

SYNTHESIS, MOLECULAR WEIGHT CHARACTERIZATION AND STRUCTURE-
PROPERTY RELATIONSHIPS OF AMMONIUM IONENES

Erika M. Borgerding

Thesis submitted to the faculty of the Virginia Polytechnic Institute and State University in
partial fulfillment of the requirements for the degree of

Master of Science
in
Chemistry

Timothy E. Long (Chair)
Judy Riffle (Member)
Richard Turner (Member)

October 29, 2007
Blacksburg, Virginia

Keywords: Ammonium Ionene, Aqueous Size Exclusion Chromatography, Thermal and
Mechanical Properties, Topology

Copyright 2007, Erika M. Borgerding

Synthesis, Molecular Weight Characterization and Structure-Property Relationships of Ammonium Ionenes

Erika M. Borgerding

ABSTRACT

Ammonium ionenes are macromolecules with quaternized nitrogen groups in the main chain. Ionenes are commonly referred to as x,y-ionene, where x and y represent the number of methylene groups between quaternized nitrogens. Synthesis of aliphatic ammonium ionenes has been studied since the early twentieth century; however, absolute molecular weight characterization has only been performed using extensive light scattering and viscosity experiments. Performing aqueous size exclusion chromatography (SEC) on ammonium ionenes provides absolute molecular weight determinations while eliminating the need for separate viscosity and light scattering experiments. We developed a mobile phase composition that provides reliable separation of aliphatic ammonium ionenes using aqueous SEC. For the first time, we report absolute molecular weights of aliphatic ammonium ionenes using this technique.

We investigated the influence of charge density and structural symmetry on thermal and mechanical properties of ammonium 6,6-, 12,6- and 12,12-ionenes. Thermal properties were measured using differential scanning calorimetry (DSC) and thermal gravimetric analysis (TGA), and mechanical properties were measured using dynamic mechanical analysis (DMA) and an Instron.

Incorporating low molecular weight polymer segments into the main chain of the ionene allows tailoring of polymer characteristics. Poly (tetramethylene oxide) segments decrease hydrophilicity and increase elastomeric character. Linear PTMO based ionenes have been synthesized previously, and we were interested in how branching affected thermal and

mechanical properties. We synthesized bis(dimethylamino) poly(tetramethylene oxide) segments, and subsequently, synthesized linear and branched ionenes to study the effects of topology on thermal and mechanical properties. Polymers were analyzed using DMA, DSC, TGA, SAXS, and an Instron.

ACKNOWLEDGMENTS

I would like to thank my advisor, Prof. Timothy Long, for his guidance and encouragement throughout my first two years of graduate school. Without his persistent pushing and enthusiasm for science, the ionene research would not have progressed as much as it has today. I would also like to thank my other committee members, Richard Turner and Judy Riffle, for their advice and support.

I would like to acknowledge John Layman for his mentorship in the lab. His expertise in aqueous size exclusion chromatography has helped the ionene research progress to a new level. Moreover, I would like to thank him for his friendship and for fighting for Dav124 (our glassware, a new air conditioner, etc...). I would also like to acknowledge Rebecca Huyck for her constant encouragement and sound advice on research and life. I would like to thank Matthew Cashion for always putting a smile on my face and for reminding me that the Tarheels are the best team in North Carolina. I would like to thank Bill Heath for teaching me purification techniques and for all his helpful synthetic advice. I would like to thank Leslie Adamczyk for her friendship and support outside of lab, as well as, my family for their constant love and support.

I would also like to thank Sharlene Williams, Mana Tamami, and Dr. Ann Fornof for their teamwork in the Kimberly-Clark and MCOE projects. Working with them has broadened and advanced the projects to levels that could not have been achieved otherwise. I would also like to acknowledge the other members of the Long research group, Matt Hunley, Andy Duncan, Akshay Kokil, Tomonori Saito, Emily Anderson, Gozde Ozturk, Dr. Brian Mather, Shijing Cheng and Vicki Long for their time, support, and helpful discussions.

TABLE OF CONTENTS

CHAPTER 1: POLYELECTROLYTES IN EMERGING TECHNOLOGIES	10
1.1 INTRODUCTION TO POLYELECTROLYTES	10
1.2 POLYELECTROLYTE MULTILAYER FILMS (PEMs)	12
1.2.1 Preparation and Applications of PEMs.....	12
1.2.2 Applications of PEMs in Biomedical Devices.....	13
1.2.2.1 Stents Coated with PEM Films	13
1.2.2.2 Friction Reduction on Mating Macromolecules	14
1.3 POLYELECTROLYTES USED FOR GENE DELIVERY.....	15
1.4 INTRODUCTION TO POLYIONENES	16
1.4.1 Synthesis and Applications of Ammonium Ionenes.....	16
1.4.2 Synthesis of PTMO Based Ammonium Ionenes	19
1.4.3 Synthesis of PEG Based Ammonium Ionenes.....	21
1.5 RESEARCH OBJECTIVES	24
1.5.1 Aliphatic Ammonium Ionenes.....	24
1.5.2 PTMO Based Ammonium Ionenes	25
1.6 REFERENCES.....	28
CHAPTER 2: ABSOLUTE MOLECULAR WEIGHT CHARACTERIZATION OF ALIPHATIC AMMONIUM IONENES USING AQUEOUS SIZE EXCLUSION CHROMATOGRAPHY	34
2.1 ABSTRACT	34
2.2 INTRODUCTION.....	35
2.3 EXPERIMENTAL	38
2.3.1 General Methods and Materials	38
2.3.2 Synthesis of N,N,N',N'-tetramethyl-1,12-dodecanediamine	39
2.3.3 Preparation of Ammonium 12,6-Ionene	39
2.3.4 Preparation of Ammonium 12,12-Ionene	40
2.3.5 Aqueous SEC of Ammonium Ionenes.....	40
2.3.6 Determination of Specific Refractive Index Increment (dn/dc)	42
2.3.7 Dynamic Light Scattering.....	42
2.4 RESULTS AND DISCUSSION	43
2.5 CONCLUSIONS	58
2.6 ACKNOWLEDGMENTS	59
2.7 REFERENCES.....	59
CHAPTER 3: INFLUENCE OF STRUCTURAL SYMMETRY AND CHARGE DENSITY ON THE THERMAL AND MECHANICAL PROPERTIES OF ALIPHATIC AMMONIUM 6,6-, 12,6- AND 12,12-IONENES	62
3.1 ABSTRACT	62
3.2 INTRODUCTION.....	63
3.3 EXPERIMENTAL	65
3.3.1 General Methods and Materials.....	65
3.3.2 Preparation of Ammonium 12,6-Ionene	67

3.3.3 Preparation of Ammonium 6,6-Ionene	67
3.3.4 Preparation of Ammonium 12,12-Ionene	67
3.3.5 Preparation of Ionene Films	68
3.4 RESULTS AND DISCUSSION	68
3.4.1 Synthesis and Molecular Weight Determinations.....	68
3.4.2 Mechanical Properties.....	70
3.4.3 Thermal Properties.....	76
3.5 CONCLUSIONS	79
3.6 ACKNOWLEDGMENTS	80
3.7 REFERENCES.....	80
CHAPTER 4: SYNTHESIS AND CHARACTERIZATION OF LINEAR AND BRANCHED POLY(TETRAMETHYLENE OXIDE) BASED IONENES	82
4.1 ABSTRACT	82
4.2 INTRODUCTION.....	83
4.3 EXPERIMENTAL	85
4.3.1 General Methods and Materials	85
4.3.2 Synthesis of Bis(dimethylamino) poly(tetramethylene oxide)	85
4.3.3 Synthesis of Linear Ionenes	87
4.3.4 Synthesis of Branched Ionenes	87
4.3.5 Characterization Methods	88
4.4 RESULTS AND DISCUSSION	89
4.4.1 Synthesis of Linear and Branched Ionenes	89
4.4.2 Mechanical Properties.....	91
4.4.3 Thermal Properties.....	96
4.4.4 Small Angle X-ray Scattering.....	98
4.5 CONCLUSIONS	99
4.6 ACKNOWLEDGMENTS	101
4.7 REFERENCES.....	101
CHAPTER 5: FUTURE DIRECTIONS	103
5.1 MOLECULAR WEIGHT DISTRIBUTIONS OF ALIPHATIC AMMONIUM IONENES USING AQUEOUS SIZE EXCLUSION CHROMATOGRAPHY	103
5.2 SYNTHESIS OF ALIPHATIC AMMONIUM IONENES WITH HIGHER EQUIVALENT MOLECULAR WEIGHTS	104
5.3 DETERMINATION OF PTMO BASED IONENE MORPHOLOGIES VIA SAXS AND TEM	106
5.4 REFERENCES	108
VITA.....	109

List of Figures

Figure 1.1: Scheme for producing a PEM film. A and B represent a polycation layer and a polyanion layer.....	13
Figure 1.2: Poly(acrylic acid) (left) and poly(allylamine hydrochloride) were used to make PEM coatings for hip replacement prostheses.	15
Figure 1.3: Synthetic scheme for ammonium x,y-ionene.....	16
Figure 1.4: The properties of molecular weight and chain rigidity are tested for their effect on antimicrobial strength. The compound on the left had great antimicrobial strength because of a stiffer chain and higher molecular weight than the compound on the right.	18
Figure 1.5: Synthesis of PTMO via a living cationic polymerization.	19
Figure 1.6: Synthetic strategy for PTMO-based ionenes.....	19
Figure 1.7: Synthesis of a PTMO-based ionene.	20
Figure 1.8: One-pot synthesis of high molecular weight PTMO-based ionene.....	21
Figure 1.9: Synthetic strategy for PEG-based water-soluble ionenes.....	22
Figure 1.10: Synthesis of a PEG-based ionene using a dihalide containing a PEG segment.	23
Figure 1.11: Synthesis of PEG-based water-soluble ionenes.	23
Figure 1.12: Synthetic strategy for bisamino poly(tetramethylene oxide)	27
Figure 1.13: Synthetic scheme for highly branched PTMO-based ionene.	28
Figure 2.1: Synthesis of aliphatic ammonium 12,y-ionenes.....	36
Figure 2.2: DLS analysis of ammonium 12,12-ionene (sample 6) in 54/23/23 (v/v/v%) water/methanol/glacial acetic acid, 0.54 M NaOAc, pH 4.0.	46
Figure 2.3: DLS analysis of ammonium 12,12-ionene (sample 6) in 54/23/23 (v/v/v%) water/methanol/glacial acetic acid, 0.54 M NaOAc, pH 4.0. Same scan as Figure 2.2, but volume (%) is shown instead of intensity (%).	46
Figure 2.4: DLS analysis of ammonium 12,12-ionene (sample 6) in 66/17/17 (v/v/v%) water/methanol/glacial acetic acid, 0.42 M NaOAc, pH 4.0.	47
Figure 2.5: DLS analysis of ammonium 12,12-ionene (sample 6) in 80/20 water/methanol (v/v/v%), 0.50 M NaOAc, pH 8.49.....	47
Figure 2.6: Determining dn/dc of ammonium 12,12-ionene in 54/23/23 (v/v/v %) water/methanol/glacial acetic acid, 0.54 M NaOAc, pH 4.0. The dn/dc was determined to be 0.168 mL/g in this example.	49
Figure 2.7: SEC chromatogram of ammonium 12,12-ionene (sample 5) showing the RI trace (dotted grey), MALLS trace (solid black), and molecular weight distribution (bold black line) in 54/23/23 (v/v/v%) water/methanol/glacial acetic acid, 0.54 M NaOAc, pH 4.0.	51
Figure 2.8: SEC chromatogram of ammonium 12,12-ionene (sample 6) showing the influence of the water/organic solvent ratio and NaOAc molarity on SEC separation. The three ratios were 74/8/18 water/methanol/acetic acid (v/v/v%), 0.57 M NaOAc, pH 4.0(solid grey), 66/17/17 water/methanol/acetic acid (v/v/v%), 0.42 M NaOAc, pH 4.0 (dotted grey), and 54/23/23 (v/v/v %) water/methanol/glacial acetic acid, 0.54 M NaOAc, pH 4.0 (solid black).....	52
Figure 2.9: SEC chromatogram of ammonium 12,6-ionene (sample 8) in the mobile phase (54/23/23 (v/v/v %) water/methanol/glacial acetic acid, 0.54 M NaOAc, pH 4.0)	53

Figure 2.10: SEC chromatogram of ammonium 12,6-ionene (sample 8) showing the RI trace (dotted grey), MALLS trace (solid black), and molecular weight distribution (bold black line) in 66/17/17 water/MeOH/AcOH (v/v/v %), 0.42 M NaOAc, pH 4.0.....	53
Figure 2.11: SEC chromatograms (MALLS trace) of aliquots obtained during a 24 h polymerization of ammonium 12,6-ionene showing molecular weight increased during the reaction.....	55
Figure 2.12: MHS plot for the ammonium 12,12-ionene (sample 5) in the mobile phase, 54/23/23 (v/v/v%) water/methanol/glacial acetic acid, 0.54 M NaOAc, pH 4.0. Measured intrinsic viscosities (black diamonds) were fitted with the logarithmic MHS relationship (dotted line).....	57
Figure 2.13: MHS plot for the ammonium 12,6-ionene (sample 8) in the mobile phase, 54/23/23 (v/v/v%) water/methanol/glacial acetic acid, 0.54 M NaOAc, pH 4.0. Measured intrinsic viscosities (black diamonds) were fitted with the logarithmic MHS relationship (dotted line).	57
Figure 3.1: Synthesis of aliphatic 12,y-ionenes.....	64
Figure 3.2: In situ FTIR spectroscopy of ammonium 12,6-ionene indicated the growth of the C-N [⊕] stretch (arrow points to peak)..	70
Figure 3.3: Reaction profile at 903 cm ⁻¹ for ammonium 12,6-ionene.	70
Figure 3.4: Crystallization of ammonium 6,6-ionene at 10x magnification under an optical microscope. The sample was prepared from a methanol solution and pipetted onto a glass slide. The methanol was allowed to evaporate under ambient conditions for 1 h, and the resultant polymer was imaged under an optical microscope. M _n 19,200 g/mol, M _w 23,000 g/mol.	71
Figure 3.5: Tan δ curves for ammonium 12,6- and 12,12-ionenes.....	72
Figure 3.6: DMA curves for ammonium 12,6-ionenes.....	74
Figure 3.7: Tensile properties of aliphatic ammonium ionenes.....	76
Figure 3.8: Samples were heated to 250 °C to erase thermal history, cooled at 3 °C/min to -90 °C, held isothermally for 30 min, and then, heated to 250 °C at 10 °C/min. The cooling cycle is shown. A cooling rate of 3 °C/min allows crystallization to occur in 12,12-40k, but not in 12,6-40k.....	78
Figure 3.9: TGA results for ammonium 6,6-, 12,6- and 12,12-ionenes.	79
Figure 4.1: Synthetic scheme for BAPTMO.....	86
Figure 4.2: Synthetic scheme for linear ionene.	87
Figure 4.3: Synthetic scheme for highly branched ionene.....	88
Figure 4.4: ¹ H NMR of BAPTMO. A comparison of the integration of peak a and peak c was used to determine the degree of polymerization and calculate the number average molecular weight.....	90
Figure 4.5: Tensile properties of linear (black) and branched (grey) ionenes.	92
Figure 4.6: Influence of crystallization on tensile properties of PTMO-based ammonium ionenes.	93
Figure 4.7: DMA results for linear (black) and branched (grey) ionenes.....	95
Figure 4.8: Tan δ curves for linear and branched PTMO-based ionenes.	96
Figure 4.9: TGA data for linear and branched ionenes.....	98
Figure 4.10: SAXS data for linear and branched ionenes.....	99
Figure 5.1: Synthesis of ammonium ionene with PTMO segments.	105
Figure 5.2: Synthesis of ionene with “block” copolymer type architecture.....	106

List of Tables

Table 2.1: The dn/dc values for aliphatic ammonium ionenes.	69
Table 2.2: Molecular weight characterization for aliphatic ammonium ionenes.....	75
Table 3.1: Molecular weights and distributions of aliphatic ammonium ionenes as determined using aqueous SEC-MALLS.....	13
Table 3.2: Thermal transitions of ammonium ionenes via DMA and DSC.....	15
Table 3.3: Tensile properties for ammonium 12,6- and 12,12-ionenes. Four repetitions per polymer sample were completed.	18
Table 4.1: Molecular weight characterization of BAPTMO.	19
Table 4.2: Tensile properties of linear and branched ionenes.	19
Table 4.3: Thermal transitions of linear and branched ionenes as measured from DSC analysis.	22

Chapter 1

POLYELECTROLYTES IN EMERGING TECHNOLOGIES

1.1 Introduction to Polyelectrolytes

Polyelectrolytes are macromolecules with ionic groups in the repeating unit.¹ Ionenenes,^{2,3} ionic liquid based polymers,⁴ zwitterionic polymers,⁵ ionomers, and branched polymers with ionic groups at pendant sites are common types of charged polymers. The charged nature of polyelectrolytes allows for electrostatic interactions with other molecules or polymers (synthetic or natural) leading to applications as gene transfection agents,^{6,7} antimicrobial agents,⁸ and polyelectrolyte multilayer films (PEMs),^{9,10,11} which have widespread uses in the biomedical field. Several comprehensive reviews have been written on charged polymers.^{12,13}

Polyelectrolytes have unique solubility properties in aqueous solutions. Polymer chains adopt an extended conformation rather than a random coiled conformation in pure water due to charge repulsion between ionic sites, a phenomenon known as the common polyelectrolyte effect. However, conformational changes occurs when salt is added, and chains collapse into random coils due to charge screening of counter ions. The valence of these counterions influences solubility. Four stages of solubility are attributed to polyelectrolyte conformations in multivalent salt solutions.^{14,15} In the first stage, polyelectrolytes dissolved in pure water will adopt an extended conformation due to the common polyelectrolyte effect. In the second stage, divalent counterions cause a phenomenon known as ion-bridging, where counter ions form electrostatic interactions with two ionic sites on the chain, and the polyelectrolyte remains soluble. In the third stage, the concentration of salt is increased, and polyelectrolytes will

precipitate from solution because of a high volume of charge screening. Finally, when the salt concentration is increased further, polyelectrolytes will re-dissolve in the solution because of a large amount of charge screening.

Counterion condensation and phase separation dictate solubility in aqueous monovalent salt solutions, and these processes are highly dependent on charge density.¹⁶ A certain amount of counterion condensation will occur depending on the amount of salt added, and polyelectrolytes with lower charge densities will precipitate at lower salt concentrations than those with higher charge densities. Phase separation occurs at lower salt concentrations for lower charge density materials because these materials are more hydrophobic than materials with higher charge densities.

Solubility properties and electrostatic interactions are two important characteristics of polyelectrolytes because of the numerous applications these properties allow. In this chapter, we will review applications of polyelectrolytes in the biomedical field. Preparation and applications of PEM films will be discussed since a broad number of biomedical applications rely on these complexes. Polyelectrolytes used in non-viral gene delivery processes will also be discussed because several types of charged polymers are able to deliver DNA to cells. Finally, we will focus on one specific type of polyelectrolytes, polyionenes, since we were interested in synthesizing and characterizing novel ionenes.

1.2 Polyelectrolyte Multilayer Films (PEMs)

1.2.1 Preparation and Applications of PEMs

Polyelectrolytes can form electrostatic bonds to oppositely charged polymers or small molecules.¹⁷ This electrostatic binding is essential for several applications, including DNA delivery and preparation of PEM films. Polyelectrolyte multilayer films, also known as layer-by-layer films or ionic self-assembled monolayers (ISAMs), have extensive applications in antimicrobial coatings for biomaterials. The synthesis of polyelectrolyte multilayer films involves submerging a substrate in one polyelectrolyte solution for 20 min, rinsing with DI water and blow drying with nitrogen, then submerging the substrate into the counter polyelectrolyte solution for 20 minutes, and repeating until the desired thickness is achieved (Figure 1.1).^{18,19} Substrates can vary from fused silica slides to poly(ethylene terphthalate) (PET) films. The average thickness for PEMs is typically less than 1 μm .²⁰ Polyelectrolytes used for biomedical devices must be biocompatible and nontoxic, such as chitosan and heparin, which are naturally occurring, biocompatible and biodegradable polymers.^{21,22,23} Other common polymers used for PEMs are poly(acrylic acid) and poly(allylamine hydrochloride) because of commercial availability.

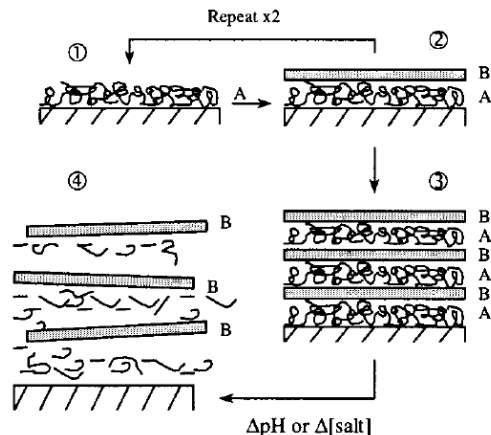


Figure 1.1: Scheme for producing a PEM film. A and B represent a polycation layer and a polyanion layer.

There are three main ways that PEM films are incorporated into biomedical devices. In the first method, both layers have antimicrobial purposes. The negatively charged layer prevents cell adhesion to biomedical devices (often made of PET), while the positively charged layer causes leakage of cellular insides.²⁴ In the second method, after the PEM film is incorporated onto a medical device and implanted in the body, the polycation will degrade or dissolve and the polyanion will be released in the cell and can perform various functions.²⁵ In the third method, the polyelectrolyte complex will serve as a scaffold for another small molecule, often a drug, which will be incorporated into the PEM film and later be eluted into the surrounding tissue.^{24,26,27}

1.2.2 Applications of PEMs in Biomedical Devices

1.2.2.1 Stents Coated with PEM Films

PEM films have been studied for applications as coatings for coronary stents, which would help prevent in-stent restenosis.²⁸ Coronary stents are biomedical devices that are used to

support the opening of blocked arteries and veins. These devices are used after transluminal coronary revascularization to prevent a second blockage due to the natural healing processes of the body (restenosis). Stents can cause a second blockage because cells adhere to the surface of biomaterials. This process is referred to as in-stent restenosis (ISR).¹⁹ The molecular mechanisms of ISR have been reviewed, which details the accepted model of bodily response to arterial injury.²⁹ This response involves a release of growth factor after the injury causing a series of events and ultimately a neointima (a new layer of cells). Vascular smooth muscle cells form a biofilm on the stent, which causes an occlusion of blood flow.³⁰ Fewer occurrences of ISR arise when the stent is coated with a PEM film prior to implantation.¹⁹ Coating a stent with a PEM film prevents cell adhesion after arterial injury, and, furthermore, incorporating a drug into that film has been shown to be more effective.³¹

1.2.2.2 PEM Films That Reduce Friction Between Mating Macromolecules

PEM films have also been shown to decrease the rate of wear behavior in mating macromolecular materials.³² Pavoov was interested in reducing friction in hip replacement prostheses without affecting the mechanical properties of the polymer implant material.³³ In this investigation, tests were performed on PEM coated materials while mimicking physiological stress levels of the hip. The authors found that hip replacement prostheses coated with the PEM films had slower wear rates due to decreased friction between the polymers. The PEM film used in this study was made from poly(acrylic acid) (PAC) and poly(allylamine hydrochloride) (PAH), two commercially available polymers via electrostatic self-assembly (Figure 1.2).

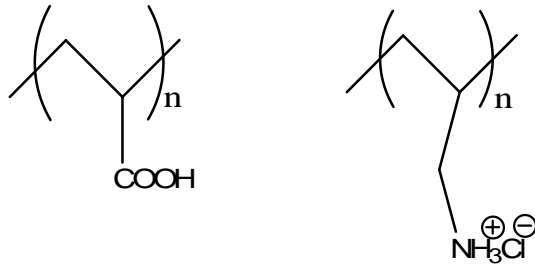


Figure 1.2: Poly(acrylic acid) (left) and poly(allylamine hydrochloride) were used to make PEM coatings for hip replacement prostheses.

Polymer brushes made of polyelectrolytes have also been shown to have low coefficient of friction values, which means these materials can be used as effective lubricants.³⁴ These types of lubricants could potentially be used to coat mating macromolecular materials, such as the hip replacement prostheses mentioned above. Polymer brushes are polymers that are attached to surfaces, but also stick out into the surrounding environment.^{27,35} They can also be used to prevent biofilm formation. Steric effects between the brush and the cells prevent the cells from adhering to the surface of a biomedical device.

1.3 Polyelectrolytes Used for Gene Delivery

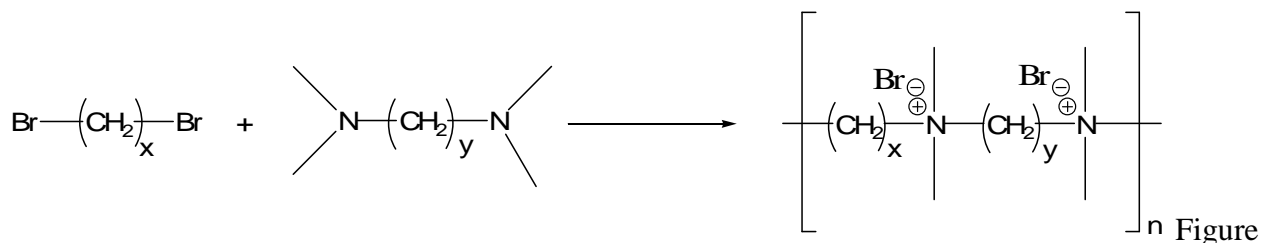
Polyelectrolytes have been widely explored as gene delivery agents to help introduce DNA into cells. Negatively charged DNA is unable to cross the cell membrane due to electrostatic repulsions with a negatively charged phospholipid bilayer. However, polycations can bind DNA and cause charge inversion,³⁶ which allows DNA to condense, cross the cell membrane and enter the cell. Many reviews have been written on gene delivery systems,^{6,7,37,38,39} and many authors have shown transfection efficiency between specific polycations and DNA.^{40,41,42,43}

Polyplex degradation inside the cell is an important parameter in gene delivery, and molecular weight has been shown to influence this process.⁴⁴ While higher molecular weight polymers condense DNA more efficiently, releasing that DNA from the complex inside the cell is more difficult. However, lower molecular weight polymers are not as efficient at condensing DNA, thus, a balance of polymer properties must be achieved in order to most effectively deliver DNA into cells. Other parameters that have been studied in developing efficient gene delivery systems include the influence of charge density,⁴⁵ solution pH,⁴⁶ and the degree of branching on DNA binding affinity.^{47,48}

1.4 Introduction to Polyionenes

1.4.1 Synthesis and Applications of Ammonium Ionenes

Polyionenes, or ionenes, are polyelectrolytes with quaternized nitrogen atoms in the backbone of the chain as opposed to pendent sites. The common nomenclature for these macromolecules is x,y-ionene, where x refers to the number of methylene spacer units in the dihaloalkane monomer, and y refers to the number of methylene spacer units between the nitrogen atoms in the di-tertiary amine monomer (Figure 1.3). The ability to easily control charge density through monomer selection provides a cornerstone for studying aliphatic ammonium ionenes.



1.3: Synthetic scheme for ammonium x,y-ionene.

Ionenes have applications in biomedical technologies as gene transfection agents,⁴⁹ polymeric cancer drugs,⁵⁰ and antimicrobials.^{51,52} Although ionenes are not ideal for DNA delivery, Langer showed that ionenes with higher charge densities positively affected the degree of transfection, where ammonium 2,10-ionene had higher transfection efficacy than 2,4- and 2,8-ionenes.²² Furthermore, Rembaum demonstrated certain ionenes selectively prevent growth of cancerous cells while normal cell growth was unaffected.²³

Antimicrobial properties of ionenes are dependent on charge density. Narita showed that ionenes with higher charge densities have increased binding affinities to yeast protoplast cells, but ionenes with lower charge densities are more cytotoxic to cells due to the ability of the longer hydrophobic segments to disrupt the cellular membranes.⁵³ Antimicrobial coatings on biomedical devices and implants are important for preventing infections since bacteria can easily invade the area.⁵⁴ Bacteria from the patient's skin or surgical instruments can enter the implant site at the time of surgery, and circulating bacteria can spontaneously become pathogenic at any time and adhere to an implant. Furthermore, the surgical area is prone to bacterial colonization because of the body's response to blunt trauma. These bacteria can form layers on the implanted devices called biofilms.⁵⁵ The sequence of events leading to biofilm formation is reviewed by Roosjen.⁵⁶ Several US Patents detail methods for coating biomedical devices with cationic antimicrobial layers, such as stents, catheters, and contact lenses.^{57,58,59}

The influence of molecular weight and chain rigidity on antimicrobial activity has also been investigated.⁶⁰ It was found that higher molecular weight polymers with stiffer chains had greater antimicrobial properties than lower molecular weight polymers with flexible chains (Figure 1.4).

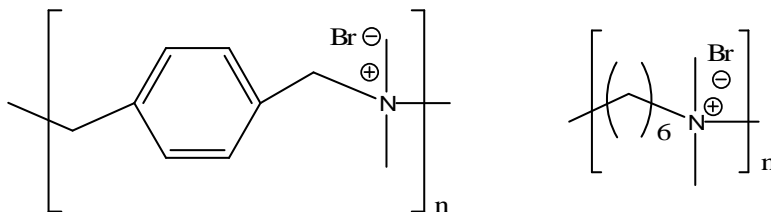


Figure 1.4: The properties of molecular weight and chain rigidity are tested for their effect on antimicrobial strength. The compound on the left had great antimicrobial strength because of a stiffer chain and higher molecular weight than the compound on the right.

Early synthetic efforts of aliphatic ammonium ionenes involved the homopolymerization of ω -halo-alkyl dialkylamines.^{61,62,63,64} However, a more conventional synthetic methodology, developed by Rembaum, is the copolymerization of a di-tertiary amine and a dihaloalkane.^{65,66} Furthermore, synthesis of non-aliphatic ionenes have also been investigated. Ionenes with poly(tetramethylene oxide) (PTMO)^{67,68,69} units or poly(ethylene glycol) (PEG)^{70,71} segments have been synthesized. The advantages of incorporating these segments into the ionene structure include adding elastomeric character, controlling solubility properties, and increasing biocompatibility. Thus, the structure-property-performance relationship of ionenes is highly dependent on monomer selection.

1.4.2 Synthesis of PTMO based Ammonium Ionenes

Ionene properties can be tailored through monomer selection, and the incorporation of PTMO is one way to alter ionene characteristics. The living cationic polymerization of tetrahydrofuran was first reported by Smith and Hubin (Figure 1.5) and has been utilized in several novel ionene polymerizations.⁷² Kohjiya chain extended living PTMO oligomers using 4,4'-bipyridine (Figure 1.6),⁷³ and other authors developed similar synthetic methodologies using

different dihaloalkanes and studied the reaction rates and mechanical properties of the resulting ionenes (Figure 1.7).^{74,75,76}

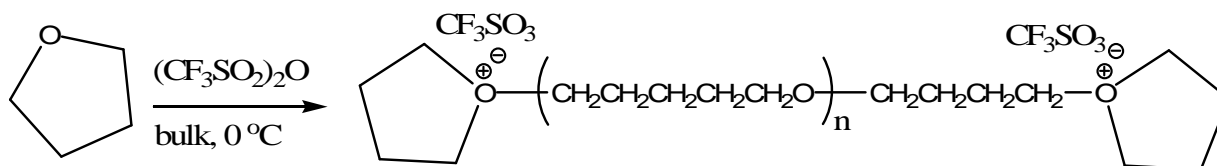


Figure 1.5: Synthesis of PTMO via a living cationic polymerization.

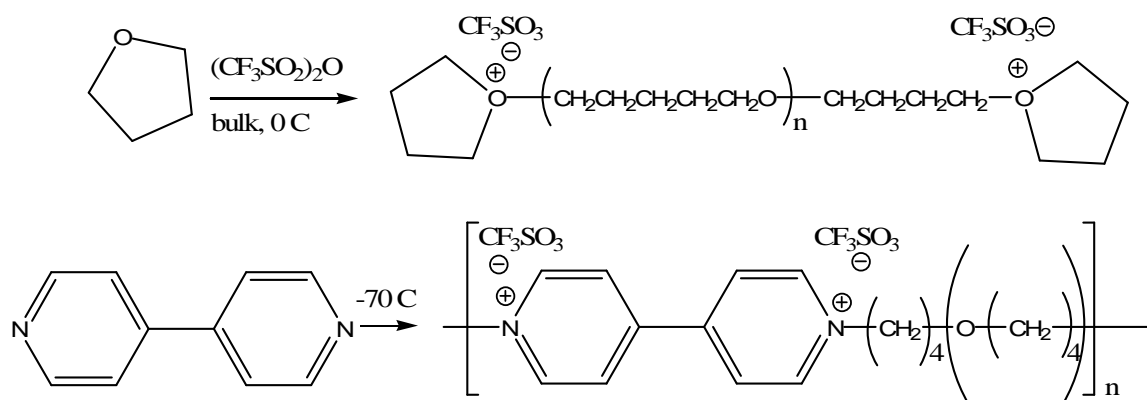


Figure 1.6: Synthetic strategy for PTMO-based ionenes.

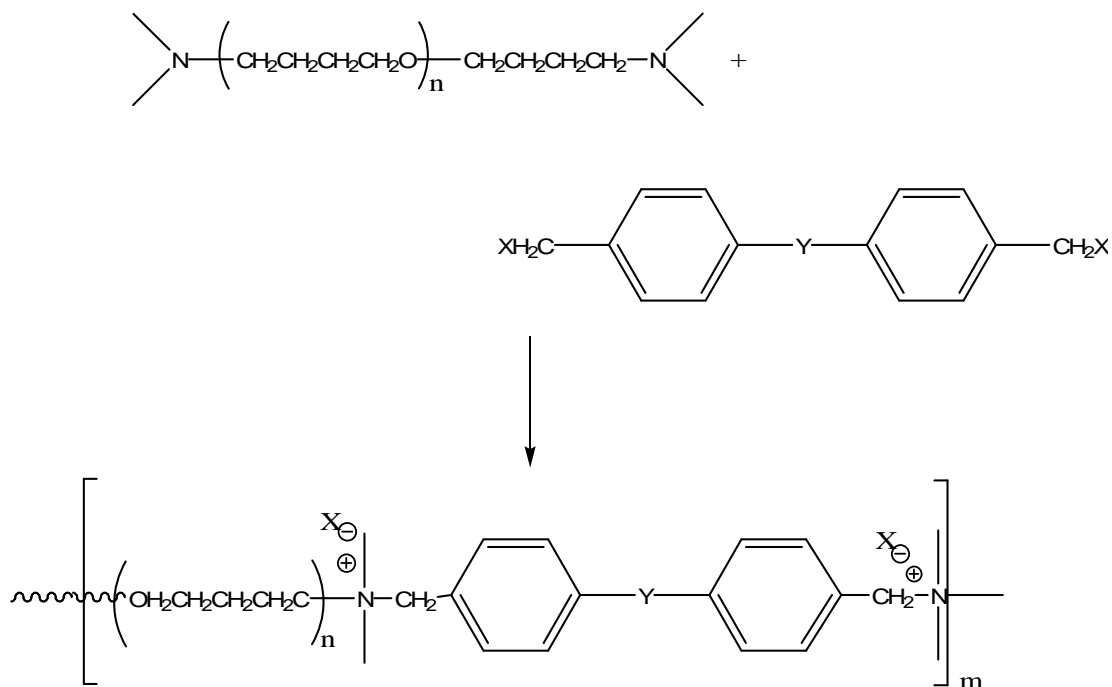


Figure 1.7: Synthesis of a PTMO-based ionene.

Ikeda developed a one-pot synthesis for high molecular weight PTMO based ammonium ionenes (Figure 1.8).⁷⁷ Reaction kinetics were crucial in this polymerization. The reaction between the N,N-dimethylaminotrimethylsilane (DMATS) and the oxonium endgroup is much slower than the reaction between a tertiary amine endcapped THF and a second oxonium compound. The authors added six equivalents of DMATS compared to 1 equivalent of initiator and allowed the reaction to proceed. Molecular weight was controlled using time; longer reaction times yielded higher molecular weights.

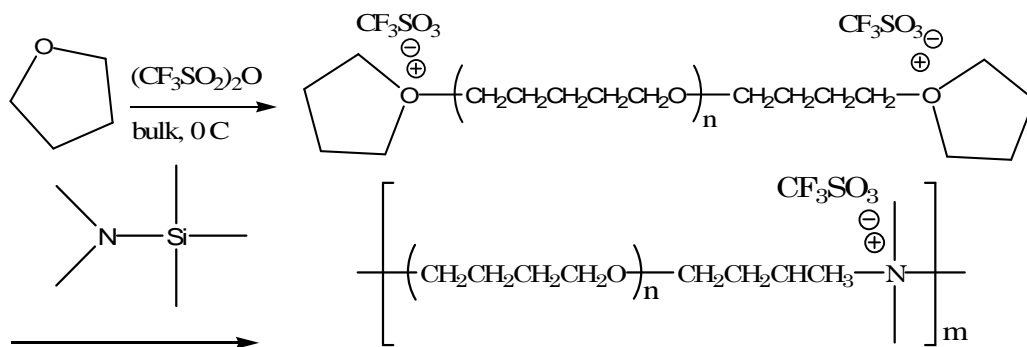


Figure 1.8: One-pot synthesis of high molecular weight PTMO-based ionene.

The elastomeric properties of PTMO-based ionenes are due to the characteristic hard-soft-hard segments familiar in common elastomers, such as polyurethane or polyureas.⁷⁸ Ionenes with low molecular weight PTMO segments have been shown to have an ordered morphology as demonstrated with small angle x-ray scattering (SAXS).⁷⁹ Microphase-separated structures have also been confirmed using transmission electron microscopy (TEM) indicating an ordered spacing between ionic aggregates or domains.⁴⁴ Regular spacing of ionic domains contributed to impressive tensile properties, where PTMO ionene had elongations of almost 1000%.⁸⁰ Furthermore, incorporating PTMO into ionenes decreases water solubility, a characteristic often associated with charged polymers, and could be desired for some applications.

1.4.3 Synthesis of PEG Based Ionenes

PEG segments have been incorporated into ionenes to increase water solubility and biocompatibility. PEG is an attractive compound for biomedical applications because of its hydrophilicity, ability to deter interactions with other proteins, and low cytotoxicity levels.^{81,82}

PEG is non-irritating when applied to the skin or beneath the skin;⁸³ its hydrophilicity is thought to be the main reason why cells cannot adsorb to its surface.^{17,84} Several novel ionenes have been synthesized with PEG segments incorporated into the backbone.

PEG-based water-soluble ionenes were synthesized using anionic polymerization techniques. Dimitrov performed the anionic polymerization of ethylene oxide initiated with N-methyldiethanolamine, followed by endcapping with hydroxyl groups, which were chain extended with dichloromethane and, subsequently, quaternized to yield a PEG based ionene (Figure 1.9).⁸⁵

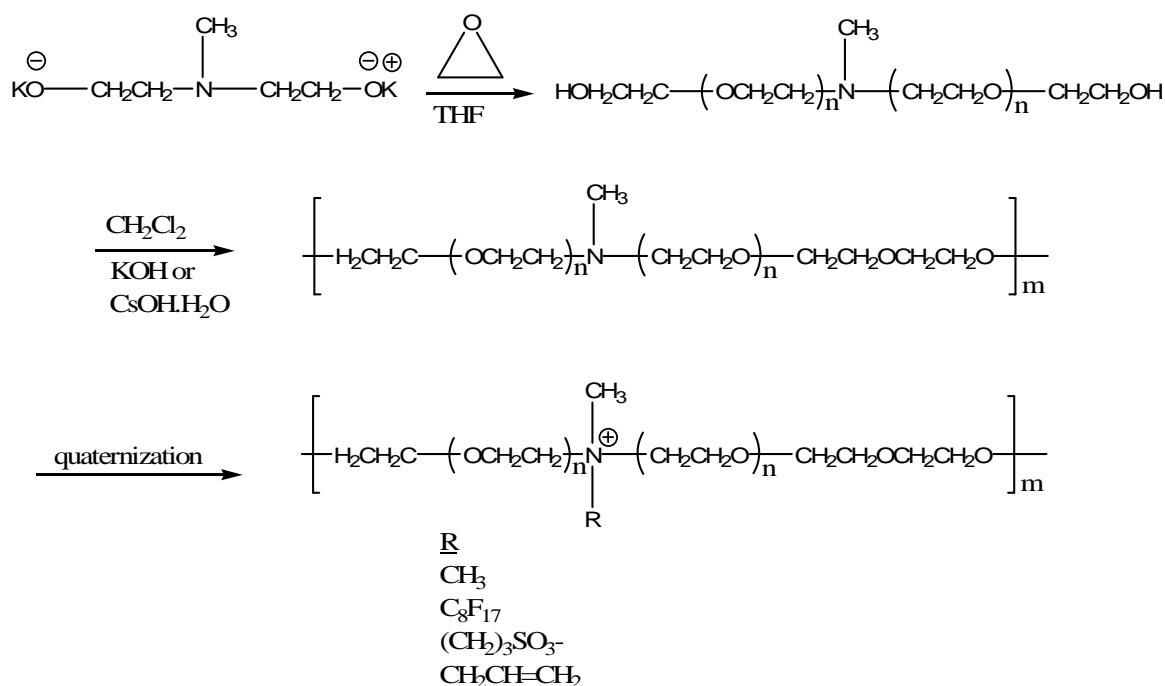


Figure 1.9: Synthetic strategy for PEG-based water-soluble ionenes.

Another incorporation of PEG into ionenes involved synthesizing a dihalide monomer where PEG was functionalized with chloroacetate end groups, which were reacted with a di-tertiary amine (Figure 1.10).⁸⁶

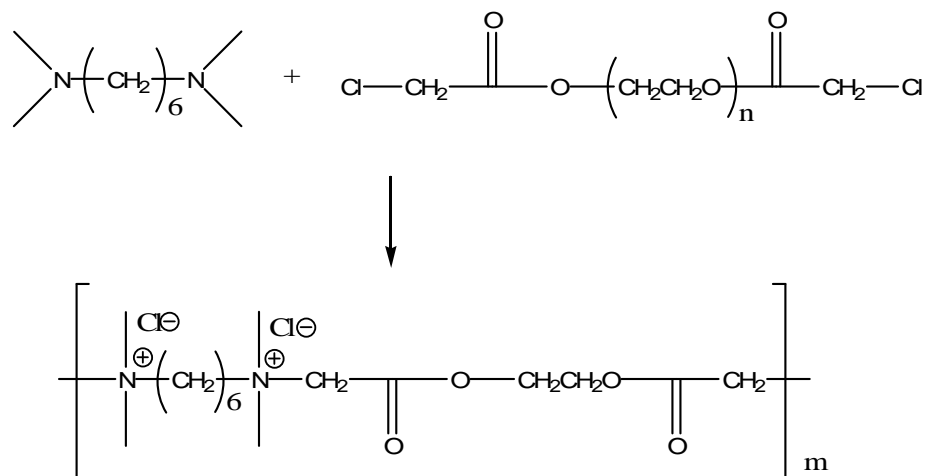


Figure 1.10: Synthesis of a PEG-based ionene using a dihalide containing a PEG segment.

Hassook has synthesized water soluble ionenes using PEG-based monomers with low molecular weight PEG segments, such as trans-1,2-bis(4-pyridyl)ethylene and di- and tri(ethylene glycol)di-p-tosylate (Figure 1.11).⁸⁷

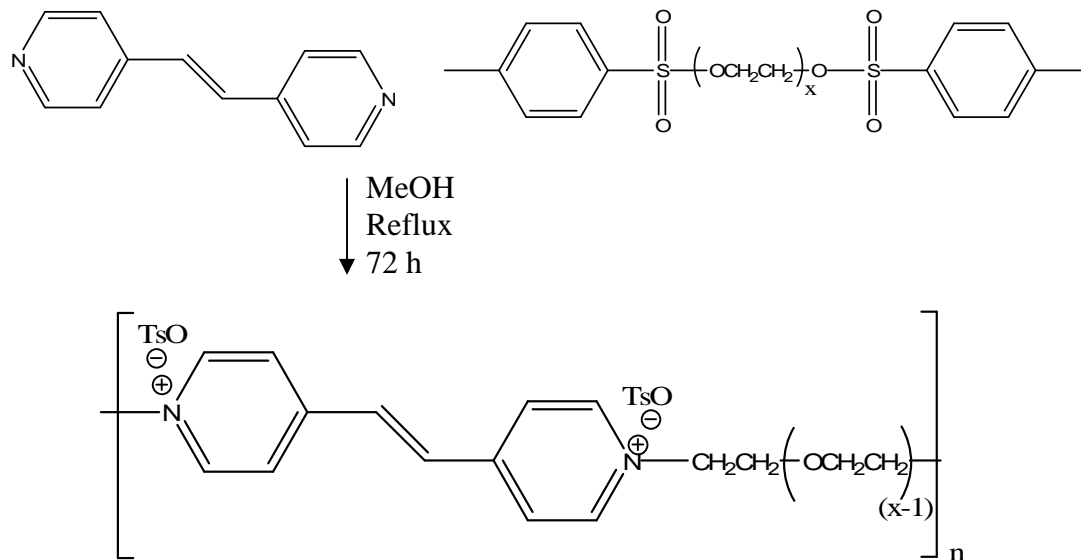


Figure 1.11: Synthesis of PEG-based water-soluble ionenes.

1.5 RESEARCH OBJECTIVES

1.5.1 Aliphatic Ammonium Ionenenes

We were interested in developing polyionenes with specific solubility properties for applications in personal hygiene items such as toilet tissue or facial tissue. It was necessary for the polymer to remain insoluble in aqueous monovalent salt solutions above 3 wt% and dissolve in salt solutions less than 3 wt% in order to both maintain the integrity of the tissue during use and allow for degradation after use. Charge density influences solubility properties of polyelectrolytes in aqueous monovalent salt solutions as previously discussed, thus, aliphatic ammonium 6,6-, 12,6- and 12,12-ionenes were synthesized from a Menshutkin reaction between a dihaloalkane and a di-tertiary amine and investigated for their solubility properties. All monomers were commercially available except N,N,N',N'-tetramethyldiaminododecane, which was synthesized from a modified literature procedure.

A major limitation in the study of aliphatic ammonium ionenes was the difficulty in performing absolute molecular weight characterization. Thermal and mechanical properties of macromolecules are highly dependent on molecular weight, which is often determined using size exclusion chromatography. The only method previously outline in the literature for determining absolute molecular weight characterization of aliphatic ammonium ionenes involved using the Mark-Houwink and Debye equations based on data from extensive viscosity and light scattering studies, respectively.⁸⁸ More recently, relative molecular weights of ammonium ionenes were calculated using aqueous size exclusion chromatography; however, measurements were based on standard-equivalent molecular weights.^{89,90} We were interested in developing a suitable aqueous SEC mobile phase composition for reliable separations and absolute molecular weight determination of aliphatic ammonium ionenes. We studied the effects of ionenes in various

water/methanol/glacial acetic acid mixtures with varying amounts of sodium acetate (NaOAc) and pH levels to arrive at the optimal mobile phase composition.

Once a suitable mobile phase composition for absolute molecular weight characterization was determined, we were interested in comparing the thermal and mechanical properties of ionenes using charge density and structural symmetry as a metric for comparison while keeping molecular weight constant. Ammonium 6,6-, 12,6- and 12,12-ionenes were selected for the study using number average molecular weights of 15,000 g/mol and 30,000 g/mol and weight average molecular weights of 20,000 g/mol and 40,000 g/mol. Dynamic mechanical analysis (DMA), tensile testing, differential scanning calorimetry (DSC), and thermal gravimetric analysis (TGA) were performed on each of the polymers to determine the role structural symmetry and charge density had on ionene performance and thermal stability.

1.5.2 PTMO-Based Ionenenes

Linear PTMO-based ammonium ionenes have been synthesized and characterized using DMA, tensile testing, SAXS, and TEM for a variety of PTMO molecular weights and chain extenders as mentioned above. These ionenes show impressive tensile properties, which suggests ionenes are good elastomers. We were interested in using topology as the metric for comparing the thermal and mechanical properties of PTMO ionenes. We thought branching would disrupt the regular ordering previously found in linear ionenes, thus decreasing their mechanical performance. Furthermore, we were interested in the morphological characteristics associated with varying both PTMO soft segment length and ionic character. Bis(dimethylamino) poly(tetramethylene oxide) segments were synthesized from the living cationic polymerization of tetrahydrofuran, followed by endcapping with methyl-

3(dimethylamino)propionate. The product was isolated, and in a reverse Michael addition reaction, sodium hydroxide cleaved methyl acrylate from the end groups yielding a di-tertiary amine endcapped PTMO segment (Figure 1.12). The low molecular weight bis-amino poly(tetramethylene oxide) polymers will be reacted with linear chain extenders such as 1,4-bis(bromomethyl)benzene to form the linear ionene, or 2,4,6-tris(bromomethyl)-mesitylene to form the highly branched ionene (both compounds are commercially available) (Figure 1.13), and the thermal and mechanical properties of the ionene films will be studied. Characterization will include DMA, TGA, DSC, tensile testing, and SAXS.

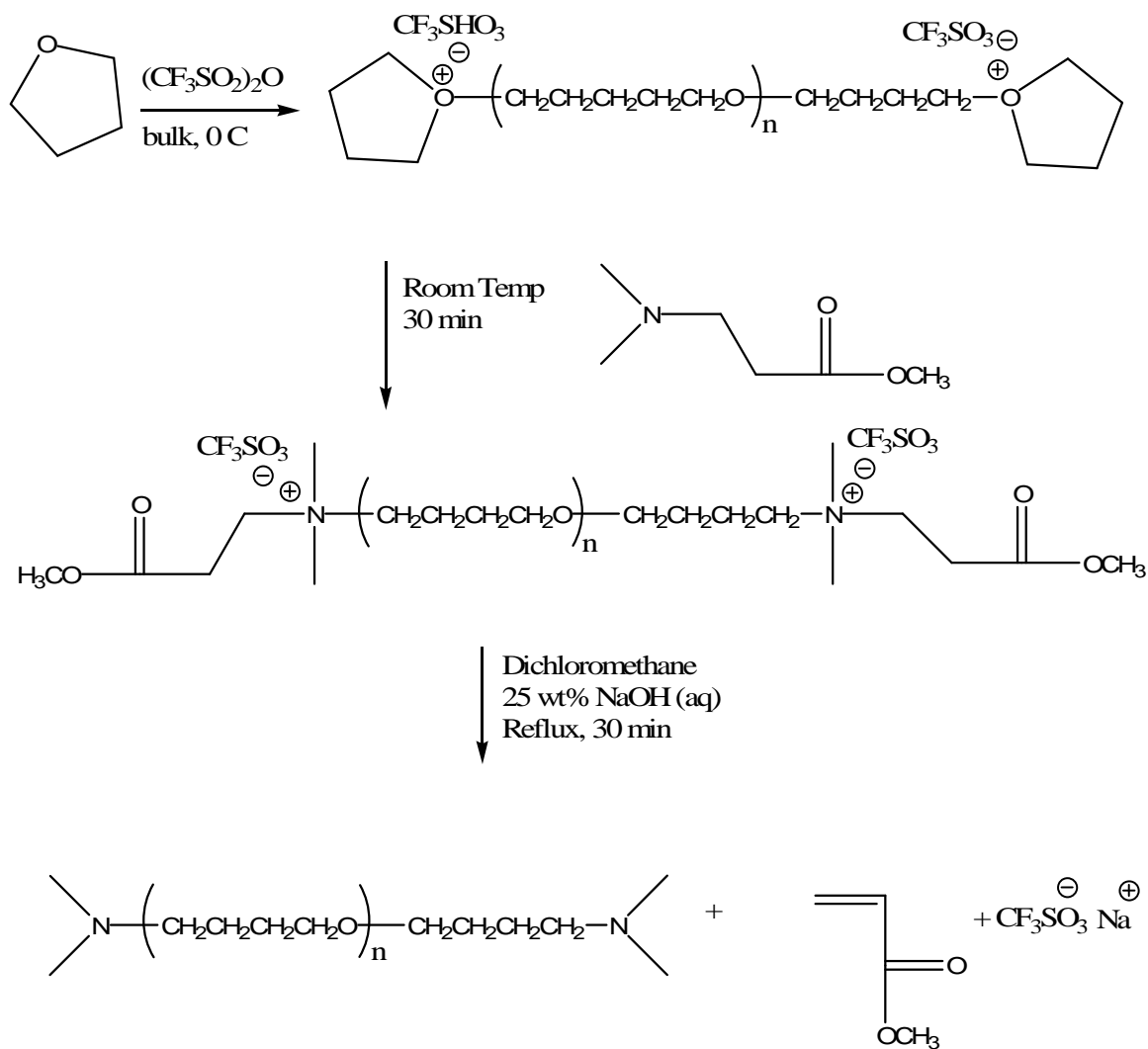


Figure 1.12: Synthetic strategy for bisamino poly(tetramethylene oxide).

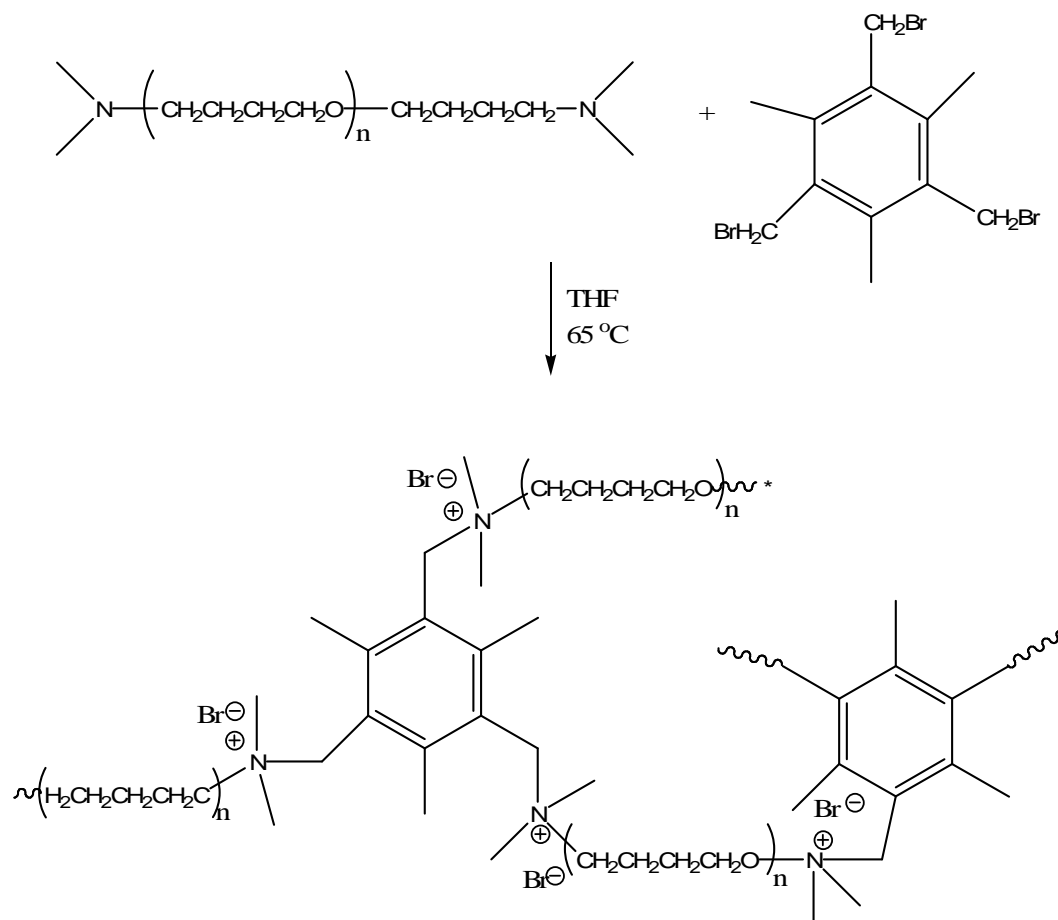


Figure 1.13: Synthetic scheme for highly branched PTMO-based ionene.

1.6 REFERENCES

- ¹ Dobrynin, A. V., Rubinstein, M., Theory of polyelectrolytes in solutions and at surfaces. *Progress in Polymer Science* **2005**, 30(11), 1049-1118.
- ² H. Noguchi and A. Rembaum, Reactions of N,N,N',N'-Tetramethyl- α,ω -diaminoalkanes with α,ω -Dihaloalkanes. I. 1-y Reactions. *Macromolecules*, **1972**, 5 (3), 253-260.
- ³ H. Noguchi and A. Rembaum, Reactions of N,N,N',N'-Tetramethyl- α,ω -diaminoalkanes with α,ω -Dihaloalkanes. II. 1-y Reactions. *Macromolecules*, **1972**, 5 (3), 261-269.
- ⁴ P. Wasserscheid and T. Welton. *Ionic Liquids in Synthesis*. Weinheim : Wiley-VCH, 2003
- ⁵ Lowe, A. B., McCormick, C. L. Synthesis and Solution Properties of Zwitterionic Polymers. *Chemical Reviews*, **2002**, 102(11), 4177-4189.
- ⁶ Li, S. D., Huang, L. Gene therapy progress and prospects: Non-viral gene therapy by systemic delivery. *Gene Therapy* **2006**, 13(18), 1313-1319.
- ⁷ Storrer, H., Mooney, D. J. Sustained delivery of plasmid DNA from polymeric scaffolds for tissue engineering. *Advanced Drug Delivery Reviews* **2006**, 58(4), 500-514.
- ⁸ Gilber, P., Moore, L. E., Cationic antiseptics: diversity of action under a common epithet. *J. Appl. Microbiology* **2005**, 99, 703-715.

-
- ⁹ Klitzing, R., Wong, J. E., Jaeger, W., Steitz, R. Short range interactions in polyelectrolyte multilayers. *Current Opinion in Colloid and Interface Science* **2004**, *9*, 158-162.
- ¹⁰ Schonhoff, M. Layered polyelectrolyte complexes: physics of formation and molecular properties. *J. Physics: Condensed Matter* **2003**, *15*, R1781-R1808.
- ¹¹ Schaaf, P., Jessel, N., Ogier-Dirrig, J., Lavalle, P., Voegel, J. C., Senger, B. Polyelectrolyte multilayer films 2005 USPatent 2006079928
- ¹² Netz, R. R., Andelman, D. Neutral and charged polymers at interfaces. *Physics Reports* **2003**, *380*(1-2), 1-95.
- ¹³ Poinignon, C., Polymer electrolytes. *Materials Science and Engineering, B: Solid-State Materials for Advanced Technology* **1989**, *B3*(1-2), 31-37.
- ¹⁴ M. Olvera de la Cruz, *J. Chem. Phys.*, **1995**, *103* (13), 5781-5791.
- ¹⁵ Solis, F. J., Olvera de la Cruz, M. Collapse of flexible polyelectrolytes in multivalent salt solutions. *Journal of Chemical Physics* **2000**, *112*(4), 2030-2035.
- ¹⁶ A. Ikegami and N. Imai, *Journal of Polymer Science*, **1962**, *56*, 133-152.
- ¹⁷ Nordmeier, E., Beyer, P. Nonstoichiometric Polyelectrolyte Complexes: A Mathematical Model and Some Experimental Results. *J. Polym. Sci. B: Polym. Physics* **1999**, *37*, 335-348.
- ¹⁸ Hong, J. D., Jung, B. D., Kim, C. H., Kim, K. Effects of Spacer chain lengths of layered nanostructures assembled with main-chain azobenzene ionenes and polyelectrolytes. *Macromolecules* **2000**, *33*, 7905-7911.
- ¹⁹ Dubas, S. T., Farhat, T. R., Schlenoff, J. B. Multiple membranes from “true” polyelectrolyte multilayers. *Journal of American Chemical Society* **2001**, *123*, 5368-5369.
- ²⁰ Grunlan, J. C., Choi, J. K., Lin, A. Antimicrobial behavior of polyelectrolyte multilayer films containing centrimide and silver. *Biomacromolecules* **2005**, *6*, 1149-1153.
- ²¹ Ren, D., Yi, H., Xie, W., Ma, X. Study on homogeneity of enzymatic degradation of chitosan as biomaterials by gel permeation chromatography. *Chinese Journal of Chromatography* **2006**, *24*(4), 407-410.
- ²² Werner, C. *Advances in Polymer Science: Polymers for Regenerative Medicine*. Springer: Dresden, 2006.
- ²³ Ruel-Gariepy, E., Leroux, J. C. Chitosan: a natural polycation with multiple applications. *ACS Symposium Series* **2006**, *934*, 243-259.
- ²⁴ Fu, J., Ji, J., Yuan, W., Shen, J. Construction of anti-adhesive and antibacterial multilayer films via layer-by-layer assembly of heparin and chitosan. *Biomaterials* **2005**, *26*, 6684-6692.
- ²⁵ Vazquez, E., Dewitt, D. M., Hammond, P. T., Lynn, D. M. Construction of hydrolytically-degradable thin films via layer-by-layer deposition of degradable polyelectrolytes. *Journal of American Chemical Society* **2002**, *124*, 13992-13993.
- ²⁶ Fiegel, J., Fu, J., Hanes, J. Poly(ether-anhydride) dry power aerosols for sustained drug delivery in the lungs. *Journal of Controlled Release* **2004**, *96*(3), 411-423.
- ²⁷ Etienne, O., Gasnier, C., Taddei, C., Voegel, J.C., Aunis, D., Schaaf, P., Metz-Boutigue, M.H., Bolcato-Bellemin, A.L., Egles, C. Antifungal coating by biofunctionalized polyelectrolyte multilayered films. *Biomaterials* **2005**, *26*, 6704-6712.
- ²⁸ Thierry, B., Winnik, F. M., Merhi, Y., Silver, J., Tabrizian, M. Bioactive coatings of endovascular stents based on polyelectrolyte multilayers. *Biomacromolecules* **2003**, *4*, 1564-1571.
- ²⁹ Indolfi, C., Mongiardo, A., Torella, D. Molecular mechanisms of In-stent restinosis and approach to therapy with eluting stents. *Trends in Cardiovascular Medicine* **2003**, *13*, 142-148.

-
- ³⁰ Salloum, D. S., Olenych, S. G., Keller, T. C., Schlenoff, J. B. Vascular Smooth muscle cells on polyelectrolyte multilayers: Hydrophobicity-directed adhesion and growth. *Biomacromolecules* **2005**, *6*, 161-167.
- ³¹ Jewell, C. M., Zhang, J., Fredin, N. J., Wolff, M. R., Hacker, T. A., Lynn, D. M. Release of plasmid DNA from intravascular stents coated with ultrathin multilayered polyelectrolyte films. *Biomacromolecules* **2006**, *7*(9), 2483-2491.
- ³² Pavoov, P. V., Gearing, B. P., Bellare, A., Cohen, R. E., Tribiological characteristics of polyelectrolyte multilayers. *Wear* **2004**, *256*, 1196-1207.
- ³³ Pavoov, P. V., Gearing, B. P., Muratoglu, O., Cohen, R. E., Bellare, A. Wear reduction of orthopaedic bearing surfaces using polyelectrolyte multilayer nanocoatings. *Biomaterials* **2006**, *27*(8), 1527-1533.
- ³⁴ Raviv, U., Giasson, S., Kamf, N., Gohy, J. F., Jerome, R., Klein, J. Lubrication by charged polymers. *Nature* **2003**, *425*, 163-165.
- ³⁵ Naji, A., Seidel, C., Netz, R. R. Theoretical approaches to neutral and charged polymer brushes. *Preprint Archive, Condensed Matter* **2005** 1-36.
- ³⁶ Nguyen, T. T., Grosberg, A. Y., Shklovskii, B. I. Screening of a charged particle by multivalent counterions in salty water: Strong charge inversion. *Journal of Chemical Physics* **2000**, *113*(3), 1110-1125.
- ³⁷ Elouahabi, A., Ruyschaert, J. M. Formation and intracellular trafficking of lipoplexes and polyplexes. *Molecular Therapy* **2005**, *11*, 336-347.
- ³⁸ Collins, L. Nonviral vectors. *Methods in Molecular Biology* **2006**, *333*, 201-225.
- ³⁹ Torchilin, V. P. Recent approaches to intracellular delivery of drugs and DNA and organelle targeting. *Annual Review of Biomedical Engineering* **2006**, *8*, 343-375.
- ⁴⁰ Funhoff, A. M., Nostrum, C. F., Lok, M. C., Fretz, M. M., Crommelin, D. J. A., Hennink, W. E. Poly(3-guanidinopropyl methacrylate): A novel cationic polymer for gene delivery. *Bioconjugate Chemistry* **2004**, *15*, 1212-1220.
- ⁴¹ Zhong, Z., Song, Y., Engbersen, J. F. J., Lok, M. C., Hennink, W. E., Feijen, J. A versatile family of degradable non-viral gene carriers based on hyperbranched poly(ester amine)s. *Journal of Controlled Release* **2005**, *109*, 317-329.
- ⁴² Kneuer, C., Ehrhardt, C., Bakowsky, H., Kumar, M. N., Oberle, V., Lehr, C. M., Hoekstra, D., Bakowsky, U. The influence of physiochemical parameters on the efficacy of non-viral DNA transfection complexes: A competitive study. *Journal of Nanoscience and Nanotechnology* **2006**, *6*(9/10), 2776-2782.
- ⁴³ Putnam, D., Gentry, C. A., Pack, D. W., Langer, R. Polymer-based gene delivery with low cytotoxicity by a unique balance of side-chain termini. *Proceedings of the National Academy of Science of the United States of America* **2001**, *98*(3), 1200-1205.
- ⁴⁴ Schaffer, D. V., Fidelman, N. A., Dan, N., Lauffenburger, D. A. Vector unpacking as a potential barrier for receptor-mediated polyplex gene delivery. *Biotechnology and Bioengineering* **2000**, *67*(5), 598-606.
- ⁴⁵ Trukhanova, E. S., Izumrudov, V. I., Litmanovich, A. A., Zelikin, A. N. Recognition and selective binding of DNA by ionenes of different charge density. *Biomacromolecules* **2005**, *6*, 3198-3201.
- ⁴⁶ Rungsardthong, U., Ehtezazi, T., Bailey, L., Armes, S. P., Garnett, M. C., Stolnik, S. Effect of polymer ionization on the interaction with DNA in nonviral gene delivery systems. *Biomacromolecules* **2003**, *4*, 683-690.

-
- ⁴⁷ Dragan, S., Cristea, M. Polyelectrolyte complexes. Formation, characterization and applications. *Recent Research Developments in Polymer Science* **2003**, *7*, 149-181.
- ⁴⁸ Twaites, B. R., de las Heras Alarcon, C., Cunliffe, D., Lavigne, M., Pennadam, S., Smith, J. R., Gorecki, D. C., Alexander, C. Thermo and pH responsive polymers gene delivery vectors: effect of polymer architecture on DNA complexation in vitro. *Journal of Controlled Release* **2004**, *97*(3), 551-556.
- ⁴⁹ Zelinkin, A. N., Putnam, D., Shastri, P., Langer, R., Izumrudov, V. A., Aliphatic Ionenes as Gene Delivery Agents: Elucidation of Structure-Function Relationship through Modification of Charge Density and Polymer Length. *Bioconjugate Chem.*, **2002**, *13*, 548-553.
- ⁵⁰ Rembaum, A. Ionene polymers for selectively inhibiting the vitro growth of malignant cells. US Patent 4,013,507 **1977**; *SciFinder Scholar* AN 1977:416039 (accessed 4/11/07).
- ⁵¹ Punyani, S., Singh, H., Preparation of Iodine Containing Quaternary Amine Methacrylate Copolymers and Their Contact Killing Antimicrobial Properties. *J. Appl. Polym. Sci.*, **2006**, *102*, 1038-1044.
- ⁵² Kourai, H., Yabuhara, T., Shirai, A., Maeda, T., Nagamune, H. Syntheses and antimicrobial activities of a series of new bis-quaternary ammonium compounds. *Eur. J. Medicinal Chem.*, **2006**, *41*, 437-444.
- ⁵³ T. Narita, R. Ohtakeyama, M. Nishino, J.P. Gong, Y. Osada, Effects of charge density and hydrophobicity of ionene polymer on cell binding and viability. *Colloid Polym. Sci.*, **2000**, *278*, 884-887.
- ⁵⁴ Wu, P., Grainger, D., W. Drug/device combinations for local drug therapies and infection prophylaxis. *Biomaterials* **2006**, *27*, 2450-2467.
- ⁵⁵ Nord, W., Gage, D. Interaction of Bovine Serum Albumin and Human Blood Plasma with PEO-Tethered Surfaces: Influence of PEO chain length, grafting density, and temperature. *Langmuir* **2004**, *20*(10), 4162-4167.
- ⁵⁶ Roosjen, A., Norde, W., Mei, H. C., Busscher, H. J. The use of positively charged or low surface free energy coatings versus polymer brushes in controlling biofilm formation. *Progress in Colloid and Polymer Science* **2000**, *132*, 138-144.
- ⁵⁷ Jen, J. S., Jones, R. E., Homesley, P., M., Petisce, J. Methods for providing biomedical devices with hydrophilic antimicrobial coatings **2006** US Patent 200568008.
- ⁵⁸ Lan, J., Vanderlaan, D., Willcox, M. Aliwarga, Y. Biomedical devices with antimicrobial cationic peptide and protein coatings. **2002**, US Patent 2001-US4524.
- ⁵⁹ Lydon, M., Gravett, D. M., Whitbourne, R. J. Antimicrobial needle coating for extended infusion. **2006**, US Patent 2005-US40512.
- ⁶⁰ Tashiro, T. Antibacterial and Bacterium Adsorbing Macromolecules. *Macromolecular Materials and Engineering* **2001**, *286*, (63-87).
- ⁶¹ C. F. Gibbs, E. R. Littman, C. S. Marvel, Quaternary Ammonium Salts from Halogenated Alkyl Dimethylamines. II. The Polymerization of Gamma-Halogenopropyl dimethylamines, *J. Am. Chem. Soc.*, **1933**, *##*, 753-757.
- ⁶² M.R. Lehman, C.D. Thompson and C.S. Marvel, Quaternary Ammonium Salts from Hologenated Alkyl Dimethylamines. III. Omega-Bromo-Heptyl-, -Octyl-, -Nonyl-, and -Decyl-dimethylamines. *J. Am. Chem. Soc.*, **1935**, *57*, 1137-1139.
- ⁶³ C.F. Gibbs and C.S. Marvel, Quaternary Ammonium Salts from Bromopropyl dialkylamines. IV. Formation of Four-Membered Rings.

-
- ⁶⁴ C.F. Gibbs and C.S. Marvel, Quaternary Ammonium Salts from Bromopropylalkylamines. V. Conversion of Cyclic Ammonium Salts to Linear Polymers.
- ⁶⁵ H. Noguchi and A. Rembaum, Reactions of N,N,N',N'-Tetramethyl- α,ω -diaminoalkanes with α,ω -Dihaloalkanes. I. 1-y Reactions. *Macromolecules*, **1972**, 5 (3), 253-260.
- ⁶⁶ H. Noguchi and A. Rembaum, Reactions of N,N,N',N'-Tetramethyl- α,ω -diaminoalkanes with α,ω -Dihaloalkanes. II. 1-y Reactions. *Macromolecules*, **1972**, 5 (3), 261-269.
- ⁶⁷ S. Smith and A.J. Hubin, Preparation and chemistry of dicationically active polymers of tetrahydrofuran. *J. Macromol. Sci. -Chem.*, **1973**, 7 (7), 1399-413.
- ⁶⁸ C.M. Leir and J.E. Stark, Ionene Elastomers from Polytetramethylene Oxide Diamines and Reactive Dihalides. I. Effect of Dihalide Structure on Polymerization and Thermal Reversibility. *J. Appl. Polym. Sci.*, **1989**, 38, 1535-47.
- ⁶⁹ S. Kohjiya, T. Ohtsiki, S. Yamashita, Polyelectrolyte Behavior of an Ionene Containing Poly(oxytetramethylene) Units. *Makromol. Chem., Rapid Commun.*, **1981**, 2, 417-20.
- ⁷⁰ I.V. Dimitrov, I.V. Berlinova, Synthesis of Poly(ethylene oxide)s Bearing Functional Groups along the Chain. *Macrom. Rapid Com.*, **2003**, 24, 551-555.
- ⁷¹ H. Han, P.R. Vantine, A.K. Nedeltchev, P.K. Bhowmik, Main-Chain Ionene Polymers Based on trans-1,2-(4-pyridyl)ethylene Exhibiting Both Thermotropic Liquid-Crystalline and Light-Emitting Properties. *J. Polym. Sci.: Part A: Polym. Chem.*, **2006**, 44, 1541-1554.
- ⁷² Smith, S., Hubin, A. J. Preparation and chemistry of dicationically active polymers of tetrahydrofuran. *Journal of Macromolecular Science, Chemistry* **1973**, 7(7), 1399-1413.
- ⁷³ S. Kohjiya, T. Hashimoto, S. Yamashita and M. Irie, Synthesis and Photochromic Behavior of Elastomeric Ionene Containing Viologen Units. *Chem. Lett.*, **1985**, 10, 1497-500.
- ⁷⁴ Feng, D., Wilkes, G. L., Lee, B., McGrath, J. M. Structure-property behavior of segmented poly(tetramethylene oxide)-based bipyridinium ionene elastomers. *Polymer* **1992**, 33(3), 526-535.
- ⁷⁵ D. Feng, L.N. Venkateshwaran, G.L. Wilkes, C.M. Leir and J.E. Stark, Structure-Property Behavior of Elastomeric Segmented PTMO-Ionene Polymers. II. *J. Appl. Polym. Sci.*, **1989**, 37, 1549-65.
- ⁷⁶ Igeda, Y., Murakami, T., Yuguchi, Y., Kajiwara, K. Synthesis and Characterization of Poly(oxytetramethylene) Ionene with 2,2'-Bipyridinium Units. *Macromolecules* **1998**, 31(4), 1246-1253.
- ⁷⁷ Ikeda, Y., Murakami, T., Urakawa, H., Kohjiya, S., Grottenmuller, R., Schmidt, M. One-pot synthesis and characterization of aliphatic poly(oxytetramethylene) ionene. *Polymer* **2002**, 43, 3483-3488.
- ⁷⁸ C. Hepburn. *Polyurethane Elastomers*. Applied Science Publishing; New York, 1982.
- ⁷⁹ Feng, D., Wilkes, G. Morphological investigation of polytetramethyleneoxide-dibromoxylene segmented ionene polymers by transmission electron microscopy and small-angle x-ray scattering. *J. Macromol. Sci.-Chem.* **1989**, A26(8), 1151-1181.
- ⁸⁰ D. Feng, L.N. Venkateshwaran, G.L. Wilkes, C.M. Leir and J.E. Stark, Structure-Property Behavior of Elastomeric Segmented PTMO-Ionene Polymers. II. *J. Appl. Polym. Sci.*, **1989**, 37, 1549-65.
- ⁸¹ Fiegel, J., Fu, J., Hanes, J. Poly(ether-anhydride) dry power aerosols for sustained drug delivery in the lungs. *Journal of Controlled Release* **2004**, 96(3), 411-423.
- ⁸² Petersen, H., Fechner, P. M., Martin, A. L., Kunath, K., Stolnik, S., Roberts, C. J., Fischer, D., Davies, M. C., Kissel, T. Polyethylenimine-graft-Poly(ethylene glycol) Copolymers: Influence

of Copolymer Block Structure on DNA Complexation and Biological Activities as Gene Delivery Systems. *Bioconjugate Chem.* **2002**, *13*, 845-854.

⁸³ Reeve, L. The poloxamers: their chemistry and medical applications. Handbook of biodegradable polymers. *Drug Targeting and delivery.* **1997**, *7*, 231-249.

⁸⁴ Kim, J. H., Kim, S., K. PEO-grafting on PU/PS IPNs for enhanced blood compatibility—effect on pendant length and grafting density. *Biomaterials* **2002**, *23*, 2015-2025.

⁸⁵ Dimitrov, I. V., Berlinova, I. V. Synthesis of Poly(ethylene oxide)s Bearing Functional Groups along the chain. *Macromolecular Rapid Communications* **2003**, *24*, 551-555.

⁸⁶ Burmistr, M. V., Sukhyy, K. M., Shilov, V. V., Pissis, P., Polizos, G., Spanoudaki, A., Gomza, Y. Structure, thermal properties and ionic conductivity of polymeric quaternary ammonium salts (polyionenes) containing ethylene oxide and aliphatic chain fragments. *Solid State Ionics* **2005**, *176*, 1787-1792.

⁸⁷ Haesook, H., Vantine, P., Nedeltchev, A., Bhowmik, P. Main-chain ionene polymers based on trans-1,2-bis(4-pyridyl)ethylene exhibiting both thermotropic liquid-crystalline and light-emitting properties. *Journal of Polymer Science, A Polymer Chemistry* **2006**, *44*, 1541-1554.

⁸⁸ Casson, D., and Rembaum, A. Solution Properties of Novel Polyelectrolytes. *Macromolecules*, **1971**, *5* (1), 75-81.

⁸⁹ Kopecká, K., Tesařová, E., Pirogov, A., Gaš, B. Ionenes acting as pseudostationary phases in capillary electrokinetic chromatography. *J. Sep. Sci.*, **2002**, *25*, 1027-1034.

⁹⁰ Reisinger, T., Meyer, W.H., Wegner, G., Haase, T., Schultes, K., Wolf, B.A. Influence of chain length on the molecular dynamics of an aliphatic ionene. *Acta Polym.*, **1998**, *49*, 710-714.

Chapter 2

Aqueous Size Exclusion Chromatography of Aliphatic Ammonium Ionenes for Absolute Molecular Weight Characterization

Erika M. Borgerding, John M. Layman, William H. Heath, Sharlene R. Williams, and Timothy E. Long

Department of Chemistry, Macromolecules and Interfaces Institute, Virginia Polytechnic Institute and State University, Blacksburg, Virginia 24061

2.1 ABSTRACT An aqueous-based SEC-MALLS mobile phase composition was determined for absolute molecular weight analysis of aliphatic ammonium ionenes, specifically 12,12- and 12,6-ionenes. The optimum solvent composition comprised a ternary mixture of 54/23/23 water/methanol/glacial acetic acid, 0.54 M NaOAc, at a pH of 4.0. The dn/dc was determined to be 0.168 mL/g for ammonium 12,12-ionene in this solvent mixture, and 0.154 mL/g for ammonium 12,6-ionene. Number average molecular weights for ammonium 12,12-ionene ranged from 3,500 – 30,700 g/mol, and weight average molecular weights ranged from 4,300 – 39,600 g/mol. Ammonium 12,6-ionenes had number average molecular weights ranging from 17,000 g/mol to 30,500 g/mol, and weight average molecular weights ranging from 22,200 – 43,300 g/mol. The molecular weight distribution ranged from 1.31 – 1.42 for ammonium 12,6-ionene and 1.26 – 1.33 for ammonium 12,12-ionene.

KEYWORDS: ammonium ionenes, cationic polyelectrolytes, aqueous SEC-MALLS, light scattering

2.2 INTRODUCTION

Ammonium ionenes are ion-containing macromolecules containing quaternary nitrogens in the main chain. The typical nomenclature for aliphatic ammonium ionenes is x,y-ionene, where x represents the number of methylene spacer units derived from the dihaloalkane monomer, and y represents the methylene spacer units in the di-tertiary amine monomer (Figure 2.1). Early efforts for the synthesis of ammonium ionenes involved the homopolymerization of ω -halo-alkyl dialkylamines;^{1,2,3,4} however, more conventional synthetic methodologies for ammonium ionenes involves the copolymerization of dihaloalkanes and di-tertiary amines, which was first reported by Rembaum et al.^{5,6} The ability to easily control charge density and counter anion through monomer selection makes ammonium ionenes an ideal model in the study of well-defined cationic polyelectrolytes. Due to their unique coulombic properties, ammonium ionenes were recently explored for several biomedical technologies including antimicrobials,^{7,8} gene transfection agents,⁹ and polymeric cancer drugs.¹⁰ Cell binding and viability studies performed using yeast protoplast revealed that ammonium ionenes with lower charge density disrupted cell membranes to a greater extent than structures with higher charge density despite less cell binding.¹¹ Furthermore, Rembaum reported ionenes as anti-tumor agents that exhibited selective inhibition of malignant cell growth without affecting normal cells.¹⁰ These examples demonstrate the potential applications of ammonium ionenes, as well as, the importance of determining their chemo-physical characteristics for conclusive structure-property relationships.

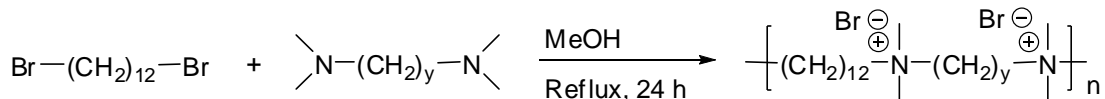


Figure 2.1: Synthesis of aliphatic ammonium 12,y-ionenes.

Determination of molecular weight and molecular weight distribution is critical when establishing structure-property-performance relationships. In earlier investigations, a comparison of the amount of non-ionic bromine in an ionene solution to the amount of total bromide in the same solution yielded “average apparent molecular weight.”¹² In Rembaum’s earlier work, extensive viscosity and light scattering studies were performed on ammonium 3,4- and 6,6-ionenes to determine molecular weights via the Mark-Houwink and Debye relationships, respectively.¹³ Absolute molecular weights were determined; however, tedious sample preparation and lengthy experiments were required to complete these calculations. Size exclusion chromatography (SEC), also referred to as gel permeation chromatography (GPC), coupled with multiangle laser light scattering (MALLS) is a well-established method for determining molecular weights. When MALLS detection is coupled with a concentration detector such as a differential refractometer (dRI), SEC provides a rapid method for determining absolute molecular weights with facile sample preparation. In addition, MALLS provides structural information, such as radius of gyration. Several texts and comprehensive reviews that describe SEC in detail are available.^{14,15,16} Despite the appreciated value of SEC-MALLS and concurrent synthetic investigations of ionenes, SEC analysis for the determination of absolute molecular weights of ammonium ionenes has not been reported earlier. This is partly attributed to the challenges associated with SEC of polyelectrolytes. Difficulties arise from ionic aggregation¹⁷ and non-size exclusion

events,^{Error! Bookmark not defined.} such as ion interaction, ion exclusion, and hydrophobic interactions in the stationary phase of the chromatographic column. SEC of cationic polyelectrolytes is especially problematic due to the negative charge common on most stationary-phase packing materials that encourages unwanted electrostatic interactions.¹⁸ To the best of our knowledge, earlier SEC analyses of ammonium ionenes were limited to relative calculation methods, which provide only standard-equivalent molecular weights. Furthermore, SEC-MALLS determination of absolute molecular weights of ammonium 12,12-ionene compositions was not reported earlier. Kopecká et al. performed SEC on ammonium 5,2- and 10,2-ionenes and determined relative molecular weights based on polyacrylamide standards.¹⁹ Similarly, Reisinger et al. performed SEC on ammonium ionenes using quaternized poly(vinylpyridinium) standards.²⁰ Although these calculations provided molecular weight trends, absolute molecular weight data is critical for the understanding of fundamental structure-property relationships. Moreover, meaningful molecular weight characterization of branched topologies is difficult when using relative calculation methods. Furthermore, our aqueous SEC-MALLS data of ammonium ionenes using two mobile phase compositions that Kopecká and Reisinger reported earlier¹ did not reveal any signals in the chromatograms.

Our research group has performed a number of studies on charge polymers.^{21,22,23} Herein, we report aqueous-based SEC-MALLS of 12,6- and 12,12-ammonium ionenes. This manuscript reports the most suitable aqueous SEC mobile-phase composition for obtaining reliable separations of aliphatic ammonium ionenes through elimination of polymer-column interactions and reduction of polymer-polymer

¹ 0.020 M NaAc in water with AcOH to adjust the pH to 5.2 (Kopecká) and 20/80 acetonitrile/0.5 M sodium sulfate, 0.5 M AcOH in water (Reisinger)

aggregation. In addition to absolute molecular weight determination, we also report dilute solution rheology of ammonium ionenes using an online, capillary-based viscosity detector. This complementary detector functions with dRI and MALLS detectors to determine the intrinsic viscosity of the sample across the molecular weight distribution.

2.3 EXPERIMENTAL

2.3.1 General Methods and Materials

HPLC grade methanol was obtained from Fischer Scientific and distilled from calcium hydride (reagent grade, 95%), which was obtained from Sigma-Aldrich and used as received. 1,12-Dibromododecane (98%) was obtained from Sigma-Aldrich, recrystallized from ethanol (AAPER Alcohol and Chemical Co.) and dried under reduced pressure. N,N,N',N'-tetramethyl-1,6-hexanediamine (99%) was obtained from Sigma-Aldrich and distilled from calcium hydride. Dimethylamine (60% in water, ~11.0 M) was obtained from Fluka and used as received. HPLC-grade tetrahydrofuran (THF), HPLC-grade water, and diethyl ether were obtained from Fischer Scientific and used as received. Sodium acetate (NaOAc) (99.0%), sodium azide (99%), and ACS grade glacial acetic acid (99.7%) were purchased from Alfa Aesar and used as received.

^1H and ^{13}C NMR spectra were recorded on a Varian Inova 400 MHz and Varian Inova 100 MHz instrument, respectively. Chemical shifts are reported in ppm downfield from TMS using the residual protonated solvent as an internal standard (CD_3OD , ^1H 4.87 ppm and ^{13}C 77.0 ppm) (D_2O , ^1H 4.79 ppm). FAB-MS was obtained on a JOEL HX110 dual focusing mass spectrometer, and FTIR data was recorded on a Perkin Elmer

Spectrum One FT-IR Spectrometer with a 1 mW He-Ne laser operating at a wavelength of 633 nm using a Spectrum v5.0.1 software package.

2.3.2 Synthesis of N,N,N',N'-tetramethyl-1,12-dodecanediamine

1,12-Dibromododecane (6.00 g, 18.3 mmol) was dissolved in THF (150 mL) and the solution was cooled to -78 °C. Dimethylamine (60% in water, 327 mL, 3.6 mol) was added to the flask, and the solution was magnetically stirred for 30 min. The solution was allowed to warm to room temperature and stir for an additional 24 h. The reaction solvent was removed with reduced pressure, and the subsequent white residue was dissolved in a 2.0 M NaOH aqueous solution (150 mL). Diethyl ether (150 mL) was added to the flask and the mixture was magnetically stirred for 2 h. The organic layer was collected and concentrated, and a yellow oil was obtained. The crude product was purified via vacuum distillation (100°C and 150 mTorr) from CaH₂ to provide a clear colorless product (yield 2.3 g, 47 %). ¹H NMR (400 MHz, CD₃OD): δ 2.26 (t, 4 H), 2.19 (s, 12 H), 1.45 (q, 4 H), 1.28 (s, 16 H). ¹³C NMR (100 MHz, CD₃OD): δ=123.8, 59.7, 44.3, 29.6, 29.5, 27.5, 27.2. FAB-MS (m/z calculated = 256.48, found = 257.29); FTIR (oil) ν = 2925.1, 2853.2, 2812.8, 2761.1, 1459.2, 1041.9 cm⁻¹.

2.3.3 Preparation of Ammonium 12,6-Ionene

1,12-Dibromododecane (1.02 g, 3.1 mmol) was transferred into a two-necked 50-mL round-bottomed flask, which was equipped with a reflux condenser and septum. Methanol (2.25 g, 70.3 mmol) was added into the flask with a cannula under nitrogen,

and the solution was heated to 80 °C. N,N,N',N'-tetramethyl-1,6-hexanediamine (0.53 g, 3.1 mmol) was transferred into the flask, and additional purging with nitrogen was performed. The reaction was magnetically stirred for 24 h. Upon completion, the methanol was quantitatively removed under reduced pressure at 25 °C to yield the polymer product. ¹H NMR (400 MHz, D₂O): δ 3.31 (m, 8 H), 3.05 (s, 12 H), 1.75 (m, 8 H), 1.31 (m, 20 H). M_n 14,000 – 41,500 g/mol, M_w 19,000 – 49,900 g/mol, PDI 1.31-1.36.

2.3.4 Preparation of Ammonium 12,12-Ionene

The 12,12-ionene was prepared as described above. ¹H NMR (400 MHz, D₂O): δ 3.31 (m, 8 H), 3.05 (s, 12 H), 1.75 (m, 8 H), 1.31 (m, 32 H). M_n 8,000 – 30,700 g/mol, M_w 11,000 – 40,000 g/mol, PDI 1.26 to 1.42.

2.3.5 Aqueous SEC of Ammonium Ionenenes

Aqueous-based SEC-MALLS was used to determine absolute molecular weights in acetate buffer solutions. The mobile phase consisted of 0.540 M sodium acetate in a ternary mixture of 54/23/23 water/methanol/glacial acetic acid v/v/v %. The pH of the resulting solution was 4.0, which was measured using a Thermo Orion 3 Star portable pH meter with a Thermo Orion Triode pH electrode. Sodium azide was added at 200 ppm to the solution as a precaution to prevent bacterial growth in the SEC system. Other compositions that employed different molarities of salt and varying mixtures of water, methanol and acetic acid, are noted in this paper. The mobile phase solutions were vacuum filtered through NALGENE® MF75™ Series Media-Plus Filter Units with a

minimum pore size of 0.200 μm . Samples were analyzed at 0.8 mL/min through 2x Waters Ultrahydrogel linear columns and 1x Waters Ultrahydrogel 250 column, with all columns measuring 7.8 x 300 mm and equilibrated to 30 $^{\circ}\text{C}$. SEC instrumentation consisted of a Waters 1515 isocratic HPLC pump, Waters 717plus Autosampler, Wyatt miniDAWN multiangle laser light scattering (MALLS) detector operating a He-Ne laser at a wavelength of 690 nm, Viscotek 270 capillary viscosity detector, and a Waters 2414 differential refractive index detector operating at a wavelength of 880 nm and 35 $^{\circ}\text{C}$. The only calibration constant, the Wyatt Astra V AUX1, was calculated using a series of aqueous sodium chloride solutions. The accuracy and reproducibility was confirmed with poly(ethylene oxide) and poly(methacrylic acid) sodium salt standards (Polymer Laboratories/Varian Inc.) ranging in molecular weight from 5,000 to 1,000,000 g/mol. Samples were processed using the Wyatt Astra V software package. Weight average molecular weights were determined from light scattering data using the following relationship:

$$\frac{K^* c}{R(\theta)} = \frac{1}{M_w P(\theta)} + 2A_2 c \quad (1)$$

where M_w is the weight average molecular weight, c is the concentration of the polymer, $R(\theta)$ is the measured excess Rayleigh ratio, $P(\theta)$ is the particle scattering function, A_2 is the second virial coefficient of the polymer-solvent system, and K^* is an optical scattering constant, following

$$K^* = \frac{4\pi^2 n_o^2 (dn/dc)^2}{\lambda_o^4 N_A} \quad (2)$$

where dn/dc is the specific refractive index increment, n_o is the refractive index of the solvent, λ_o is the wavelength of the incident laser in a vacuum, and N_A is Avogadro's number.

2.3.6 Determination of Specific Refractive Index Increments (dn/dc)

A Wyatt OptiRex differential/absolute refractive index detector operating at a wavelength of 690 nm and 30 °C was used for all specific refractive index increment measurements. Polymer samples (0.076 – 1.512 mg/mL) were allowed to dissolve in the appropriate solvent overnight. Samples were metered at 0.8 mL/min into the RI detector at 30 °C using a ^{kd}Scientific syringe pump and a syringe affixed with a 0.45 μm PTFE syringe filter. The dn/dc values were determined using the Wyatt Astra V software package.

2.3.7 Dynamic Light Scattering

Dynamic light scattering measurements were performed on a Malvern Zeta Sizer Nano Series Nano-ZS instrument using Dispersion Technology Software (DTS) version 4.20 at a wavelength of 633 nm using a 4.0 mW, solid state He-Ne laser at a scattering angle of 173°. The experiments were performed at a temperature of 25 °C. Polymer samples were prepared at 1 mg/mL and allowed to dissolve in the appropriate solvent overnight. Samples were syringed through 0.45 μm PTFE syringe filters directly into clean cuvettes. Data was observed for the presence or absence of aggregation peaks based on particle diameter size.

2.4 RESULTS AND DISCUSSION

The synthesis of 12,6-ionenes were performed with commercially available monomers. N,N,N',N'-tetramethyl-1,12-dodecanediamine was synthesized according to a modified literature procedure from dimethyl amine and α,ω -dibromododecane.²⁴ The synthesis of aliphatic ammonium ionenes was performed via the Menshutken reaction between the appropriate dihalide and di-tertiary amine in a methanolic solution under reflux for 24 h. Reaction progress was analyzed via *in situ* FTIR spectroscopy and growth of the C-N[⊕] stretch at 920 cm⁻¹ was observed. The polymerization was complete after 20 h, based on the lack of further increase in the C-N[⊕] stretch (data not shown).²⁵ Our research group has shown *in situ* FTIR spectroscopy is a useful technique to monitor reaction progress and determine reaction kinetics.^{26,27} Upon removal of methanol, the resulting polymers formed colorless, transparent, and ductile films.

The structures of ammonium 12,6- and 12,12-ionenes were confirmed via ¹H NMR spectroscopy. Both ionene structures exhibited similar chemical shifts, differing only in their relative peak integrations. A singlet at δ 3.05 ppm corresponded to the methyl groups bonded to quaternized nitrogen atoms (CH₃-N[⊕]). A broad resonance centered at δ 3.31 ppm corresponded to the methylene directly bonded to quaternized nitrogen atoms (-CH₂-N[⊕]). The methylene units beta to the quaternized nitrogen atoms had a broad resonance centered at δ 1.75 ppm (-CH₂CH₂N[⊕]). A broad resonance centered at δ 1.31 ppm corresponded to the methylene spacer units three or more units away from the quaternized nitrogen atoms (-CH₂-CH₂-).

Successful size exclusion chromatography of polyelectrolytes requires the elimination of polymer-polymer and polymer-stationary phase interactions. It is widely

recognized that electrostatic interactions between polymer chains or between the polymer and the stationary phase are effectively eliminated with an increase in ionic strength of the mobile phase.²⁶ Thus, sodium acetate was used in these studies; however, as the ionic strength of the solvent increased, it was presumed that hydrophobic interactions become more prevalent; thus, in order to overcome both polymer-polymer and polymer-stationary phase hydrophobic interactions, methanol was added to the mobile phase and glacial acetic acid was also determined to improve SEC separations. The acetic acid likely functions as both an organic modifier to eliminate hydrophobic interactions, as well as, a proton donor to increase ionic strength of the solvent. An increase in the ionic strength of the solvent is known to shield electrostatic interactions, which reduces the Debye screening length.²⁸ As this occurs, the persistence length of the polymer decreases resulting in random coil conformation of the polymer chain, similar to neutral polymers.²⁹ Random coils are the preferred conformation for reliable SEC since chain-extended conformations fail to sample the available pore volume resulting in non-Gaussian distributions.¹⁷ Decreasing the Debye screening length also helps to eliminate electrostatic interaction between the polyelectrolyte and the stationary phase, which can delay the elution of polyelectrolytes leading to tailing in chromatograms.³⁰ Charge screening also functions to eliminate ion-exclusion effects, which prevent polyelectrolyte chains from sampling smaller pore sizes leading to premature sample elution. The ionic strength that is necessary for reducing these effects depends on the chemo-physical properties of a given polymer/solvent/column system.

Ionic aggregation is generally considered detrimental to successful SEC since larger aggregates may impede instrumentation flow, elute prematurely, and/or skew

measurements of the molecular weight distribution.²⁷ In order to determine if the ionenes were aggregating in solution, dynamic light scattering was first performed in a variety of potential mobile phase compositions. Ammonium 12,12-ionene samples that were dissolved in the mobile phase (54/23/23 v/v/v % water/methanol/glacial acetic acid, 0.54 M NaOAc, pH 4.0) showed insignificant aggregation behavior (Figure 2.2), and this observation suggested that the polymer-solvent composition fulfilled one of the requirements necessary for reliable SEC. Furthermore, when plotted in volume (%) versus diameter size, DLS data indicates the average diameter size was determined to be 12 nm, which is typical for polyelectrolytes in aqueous mobile phases (Figure 2.3). Other solvent compositions consisting of lower amounts of organic co-solvent, lower sodium acetate concentrations, and/or higher pH exhibited notable aggregation; thus, these compositions were eliminated as mobile phases for the SEC of aliphatic ammonium ionenes. As shown in Figure 2.4, a decrease in the amount of methanol and glacial acetic, from 23 to 17 vol. %, resulted in bimodal DLS curves. Also, completely eliminating glacial acetic acid from the mobile phase composition promoted polymer aggregation (Figure 2.5). These mobile phase compositions were not pursued as possible mobile phases for the SEC of ammonium ionenes since they encouraged aggregation.

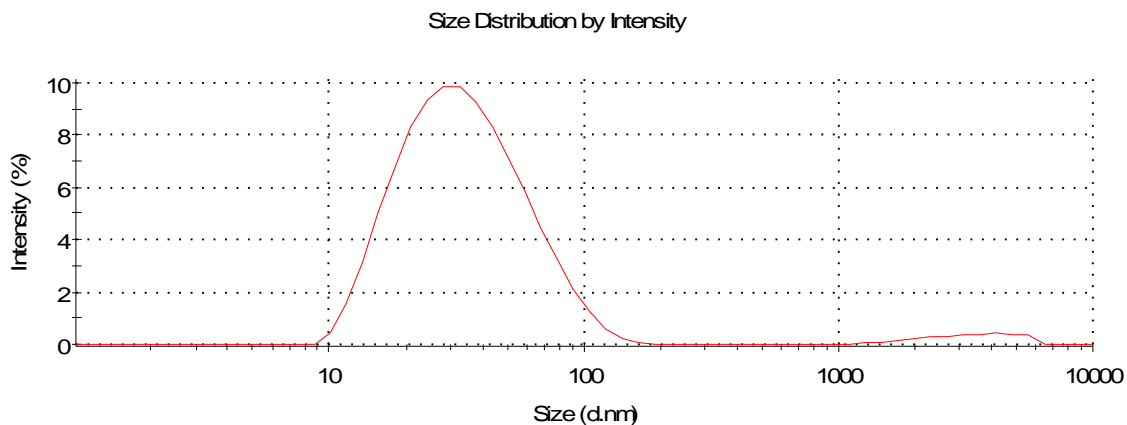


Figure 2.2: DLS analysis of ammonium 12,12-ionene (sample **6**) in 54/23/23 (v/v/v%) water/methanol/glacial acetic acid, 0.54 M NaOAc, pH 4.0.

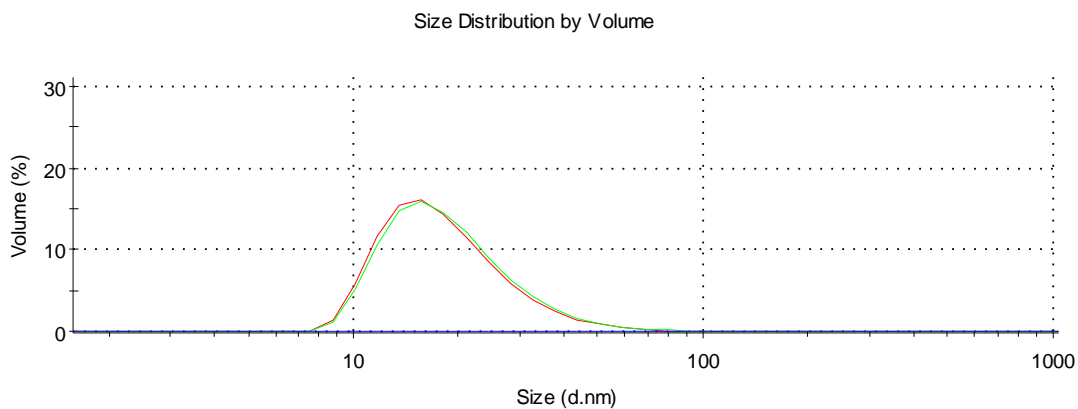


Figure 2.3: DLS analysis of ammonium 12,12-ionene (sample **6**) in 54/23/23 (v/v/v%) water/methanol/glacial acetic acid, 0.54 M NaOAc, pH 4.0. Same scan as Figure 2.2, but volume (%) is shown instead of intensity (%).

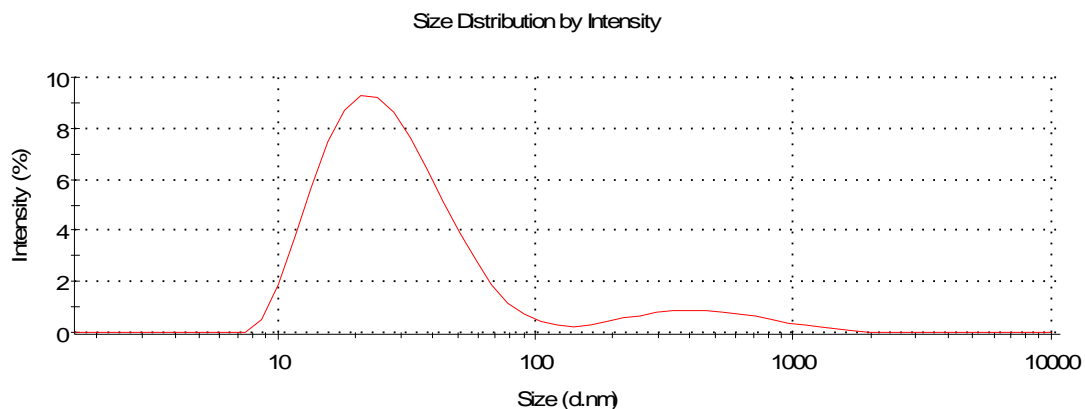


Figure 2.4: DLS analysis of ammonium 12,12-ionene (sample **6**) in 66/17/17 water/methanol/glacial acetic acid (v/v/v %), 0.42 M NaOAc, pH 4.0.

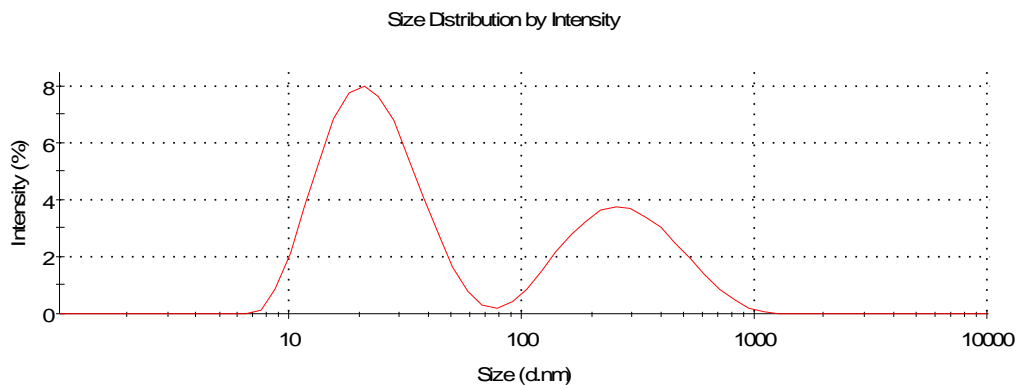


Figure 2.5: DLS plot of ammonium 12,12-ionene (sample **6**) in 80/20 water/methanol (v/v/v %), 0.50 M NaOAc, pH 8.49.

The specific refractive index increment (dn/dc) corresponds to the dependence of the solution's refractive index on solute concentration.¹⁴ The dn/dc of a polymer depends on the chemical composition of solute, solvent used to dissolve the solute, temperature, and wavelength of the incident laser.³¹ Thus, maintaining constant laser wavelength and temperature enables the calculation of dn/dc for each combination of polymer and solvent before successful SEC-MALLS for accurate molecular weight determination. The dn/dc of a polymer is usually considered as a constant in a given solvent; however, the

contribution of end-groups becomes significant at lower molecular weights leading to dissimilar chemical compositions.³² In the SEC-MALLS analysis of neutral polymers, dn/dc values are readily calculated online using 100% mass recovery methods. However, counter-ion dissociation and non-quantitative sample recovery prevent online determination for SEC analysis of polyelectrolytes. Therefore, individual offline batch-mode measurements must be performed to determine accurate dn/dc values. In this study, an off-line determination was performed on the ammonium ionenes to obtain dn/dc values. Various polymer concentrations were prepared ranging from 0.076 mg/mL to 1.512 mg/mL. Differential refractive index data were obtained for each solution and plotted versus concentration using the Wyatt Astra V software package. The slope of the linear fit is the dn/dc of the polymer for this particular solvent. A typical dn/dc plot for an ammonium 12,12-ionene (sample 5) in the mobile phase, 54/23/23 (v/v/v%) water/methanol/glacial acetic acid, 0.54 M NaOAc, pH 4.0, is shown in Figure 2.6. The dn/dc values for ammonium 12,12- and 12,6-ionenes in this mobile phase are shown in Table 2.1.

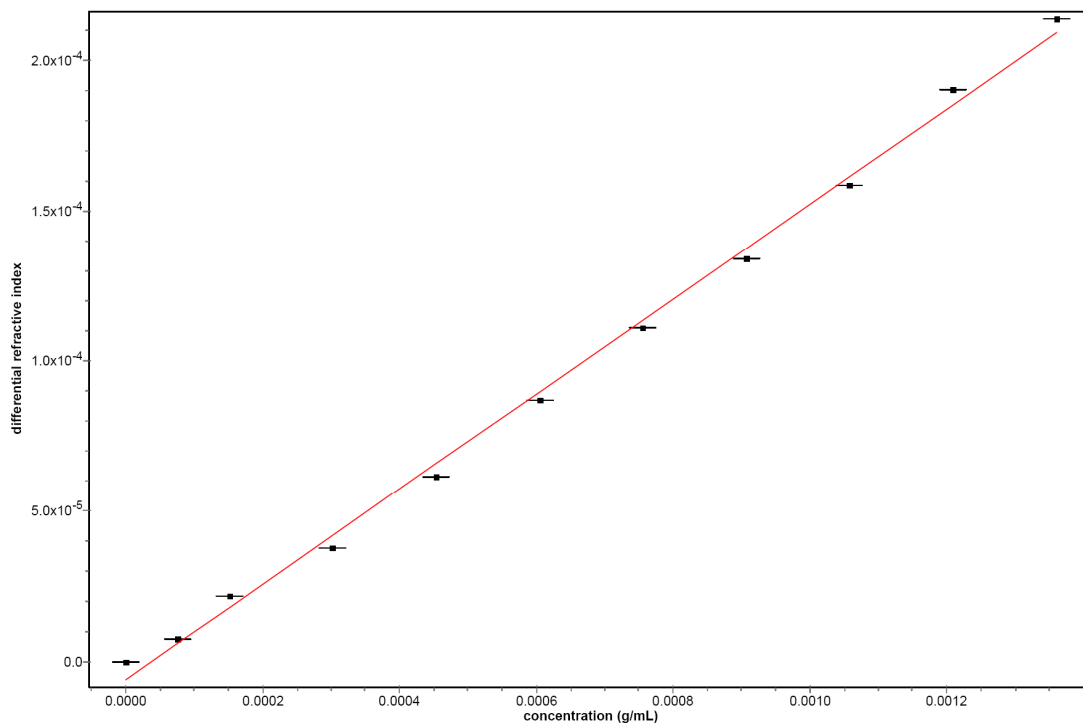


Figure 2.6: Determining dn/dc of ammonium 12,12-ionene in 54/23/23 (v/v/v %) water/methanol/glacial acetic acid, 0.54 M NaOAc, pH 4.0. The dn/dc was determined to be 0.168 mL/g in this example.

Table 2.1: The dn/dc values for aliphatic ammonium ionenes.

	^a dn/dc (mL/g)
Ammonium 12,12-ionene	0.168
Ammonium 12,6-ionene	0.154

^a Each dn/dc was measured using 11 concentrations varying from 0.076 – 1.55 mg/mL in the mobile phase, 54/23/23 (v/v/v%) water/methanol/glacial acetic acid, 0.54 M NaOAc, pH 4.0.

Absolute moments of the molecular weight distribution were determined for ammonium 12,6- and 12,12-ionenes using 54/23/23 (v/v/v%) water/methanol/glacial acetic acid, 0.54 M NaOAc, pH 4.0 and are summarized in Table 2.2. Ammonium 12,12-ionene prepared from various dihalide:diamine monomer stoichiometries had number average molecular weights between 3,500 and 30,700 g/mol and weight average molecular weights between 4,300 and 39,600 g/mol. Ammonium 12,6-ionene prepared

from various dihalide:diamine molar ratios had number average molecular weights between 17,000 and 30,500 g/mol and weight average molecular weights between 22,200 and 43,300 g/mol. As expected for a step-growth polymerization, molecular weights for ammonium ionenes increased as the molar ratios approached 1:1. Molecular weight distributions for all ammonium ionene polymers ranged from 1.27 to 1.42.

Table 2.2: Molecular weight characterization for aliphatic ammonium ionenes.

Sample	Ammonium x,y-Ionene	Monomer Stoichiometry (diamine:dihalide)	^a M _n (g/mol)	^a M _w (g/mol)	^a M _w /M _n
1	12,12	1:1.10	3,500	4,300	1.26
2	12,12	1:1.07	9,700	12,300	1.27
3	12,12	1:1.05	11,600	14,600	1.26
4	12,12	1:1.03	14,000	17,800	1.27
5	12,12	1:1	18,700	24,900	1.33
6	12,12	1:1	20,600	26,000	1.26
7	12,12	1:1	30,700	39,600	1.29
8	12,6	1:1	17,000	22,200	1.31
9	12,6	1:1	30,500	43,300	1.42

^aMolecular weights determined via SEC-MALLS in 54/23/23 (v/v/v%) water/methanol/glacial acetic acid, 0.54 M NaOAc, pH 4.0.

The SEC chromatogram for a typical ammonium 12,12-ionene in the mobile phase (54/23/23 (v/v/v %) water/methanol/glacial acetic acid, 0.54 M NaOAc, pH 4.0) including the RI trace, MALLS trace, and molecular weight as a function of the molecular weight distribution is shown in Figure 2.7. The mono-modal, symmetrical peak in the MALLS and RI chromatograms demonstrated reliable sample separation and provided additional support for the absence of polymer aggregation in solution. Thus, in addition to fulfilling the non-aggregating requirement, this mobile phase successfully reduced polymer-stationary phase interactions, which indicated that the ionic strength of the tested mobile phase was sufficient to discourage any electrostatic interactions that

would otherwise lead to ion interaction or ion exclusion effects. When the organic content of the solvent was decreased, poor SEC separation was observed. In the case of the 12,12-ionene, decreasing the relative amount of methanol and glacial acetic acid, both from 23 to 17 vol. %, resulted in bimodality and tailing in the SEC chromatograms (Figure 2.8). Similar to the 12,12-ionene, SEC-MALLS of the ammonium 12,6-ionene in the same mobile phase also showed mono-modal peaks (Figure 2.9). However, unlike the 12,12-ionene, the asymmetric 12,6-ionene also showed reliable separations in the mobile phase, 66/17/17 (v/v/v%) water/MeOH/AcOH, 0.42 M NaOAc, pH 4.0 solvent composition (Figure 2.10). Although this mobile phase works well for the ammonium 12,6-ionene, the mobile phase, 54/23/23 (v/v/v %) water/methanol/glacial acetic acid, 0.54 M NaOAc, pH 4.0, is more versatile since it provides reliable separations for both of the ionenes tested.

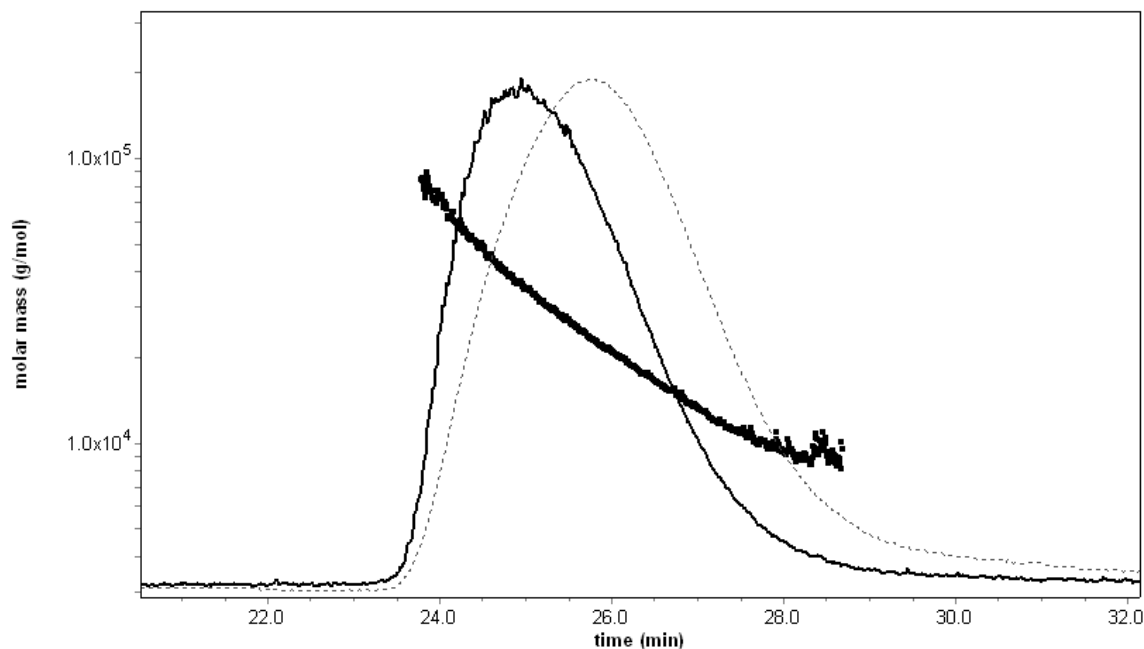


Figure 2.7: SEC chromatogram of ammonium 12,12-ionene (sample 5) showing the RI trace (dotted grey), MALLS trace (solid black), and molecular weight distribution (bold black line) in 54/23/23 (v/v/v %) water/methanol/glacial acetic acid, 0.54 M NaOAc, pH 4.0.

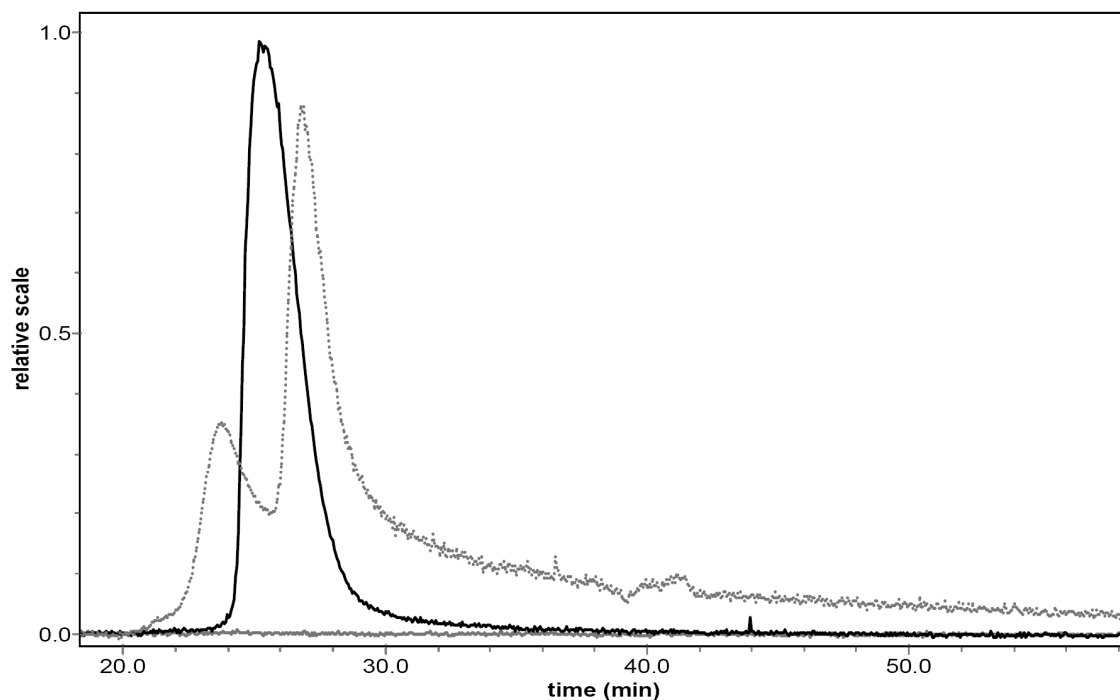


Figure 2.8: SEC chromatogram of ammonium 12,12-ionene (sample **6**) showing the influence of the water/organic solvent ratio and NaOAc molarity on SEC separation. The three ratios were 74/8/18 water/methanol/acetic acid (v/v/v%), 0.57 M NaOAc, pH 4.0 (solid grey), 66/17/17 water/methanol/acetic acid (v/v/v%), 0.42 M NaOAc, pH 4.0 (dotted grey), and 54/23/23 (v/v/v %) water/methanol/glacial acetic acid, 0.54 M NaOAc, pH 4.0 (solid black).

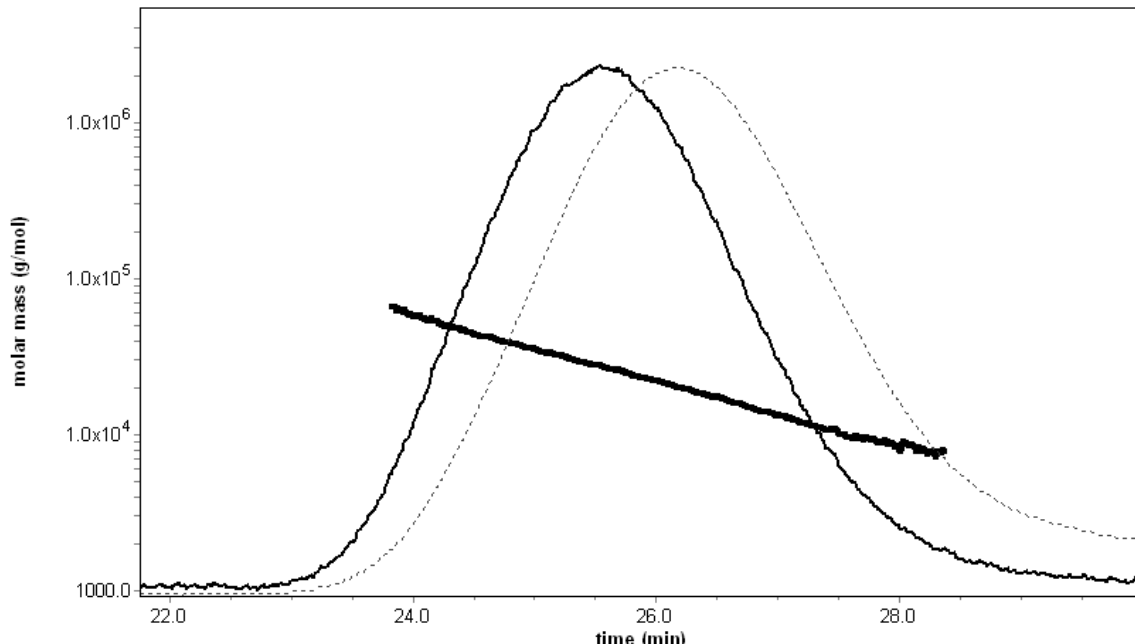


Figure 2.9: SEC chromatogram of ammonium 12,6-ionene (sample **8**) in the mobile phase (54/23/23 (v/v/v %) water/methanol/glacial acetic acid, 0.54 M NaOAc, pH 4.0).

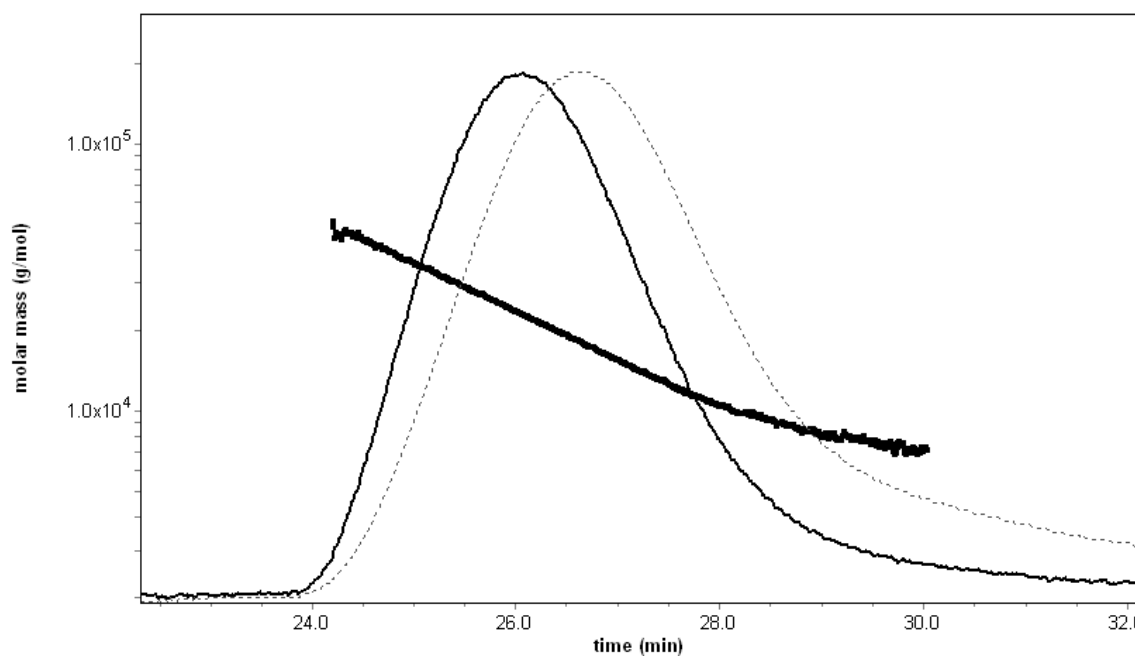


Figure 2.10: SEC chromatogram of ammonium 12,6-ionene (sample **8**) showing the RI trace (dotted grey), MALLS trace (solid black), and molecular weight distribution (bold black line) in 66/17/17 water/MeOH/AcOH (v/v/v %), 0.42 M NaOAc, pH 4.0.

The expected molecular weight distribution for step-growth polymerization is approximately 2.0; however, the molecular weight distributions for ammonium ionenes

ranged from 1.26 to 1.42. Molecular weight distributions less than 2.0 in step-growth polymerizations can occur because of fractionation in the purification process or sample exclusion within the chromatography columns.¹⁴ We can exclude the possibility of fractionation since we solution-cast ionenes directly from the reaction mixture. Furthermore, samples were analyzed a second time using columns with a higher resolution (PL aquagel-OH 30 and PL aquagel-OH 40 measuring 7.5 x 300 mm), and we eliminated the possibility of excluding sample volume from the column pores. Thus, it is presumed that the molecular weight distributions that were determined for aliphatic ammonium ionenes using aqueous size exclusion chromatography were substantial.

Another reason step-growth polymerizations may produce polymers with narrow molecular weight distributions is if the reactivity of monomers is different than the reactivity their polymer chains.³³ Nanda demonstrated that distributions less than 2 are achieved if reactivity decreases with increasing molecular weight.³⁴ We have demonstrated that molecular weight increases throughout the polymerization process from measuring molecular weights of aliquots obtained during a 24 h polymerization of ammonium 12,6-ionene (Figure 2.11), and we are currently studying the reaction kinetics to determine if the reactivity of monomers is greater than that of polymer chains. Wegner has studied the reaction kinetics of aliphatic ammonium ionenes with *in situ* NMR and demonstrated that monomer reactivity varied depending on the stage of polymerization.³⁵ For these reasons, reaction kinetics may be one reason for our narrow molecular weight distributions. On the other hand, while we have demonstrated that our mobile phase composition allows for reliable separations of aliphatic ammonium ionenes to achieve appropriate magnitudes of the molecular weight, this mobile phase composition may not

be best suited for determining molecular weight distributions based on the narrow distributions obtained for our samples. However, determining the magnitude of molecular weight for ionenes allows for fair comparisons of thermal and mechanical properties and other characteristics dependent on molecular weight.

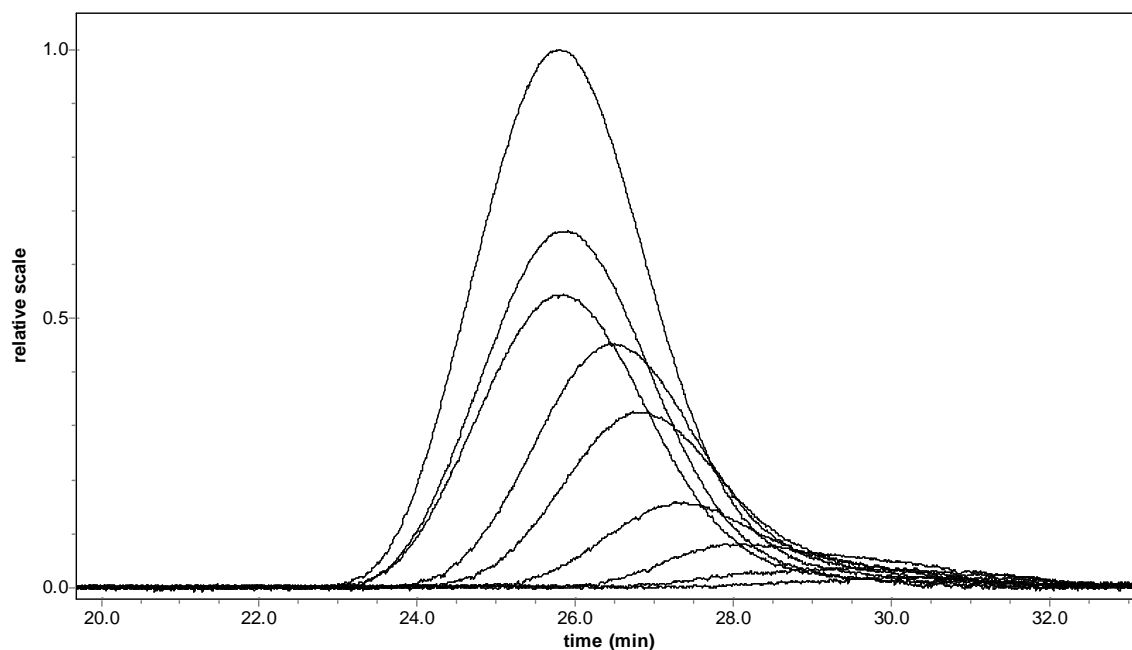


Figure 2.11: SEC chromatograms (MALLS trace) of aliquots obtained during a 24 h polymerization of ammonium 12,6-ionene showing molecular weight increased during the reaction.

The solvent compositions that were employed in previous calibrated SEC-dRI investigations of ammonium ionenes were evaluated.^{19,20} In two prior studies, one mobile phase consisted of 0.020 M NaOAc in water with acetic acid added to adjust the pH to 5.2, and a second mobile phase comprised 20/80 acetonitrile/0.5 M sodium sulfate, 0.5 M acetic acid in water. However, peaks corresponding to polymer were not observed in either the RI or MALLS chromatograms in either of these solvents.

Utilizing an online viscosity detector, the intrinsic viscosity was determined as a function of the molecular weight distribution. When plotted as the logarithm of intrinsic

viscosity as a function of the logarithm of molecular weight, a linear fit to the data yields constants for the well known Mark-Houwink-Sakurada (MHS) relationship, which is given as

$$\log[\eta] = \alpha \log M - \log k \quad (3)$$

where $[\eta]$ is the intrinsic viscosity, and α and k are constants, which depend on the polymer and solvent used at a given temperature.³⁶ The MHS alpha parameter provides information about the solvent quality or chain stiffness for a polymer in solution. Typically, alpha values around 0.50 indicate theta solvent conditions whereas values around 0.80 indicate good solvent conditions.³⁰ Data obtained for both the 12,12- and 12,6-ionenes fit well to the linear MHS relationship. As shown in Figure 2.12, the MHS plot for the ammonium 12,12-ionene (sample **5**) in the mobile phase (54/23/23 (v/v/v %) water/methanol/glacial acetic acid, 0.54 M NaOAc, pH 4.0) at 30 °C yielded an alpha parameter of 0.63 and a k value of 5.3×10^{-4} dL/g. As shown in Figure 2.13, the MHS plots for the ammonium 12,6-ionene (sample **8**) in the same mobile phase at 30 °C yielded an alpha value of 0.75 and a k value of 1.6×10^{-4} dL/g. The higher alpha parameter of 0.75 for the 12,6-ionene suggested that the mobile phase is a better solvent for this sample than for the 12,12-ionene which had an alpha value of 0.63.

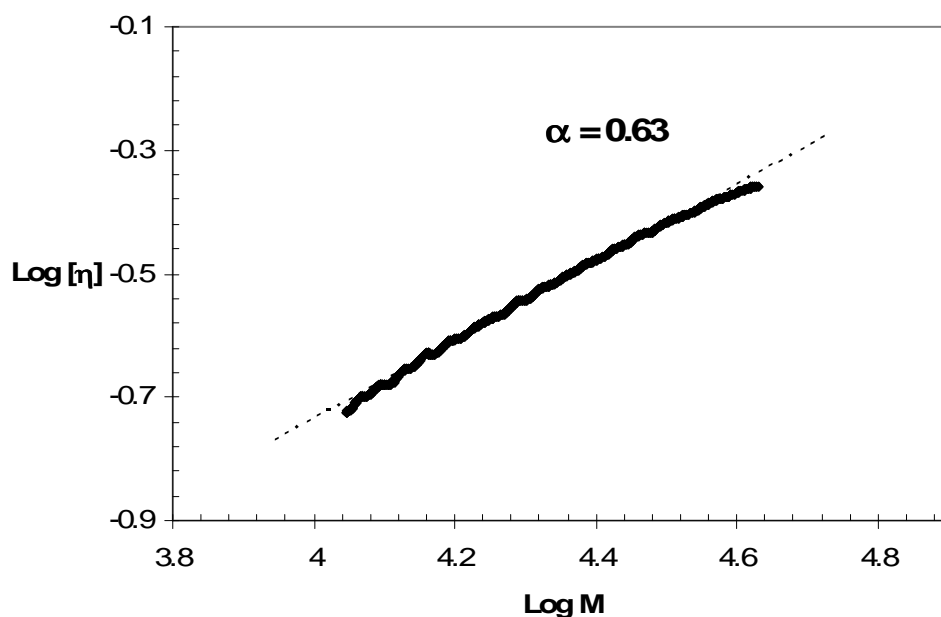


Figure 2.12: MHS plot for the ammonium 12,12-ionene (sample 5) in the mobile phase, 54/23/23 (v/v/v%) water/methanol/glacial acetic acid, 0.54 M NaOAc, pH 4.0. Measured intrinsic viscosities (black diamonds) were fitted with the logarithmic MHS relationship (dotted line).

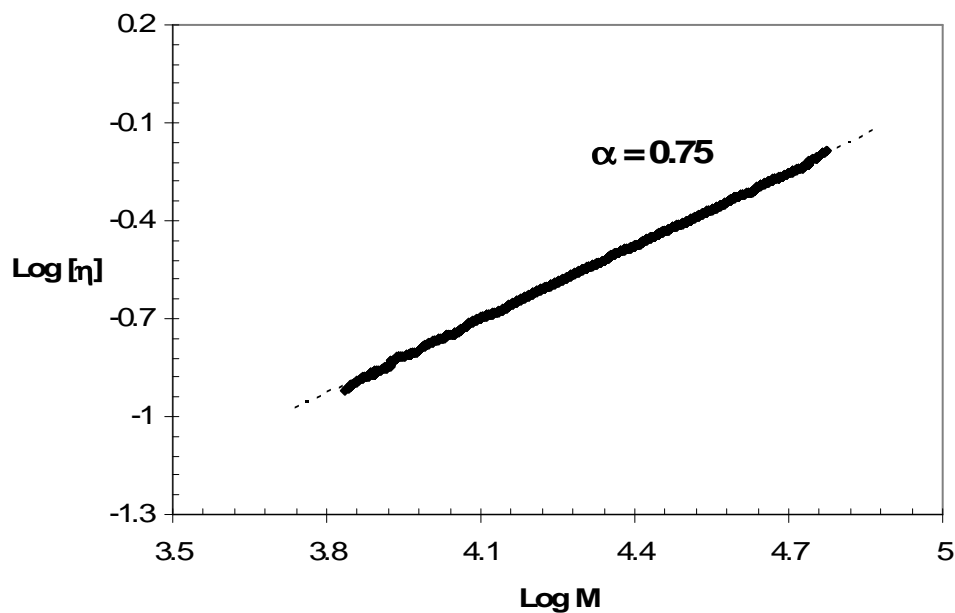


Figure 2.13: MHS plot for the ammonium 12,6-ionene (sample 8) in the mobile phase, 54/23/23 (v/v/v%) water/methanol/glacial acetic acid, 0.54 M NaOAc, pH 4.0. Measured

intrinsic viscosities (black diamonds) were fitted with the logarithmic MHS relationship (dotted line).

2.5 CONCLUSIONS

Absolute molecular weight characterization of aliphatic ammonium ionenes was successfully accomplished using aqueous-based SEC-MALLS. A suitable mobile phase composition of 54/23/23 (v/v/v%) water/methanol/acetic acid and 0.54 *M* NaOAc at pH 4.0 was developed to reduce polymer-polymer and polymer-stationary phase interactions. Using this mobile phase composition, reliable separations were obtained and accurate measurements of molecular weight were achieved. Ammonium 12,6-ionene had number average molecular weights ranging from 17,000 – 30,500 g/mol and weight average molecular weights ranging from 22,200 g/mol – 43,300 g/mol with molecular weight distributions ranging from 1.31 – 1.42. Ammonium 12,12-ionene had number average molecular weights ranging from 3,500 – 30,700 g/mol and weight average molecular weights ranging from 4,300 – 39,600 g/mol with molecular weight distributions ranging from 1.26 – 1.33.

Molecular weight distributions less than 2.0 for step-growth polymerization are unusual; however, in our opinion, the distributions determined in our mobile phase composition using aqueous SEC are substantial. We have eliminated the possibilities of fractionation during purification and pore volume exclusion in the column, and we are currently investigating the reaction kinetics of aliphatic ammonium ionene polymerizations. Aqueous SEC provided reliable separations of aliphatic ammonium ionenes, which allowed for accurate measurements of molecular weight; however, this

mobile phase may not be best suited for determining molecular weight distribution of aliphatic ammonium ionenes

Additionally, intrinsic viscosity data was collected for ammonium 12,12- and 12,6-ionenes as a function of molecular weight distribution to determine MHS parameters.

2.6 ACKNOWLEDGMENTS

This material is based upon work supported in part by the U.S. Army Research Laboratory and the U.S. Army Research Office under grant number DAAD19-02-1-0275 Macromolecular Architecture for Performance (MAP) MURI. Additionally, the authors acknowledge the generous support of Kimberly-Clark Corporation for funding.

2.7 REFERENCES

¹ C. F. Gibbs, E. R. Littman, C. S. Marvel, Quaternary Ammonium Salts from Halogenated Alkyl Dimethylamines. II. The Polymerization of Gamma-Halogenopropyl dimethylamines, *J. Am. Chem. Soc.*, **1933**, 753-757.

² M.R. Lehman, C.D. Thompson and C.S. Marvel, Quaternary Ammonium Salts from Halogenated Alkyl Dimethylamines. III. Omega-Bromo-Heptyl-, -Octyl-, -Nonyl-, and -Decyl-dimethylamines. *J. Am. Chem. Soc.*, **1935**, 57, 1137-1139.

³ C.F. Gibbs and C.S. Marvel, Quaternary Ammonium Salts from Bromopropyl dialkylamines. IV. Formation of Four-Membered Rings.

⁴ C.F. Gibbs and C.S. Marvel, Quaternary Ammonium Salts from Bromopropyl dialkylamines. V. Conversion of Cyclic Ammonium Salts to Linear Polymers.

⁵ H. Noguchi and A. Rembaum, Reactions of N,N,N',N'-Tetramethyl- α,ω -diaminoalkanes with α,ω -Dihaloalkanes. I. 1-y Reactions. *Macromolecules*, **1972**, 5 (3), 253-260.

⁶ H. Noguchi and A. Rembaum, Reactions of N,N,N',N'-Tetramethyl- α,ω -diaminoalkanes with α,ω -Dihaloalkanes. II. 1-y Reactions. *Macromolecules*, **1972**, 5 (3), 261-269.

-
- ⁷ Punyani, S., Singh, H., Preparation of Iodine Containing Quaternary Amine Methacrylate Copolymers and Their Contact Killing Antimicrobial Properties. *J. Appl. Polym. Sci.*, **2006**, *102*, 1038-1044.
- ⁸ Kourai, H., Yabuhara, T., Shirai, A., Maeda, T., Nagamune, H. Syntheses and antimicrobial activities of a series of new bis-quaternary ammonium compounds. *Eur. J. Medicinal Chem.*, **2006**, *41*, 437-444.
- ⁹ Zelinkin, A. N., Putnam, D., Shastri, P., Langer, R., Izumrudov, V. A., Aliphatic Ionenes as Gene Delivery Agents: Elucidation of Structure-Function Relationship through Modification of Charge Density and Polymer Length. *Bioconjugate Chem.*, **2002**, *13*, 548-553.
- ¹⁰ Rembaum, A. Ionene polymers for selectively inhibiting the vitro growth of malignant cells. US Patent 4,013,507 **1977**; *SciFinder Scholar* AN 1977:416039 (accessed 4/11/07).
- ¹¹ T. Narita, R. Ohtakeyama, M. Nishino, J.P. Gong, Y. Osada, Effects of charge density and hydrophobicity of ionene polymer on cell binding and viability. *Colloid Polym. Sci.*, **2000**, *278*, 884-887.
- ¹² M.R. Lehman, C.D. Thompson and C.S. Marvel, Quaternary Ammonium Salts from Hologenated Alkyl Dimethylamines. III. Omega-Bromo-Heptyl-, -Octyl-, -Nonyl-, and -Decyl-dimethylamines. *J. Am. Chem. Soc.*, **1935**, *57*, 1137-1139.
- ¹³ Casson, D., and Rembaum, A. Solution Properties of Novel Polyelectrolytes. *Macromolecules*, **1971**, *5* (1), 75-81.
- ¹⁴ Wu, C. Handbook of Size Exclusion Chromatography; Marcel Dekker: New York, 1995.
- ¹⁵ Garcia, R., Porcar, I., Campos, A., Soria, V., Figueruelo, J. E. Solution Properties of Polyelectrolytes. VII. A comparative study of the elution behavior on two organic-based packings. *J. Chromatogr. A*, **1993**, *655* (2), 191-198.
- ¹⁶ Barth, H. G., Boyes, B. E., Jackson, C. Size Exclusion Chromatography, *Anal. Chem.*, **1996**, *68*, 445R-466R.
- ¹⁷ Wittgren, B.; Welinder, A.; Porsch B. Molar mass characterization of cationic methacrylate ethyl acrylate copolymers using size-exclusion chromatography with online multi-angle light scattering and refractometric detection. *J. Chromatogr. A* 2003, *1002*:101Y109.
- ¹⁸ Jiang, X.; van der Horst, A.; van Steenberg, M.J.; Akeroyd, N.; van Nostrum, C.F.; Schoenmakers, P.J.; Hennink, W.E. Molar-Mass Characterization of Cationic Polymers for Gene Delivery by Aqueous Size-Exclusion Chromatography. *Pharmaceutical Research*, **2006**, *23*(3), 595-603.
- ¹⁹ Kopecká, K., Tesařová, E., Pirogov, A., Gaš, B. Ionenes acting as pseudostationary phases in capillary electrokinetic chromatography. *J. Sep. Sci.*, **2002**, *25*, 1027-1034.
- ²⁰ Reisinger, T., Meyer, W.H., Wegner, G., Haase, T., Schultes, K., Wolf, B.A. Influence of chain length on the molecular dynamics of an aliphatic ionene. *Acta Polym.*, **1998**, *49*, 710-714.
- ²¹ Mather, B. D., Baker, M. B., Beyer, F. L., Green, M. D., Berg, M. A. G., Long, T. E., Multiple Hydrogen Bonding for the Noncovalent Attachment of Ionic Functionality in Triblock Copolymers. *Macromolecules*, **2007**, *40*, 4396-4398.

-
- ²² McKee, M. G., Hunley, M. T., Layman, J. M., Long, T. E. Solution Rheological Behavior and Electrospinning of Cationic Polyelectrolytes. *Macromolecules*, **2006**, *39*, 575-583.
- ²³ Kang, H., Lin, Q., Armentrout, R. S., Long, T. E. Synthesis and Characterization of Telechelic Poly(ethylene terephthalate) Sodiosulfonate Ionomers, *Macromolecules*, **2002**, *35*, 8738-8744.
- ²⁴ T. A. Spencer, T. J. Onofrey, O. Reginald, S. J. Russel, L. E. Lee, D. E. Blanchard, A. Castro, P. Gu, G. Jiang, I. Shechter, Zwitterionic Sulfobetaine Inhibitors of Squalene Synthesis, *J. Org. Chem.*, **1999**, *64* (3), 818.
- ²⁵ Colthup, N. B., Daly, L. H., Wiberley, S. E. *Introduction to Infrared and Raman Spectroscopy*, 3rd Ed.; Academic Press: New York, **1975** (page 344).
- ²⁶ Lizotte, J., Long, T. E., Stable Free Radical Kinetics of Alkyl Acrylate Monomers Using in situ FTIR Spectroscopy: Influence of Hydroxyl Containing Monomers and Additives, *Macromol. Chem. Phys.*, **2004**, *205*, 692-698.
- ²⁷ Pasquale, A. J., Allen, R. D., Long, T. E. Fundamental Investigations of the Free Radical Copolymerization and Terpolymerization of Maleic Anhydride, Norbornene, and Norbornene-tert-Butyl Ester: In-Situ Mid-Infrared Spectroscopic Analysis, *Macromol.*, **2001**, *34*, 8064-8071.
- ²⁸ Garcia, R., Porcar, I., Campos, A., Soria, V., Figueruelo, J. E., X. Influence of ionic strength on the electrostatic secondary effects in size-exclusion chromatography, *J. Chromatogr. A*, **1994**, *662*, 61-69.
- ²⁹ Mourey, T., Le, K., Bryan, T., Zheng, S., Bennett, G., Determining persistence length by size-exclusion chromatography. *Polymer*, **2005**, *46*, 9033-9042.
- ³⁰ Barth, H. Characterization of water-soluble polymers using size-exclusion chromatography, *Advances in Chemistry Series*, **1986**, 31-55.
- ³¹ Coto, B., Escola, J. M., Suarez, I., Caballero, M. J., Determination of dn/dc values for ethylene-propylene copolymers. *Polymer Testing*, **2007**, *26*, 568-575.
- ³² Grinshpun, V., Rudin, A., A New Method for Determining Molecular Weight Distributions of Copolymers. *J. Appl. Polym. Sci.* **1986**, *32*, 4303-4311.
- ³³ Gupta, S. K., Kumar, A., Bhargava, A. Molecular weight distribution and moments for condensation polymerization of monomers having reactivity different from their homologues. *Polymer*, **1979**, *20*, 305-310.
- ³⁴ Nanda, V. S., Jain, S. C. Effect of variation of the biomolecular rate constant with chain length on the statistical character of condensation polymers. *The Journal of Chemical Physics*, **1968**, *49*(3), 1318-1320.
- ³⁵ Wang, J., Meyer, W. H., Wegner, G. On the polymerization of N,N,N',N'-tetramethyl- α,ω -alkanediamines with dibromoalkanes – an *in-situ* NMR study. *Macromolecular Chemistry and Physics*, **1994**, *195*, 1777-1795.
- ³⁶ Brandrup, J., Immergut, E. H. *Polymer Handbook*, 4th ed., Wiley-Interscience: New York, 1989.

Chapter 3

INFLUENCE OF STRUCTURAL SYMMETRY AND CHARGE DENSITY ON THE THERMAL AND MECHANICAL PROPERTIES OF ALIPHATIC AMMONIUM 6,6-, 12,6- AND 12,12-IONENES

Erika M. Borgerding, Sharlene R. Williams, John M. Layman, and Timothy E. Long*

Department of Chemistry, Macromolecules and Interfaces Institute, Virginia Polytechnic Institute and State University, Blacksburg, Virginia 24061

3.1 ABSTRACT

The thermal and mechanical properties of ammonium 6,6-, 12,6- and 12,12-ionenes were investigated as a function of charge density and structural symmetry. Number average molecular weights between 14,600 and 19,200 g/mol with weight averages between 20,300 and 23,000 g/mol were investigated and compared to ionenes with number average molecular weights between 25,300 and 30,700 g/mol and weight average molecular weights between 39,300 and 43,300 g/mol. Structural symmetry enhanced the ability of ionenes to crystallize, as observed with differential scanning calorimetry and optical microscopy. The crystallinity reduced chain mobility and increased the onset of degradation temperature as observed with thermal gravimetric analysis (TGA). Ammonium 6,6-ionene crystallized readily at room temperature, and 12,12-ionene showed a small crystallization peak in the DSC trace when the cooling rate was slow, but ammonium 12,6-ionene did not crystallize. Dynamic mechanical analysis (DMA) indicated three transitions occur for ammonium 12,6- and 12,12-ionenes, which were attributed to glass transition temperature (T_g), motions of ionic groups, and mobility of methylene chains. Increasing molecular weight positively influenced tensile properties

of ammonium ionenes, and ammonium 12,12-ionene had higher tensile strengths at yield and break than ammonium 12,6-ionene.

Keywords: ammonium ionene, charge density, structural symmetry, mechanical properties, thermal properties

3.2 INTRODUCTION

Ammonium polyionenes are macromolecules with quaternary ammonium groups in the backbone of the chain as opposed to pendant side chains. Ionenes are commonly referred to using the nomenclature x,y-ionene, where x refers to the number of methylene spacer units in the dihaloalkane and y refers to the number of methylene spacer units in the di-tertiary amine (Figure 3.1). Although ammonium ionenes have been of synthetic interest since the early 1930s^{1,2,3,4,5,6} and investigated for biomedical applications as antimicrobials⁷ and gene transfection agents,⁸ less attention has been paid to the thermal and mechanical properties of these polymers. One reason for this slowed progress is that molecular weight determination, a critical parameter for the thermal and mechanical characterization of polymers, is difficult to perform on ammonium ionenes due to the problems associated with using aqueous size exclusion chromatography (SEC) to establish molecular weights of polycations.^{9,10} However, our research group recently determined a suitable aqueous SEC-MALLS mobile phase composition that allowed for reliable separation of ammonium ionenes,¹¹ which has provided a metric for comparing thermal and mechanical properties of ammonium 12,6- and 12,12-ionenes using absolute molecular weight characterization. We have shown that increasing molecular weight positively influences the thermal and mechanical properties of ammonium 12,12-

ionene,¹² and we were interested in comparing thermal and mechanical properties of ionenes with the same molecular weights with varying charge densities and structural symmetries.

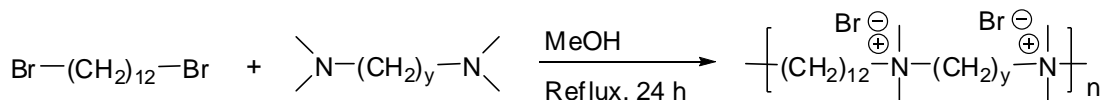


Figure 3.1: Synthesis of aliphatic 12,y-ionenes.

Aliphatic ammonium ionenes have been previously characterized via torsional braid analysis (TBA) and wide angle x-ray scattering (WAXS). Tanaka analyzed several x,y-ionenes using TBA and determined that aliphatic ammonium ionenes exhibit three mechanical relaxations, which were attributed to glass transition temperature (T_g, T_α), ionic portions of the polymer (T_β), and motions of the methylene groups (T_γ).¹³ WAXS analysis indicated that ionenes with higher charge densities possessed higher crystallinities than ionenes with lower charge densities.¹³ Furthermore, Tanaka investigated the effects of hygroscopicity and counter anion selection on mechanical relaxations.¹⁴ It was determined that both larger counterions and water uptake caused a decrease in T_α and T_β relaxations, but had little effect on the T_γ relaxation. Similar TBA and WAXS results were found for oxyethylene ionenes.¹⁵

While performing TBA and WAXS experiments provided valuable information on aliphatic ammonium ionenes, we were also interested in investigating other thermal and mechanical properties. Strong tensile properties have been reported for other ammonium ionene systems, such as PTMO-based ammonium ionenes,¹⁶ but have yet to be determined for aliphatic ammonium ionenes. Furthermore, dynamic mechanical analysis (DMA), differential scanning calorimetry (DSC), and thermal gravimetric analysis (TGA) have not been performed on ammonium 12,6- and 12,12-ionenes.

Herein, we report on a series of well-defined ammonium 6,6-, 12,6- and 12,12-ionenes used to probe the influence of structural symmetry and charge density on thermal and mechanical properties. Ionenes with number average molecular weights of 15,000 g/mol and 30,000 g/mol with weight average molecular weights of 20,000 g/mol and 40,000 g/mol, respectively, were examined. In this study, ionenes are referred to as x,y-MW; for example, 12,6-20k refers to ammonium 12,6-ionene with a weight average molecular weight of 20,000 g/mol. DMA, TGA, DSC, SEC, and tensile properties were determined.

3.3 EXPERIMENTAL

3.3.1 General Methods and Materials

HPLC grade methanol was obtained from Fischer Scientific and distilled from calcium hydride (reagent grade, 95%), which was obtained from Sigma-Aldrich chemical company and used as received. 1,12-Dibromododecane (98%) was obtained from Sigma-Aldrich chemical company and recrystallized from 200 proof ethyl alcohol (AAPER Alcohol and Chemical Co.) and dried under reduced pressure. N,N,N',N'-tetramethyl-1,6-hexanediamine (99%) was obtained from Sigma-Aldrich chemical company and distilled from calcium hydride. Dimethylamine (60% in water, ~11.0 M) was obtained from Fluka and used as received. HPLC grade tetrahydrofuran (THF), HPLC grade water, and diethyl ether were obtained from Fischer Scientific and used as received. Sodium acetate (NaOAc) (99.0%), sodium azide (99%), and ACS grade glacial acetic acid (99.7%) were purchased from Alfa Aesar chemical company and used as received.

N,N,N',N'-tetramethyl-1,12-dodecanediamine was prepared from a modified literature procedure as discussed in our previous work.¹¹

Dynamic mechanical analysis (DMA) was performed on a DMA Q800 instrument in tension mode at 3°C/min and 1 Hz. Tensile testing was performed on an Instron Model 1123 Universal Testing system using mini dog-bone-shaped samples cut using a bench-top die (2.91 mm x 10 mm) from cast films and a Bluehill software package. Samples were dried at 100 °C for 24 h and, subsequently, kept in a dessicator until testing was begun. Four repetitions per polymer sample were completed, and films were deformed until failure at a cross-head speed of 10 mm/min at ambient conditions. Differential scanning calorimetry (DSC) was performed using a Q1000 instrument with a heating rate of 10°C/min under a nitrogen flow of 50 ml/min. A Thermal Gravimetric Analysis (TGA) 2950 was used with a heating rate of 10°C/min from 25°C to 600°C, under nitrogen. Samples were dried at 100 °C for 24 h prior to testing. *In situ* FTIR analysis was performed per a Metler Toledo ReactIR 4000 instrument with a stainless steel ATR probe. An average absorbance was plotted every 5 min from 126 infrared scans for 24 h.

Aqueous size exclusion chromatography (SEC) was performed according to a procedure recently developed in our research group¹¹ using a mobile phase composition comprising a ternary mixture of 54/23/23 (v/v/v%) water/methanol/glacial acetic acid, 0.54 M NaOAc, pH 4.0. The mobile phase solutions were vacuum filtered through NALGENE® MF75™ Series Media-Plus Filter Units with a minimum pore size of 0.200 µm. Samples were analyzed at 0.8 mL/min through 2x Waters Ultrahydrogel linear columns and 1x Waters Ultrahydrogel 250 column, with all columns measuring 7.8 x 300

mm and equilibrated to 30 °C. SEC instrumentation consisted of a Waters 1515 isocratic HPLC pump, Waters 717plus Autosampler, Wyatt miniDAWN multiangle laser light scattering (MALLS) detector operating a He-Ne laser at a wavelength of 690 nm, Viscotek 270 capillary viscosity detector, and a Waters 2414 differential refractive index detector operating at a wavelength of 880 nm and 35 °C.

3.3.2 Preparation of Ammonium 12,6-Ionene

1,12-Dibromododecane (2.988 g, 9.1 mmol) was transferred into a two-necked 50-mL round bottom flask, which was equipped with a septum and a condenser, and heated to 80 °C. Methanol (4.55 g) and N,N,N',N'-tetramethyl-1,6-hexanediamine (1.56 g, 9.1 mmol) were transferred into the flask, which was purged with nitrogen. The reaction was magnetically stirred for 24 h. Upon completion, films were cast from a methanol solution.

3.3.3 Preparation of Ammonium 6,6-Ionene

Ammonium 6,6-ionene was prepared from the above procedure using 1,6-dibromohexane.

3.3.4 Preparation of Ammonium 12,12-Ionene

Ammonium 12,12-ionene was prepared from the above procedure using N,N,N',N'-tetramethyl-1,12-dodecanediamine.

3.3.5 Preparation of Ionene Films

Methanol (5 mL) was added to the reaction product to reduce the viscosity of the polymer. The ionene was poured into Teflon molds (30 mm x 25 mm) to yield 0.5 g films, which were dried in the hood with minimal air flow for 48-72 h. The films were placed on a hot plate at 70°C for 48 h. Films were dried under reduced pressure at room temperature for 24 hours and, subsequently dried at 100°C for 24 h. Films were kept in a dessicator until testing began.

3.4 RESULTS AND DISCUSSION

3.4.1 Synthesis and Molecular Weight Determination

Tailoring polymer characteristics through judicious monomer selection is a cornerstone for studying aliphatic ammonium ionenes. The ability to easily control charge density and counter ion through monomer selection provides a systematic method for studying ammonium ionenes. Ammonium ionenes were synthesized via a Menshutkin reaction between a dihaloalkane and a di-tertiary amine in a methanolic solution for 24 h at 80 °C, as described previously.¹¹ Absolute molecular weights were determined using aqueous size exclusion chromatography and samples with weight average molecular weights of 20,000 and 40,000 were chosen for comparison (Table 3.1).

Our interest in ammonium 6,6-, 12,6- and 12,12-ionenes allowed us to determine the effects that both structural symmetry and charge density have on thermal and mechanical properties. Ammonium 12,12- and 6,6-ionenes are structurally symmetric since the same number of methylene groups are present on each side of the quaternized nitrogen atom; furthermore, ammonium 6,6-ionene has a charge density twice that of

ammonium 12,12-ionene, which influences both the ordering of polymer chains and properties of the ionene. Ammonium 12,6-ionene has asymmetric structural composition since the number of methylene groups on each side of the quaternized nitrogen atom is different, thus, making it a good model to compare to the symmetrical ionenes.

Table 3.1: Molecular weights and distributions of aliphatic ammonium ionenes as determined using aqueous SEC-MALLS.

	M_n (g/mol)	M_w (g/mol)	M_w/M_n
6,6-20k	19,200	23,000	1.20
12,6-20k	16,300	20,300	1.25
12,12-20k	14,600	20,700	1.42
6,6-40k	25,300	39,300	1.55
12,6-40k	30,500	43,300	1.42
12,12-40k	30,700	40,000	1.29

The reaction of ammonium 12,6-ionene was followed with *in situ* FTIR spectroscopy to monitor absorbance at the wavenumber 903 cm^{-1} , which corresponds to the formation of the C-N^{\oplus} bond (Figure 3.2).¹⁷ The reaction of ammonium 12,6-ionene proceeds for 20 h in a 30 wt% solids methanol solution (Figure 3.3). Second order kinetics were previously observed for the polymerization of aliphatic ammonium ionenes.¹⁸ Ammonium 12,12-ionene showed identical behavior when monitored using *in situ* FTIR spectroscopy (data not shown).

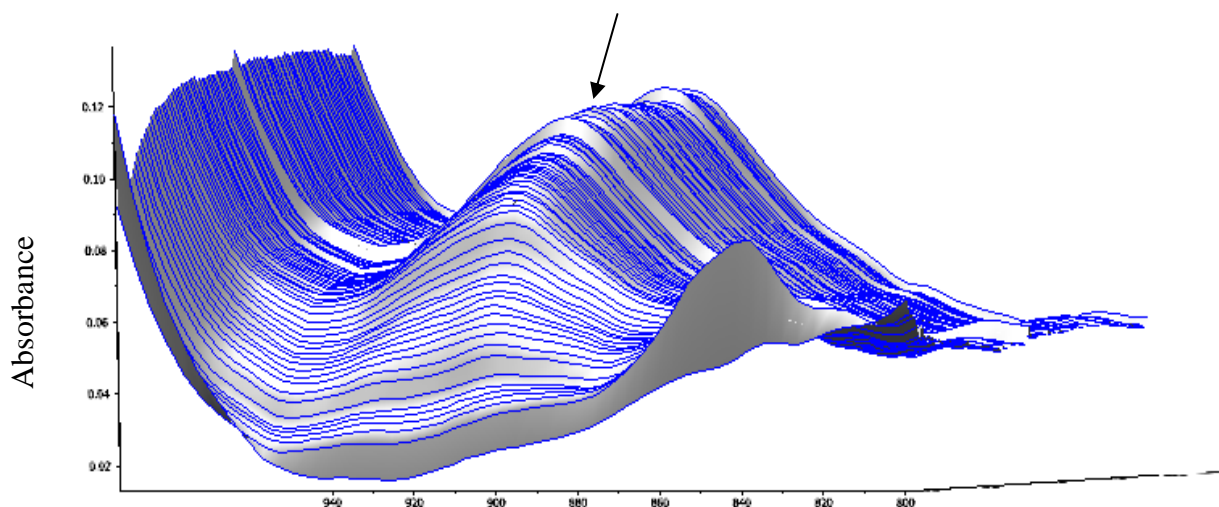


Figure 3.2: *In situ* FTIR spectroscopy of ammonium 12,6-ionene indicated the growth of the C-N[⊕] stretch (arrow points to peak).

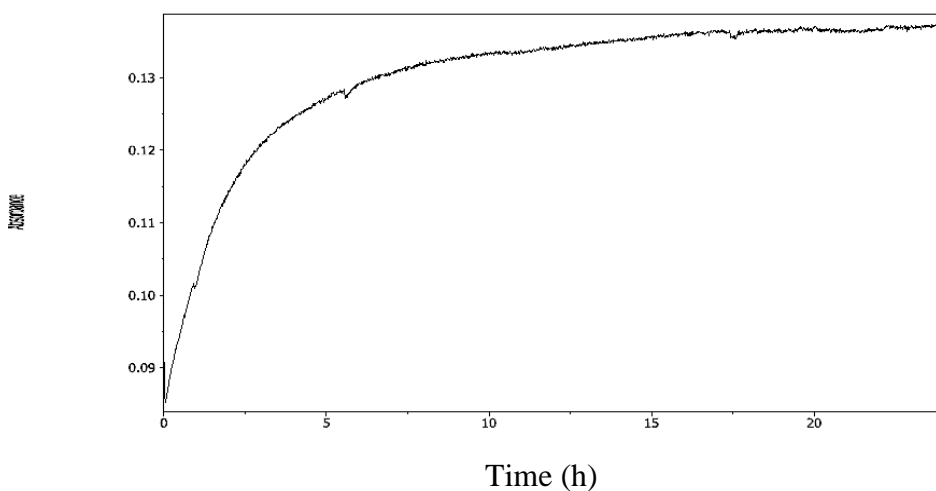


Figure 3.3: Reaction profile at 903 cm⁻¹ for ammonium 12,6-ionene.

3.4.2 Mechanical Properties

Dynamic mechanical analysis (DMA) was performed on ammonium 12,6- and 12,12-ionenes to determine the influence of temperature on storage modulus. Ammonium 6,6-ionene was not tested since it did not form uniform films due to a highly ordered crystalline structure (Figure 3.4). Three mechanical relaxations occurred for

each ionene as seen in the $\tan \delta$ plot (Figure 3.5), similar to the results Tanaka observed using TBA.¹³ The first thermal transition was attributed to the glass transition temperature of the polymer, which occurred at 63 °C and 66 °C for 12,6-20k and 12,6-40k, respectively, and at 56 °C and 44 °C for 12,12-20k and 12,12-40k, respectively (Figure 3.6). Ammonium ionenes are hygroscopic and water uptake from the atmosphere readily causes plasticization, thus, lowering the T_g .¹⁹ Therefore, comparison of the first DMA transition to that of the T_g calculated from DSC results, where ionenes were dried under reduced pressure at 100 °C for 4 days prior to testing, indicated that water uptake occurred during sample preparation for DMA (Table 3.2).

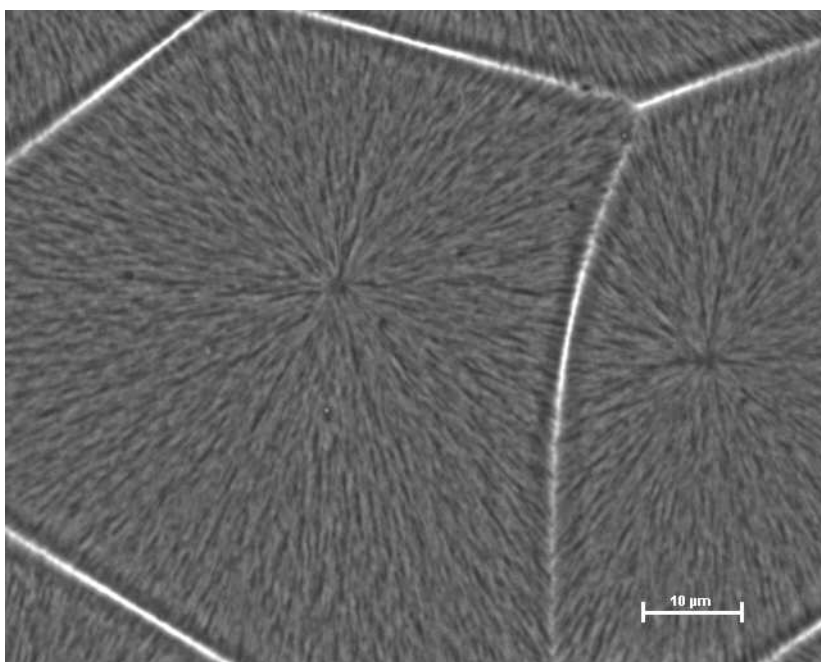


Figure 3.4: Crystallization of ammonium 6,6-ionene at 10x magnification under an optical microscope. The sample was prepared from a methanol solution and pipetted onto a glass slide. The methanol was allowed to evaporate under ambient conditions for 1 h, and the resultant polymer was imaged under an optical microscope. M_n 19,200 g/mol, M_w 23,000 g/mol.

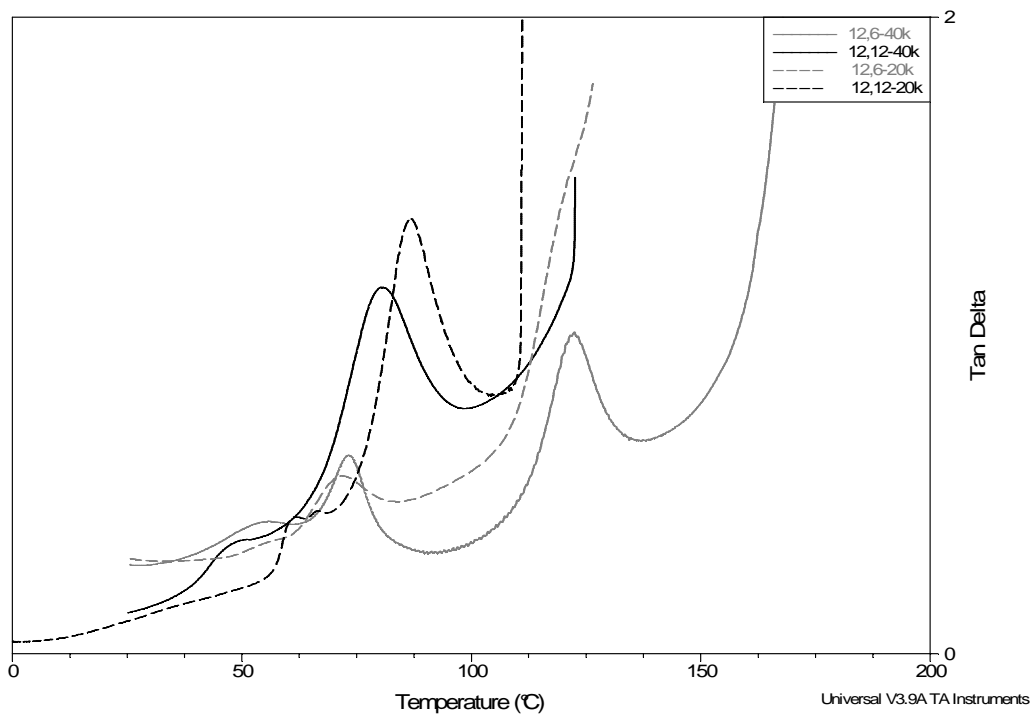


Figure 3.5: Tan δ curves for ammonium 12,6- and 12,12-ionenes.

Table 3.2: Thermal transitions of ammonium ionenes via DMA and DSC.

	DMA Transitions ($^{\circ}\text{C}$)			DSC T_g ($^{\circ}\text{C}$)
	T_1	T_2	T_3	
12,6-20k	63	94	126	90
12,12-20k	56	78	110	69
12,6-40k	66	112	161	104
12,12-40k	44	69	125	69

The second transition was attributed to the movement of ionic groups in the polymer chains. Clustering of ionic groups is common in polyelectrolytes due to electrostatic interactions between the charged segments and counterions, which can also lead to ion channel formation.²⁰ This relaxation occurred at 94 °C and 112 °C for 12,6-20k and 12,6-40k and at 78 °C and 69 °C for 12,12-20k and 12,12-40k, respectively. The transition temperatures for 12,6-20k and 12,6-40k were higher than those for the corresponding ammonium 12,12-ionenes. At comparable molecular weights, the degree of polymerization for ammonium 12,6-ionene is higher since the molecular weight of its repeating unit is lower than that of 12,12-ionene, which means more quaternized nitrogen groups were present in ammonium 12,6-ionene samples. Thus, ionic aggregation was more prevalent, and more thermal energy was needed to dissociate the aggregates and mobilize the chains, leading to higher DMA transition temperatures.

The third transition was attributed to polymer flow. This transition occurred at 126 °C for 12,6-20k and 161 °C for 12,6-40k, compared to 12,12-20k and 12,12-40k, which were observed at 109 °C and 125 °C, respectively. Higher transition temperatures and longer rubbery plateaus were observed for ionenes with higher molecular weights. The rubbery plateau that preceded flow was attributed to the mobility of methylene groups following the dissociation of ionic groups. The rubbery plateau for 12,12-20k extended from 85 °C to 109 °C compared to that of 12,12-40k, which extended from 85 °C to 125 °C. Similar results were found for 12,6-ionene, where the rubbery plateau for 12,6-20k extended from 120 °C to 126 °C and that for 12,6-40k extended from 120 °C to 160 °C.

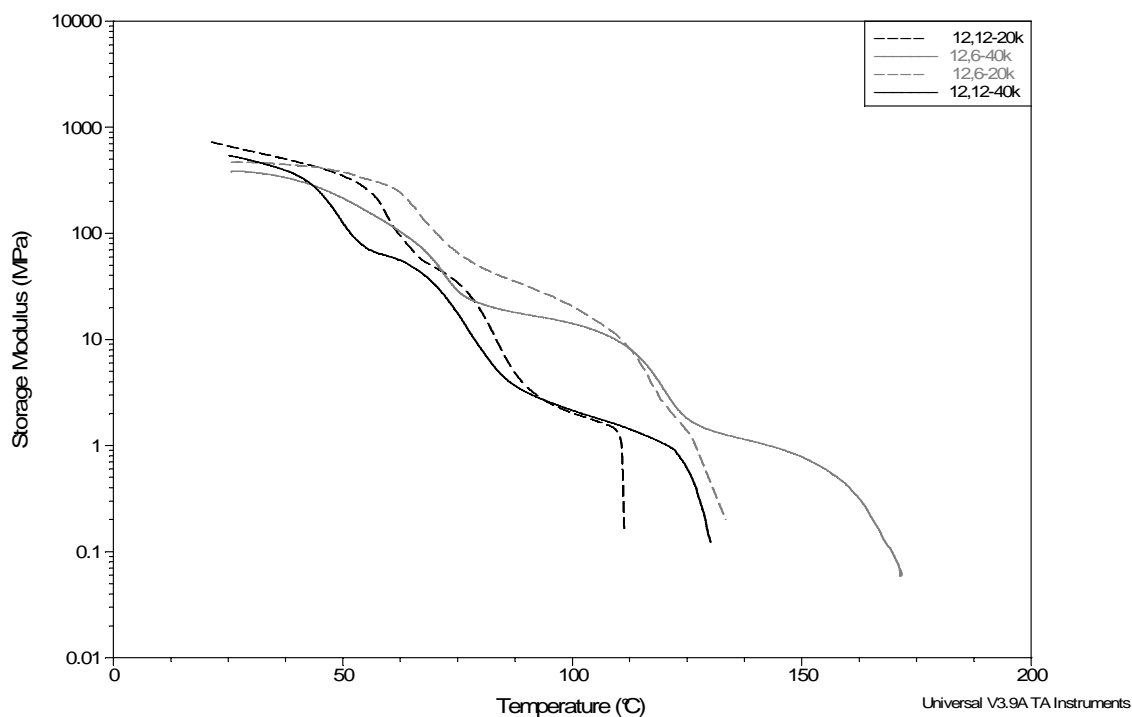


Figure 3.6: DMA curves for ammonium 12,6- and 12,12-ionenes.

Mechanical properties were also tested using an Instron to determine the tensile strengths and elongations associated with aliphatic ammonium ionenes (Figure 3.7, Table 3.3). Ammonium ionenes containing PTMO soft segments have been shown to elongate more than 1000%¹⁶, and we were interested to see if aliphatic ammonium ionenes also exhibited strong tensile properties. 12,6-20k was brittle and exhibited poor tensile properties breaking at less than 10% elongation and having tensile strengths at yield and break of 9 MPa. Because the polymer was brittle, only one sample was able to withstand breaking in the grips. However, ammonium 12,12-ionene at the same molecular weight exhibited elongations greater than 200% and tensile stresses at yield and break of 6 and

10 MPa, respectively. Higher molecular weights positively influenced tensile properties. 12,6-40k had tensile strengths at yield and break of 13 and 16 MPa with elongations above 300%, and 12,12-40k had tensile strengths at yield and break of 35 and 24 MPa with elongations above 100%, respectively. It is important to note that the hygroscopic nature of the polymers can influence the mechanical properties. Since tests were performed under ambient conditions, samples were first dried at 100 °C in vacuo, and subsequently, kept in a dessicator until tested. Hygroscopicity may be the reason for large error in Table 3.3 since we have observed that water plasticizes aliphatic ammonium ionenes. Water uptake may contribute to higher strains at break or lower moduli. Although, we were careful to keep our samples as dry as possible, further testing in a dry environment is needed to fully understand the effect of charge density on tensile properties.

Table 3.3: Tensile properties for ammonium 12,6- and 12,12-ionenes. Four repetitions per polymer sample were completed.

	Stress at Break (MPa)	Strain at Break (%)	Stress at Yield (MPa)	Modulus (MPa)
12,6-20k	--	9	9	278
12,12-20k	10 ± 4	206 ± 121	6 ± 0.4	231 ± 113
12,6-40k	16 ± 5	313 ± 41	13 ± 3	132 ± 63
12,12-40k	24 ± 2	235 ± 6	35 ± 4	489 ± 55

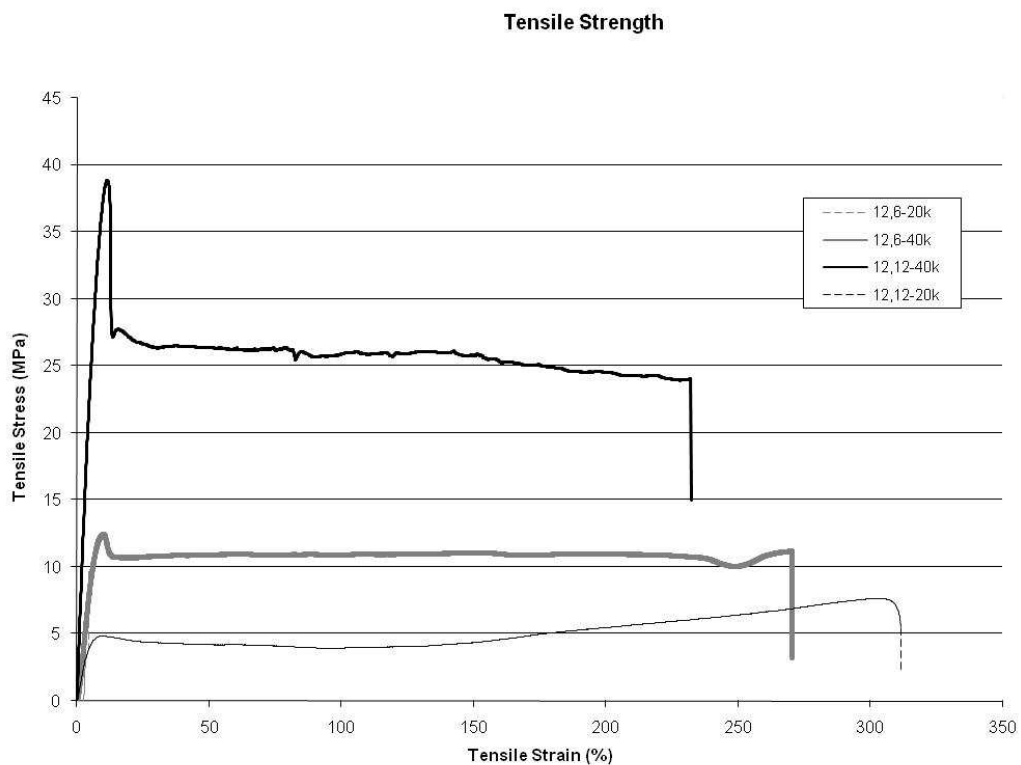


Figure 3.7: Tensile properties of aliphatic ammonium ionenes.

3.4.3 Thermal Properties

Thermal properties were investigated using differential scanning calorimetry (DSC) to determine thermal transitions and morphologies. A single transition in the third cycle of the DSC trace for ammonium 12,6- and 12,12-ionenes indicated a T_g corresponding to an amorphous morphology, but no T_m or T_c were observed. Prior to testing, the hygroscopic samples were heated to 100 °C for 48 h to ensure solvent removal and to prevent plasticization.²¹ Both 12,12-20k and 12,12-40k exhibited a T_g at 69 °C, while 12,6-20k showed a T_g at 90 °C, and 12,6-40k had a T_g at 104 °C (Table 3.1). Ammonium 6,6-ionene did not exhibit a T_g in the DSC trace, which was expected since the morphology was crystalline; however, T_m and T_c were not observed, either. The crystalline melting temperature of ammonium 6,6-ionene was speculated to be higher

than the degradation temperature, thus, no melting or crystallization peaks were observed in the DSC curve.

In a second DSC test, samples were heated to just below their onset of degradation temperature to erase thermal history and, subsequently, cooled at 3 °C/min to -90 °C to induce crystallization. The samples were held at -90 °C for 30 min, and then, heated to 250 °C. 12,12-40k had a crystallization peak at 63 °C (Figure 3.8), which was attributed to the symmetric structural composition, which allowed the chains to become ordered during the slow cooling process; however, an exothermic peak corresponding to crystallization was not observed for 12,6-40k, which was speculated to be due to the irregularity in structural composition. However, since testing conditions may have been better suited towards crystallization in ammonium 12,12-ionene, and because T_g values and T_m values overlapped (data not shown), a more in depth study using modulated DSC is planned for future work.

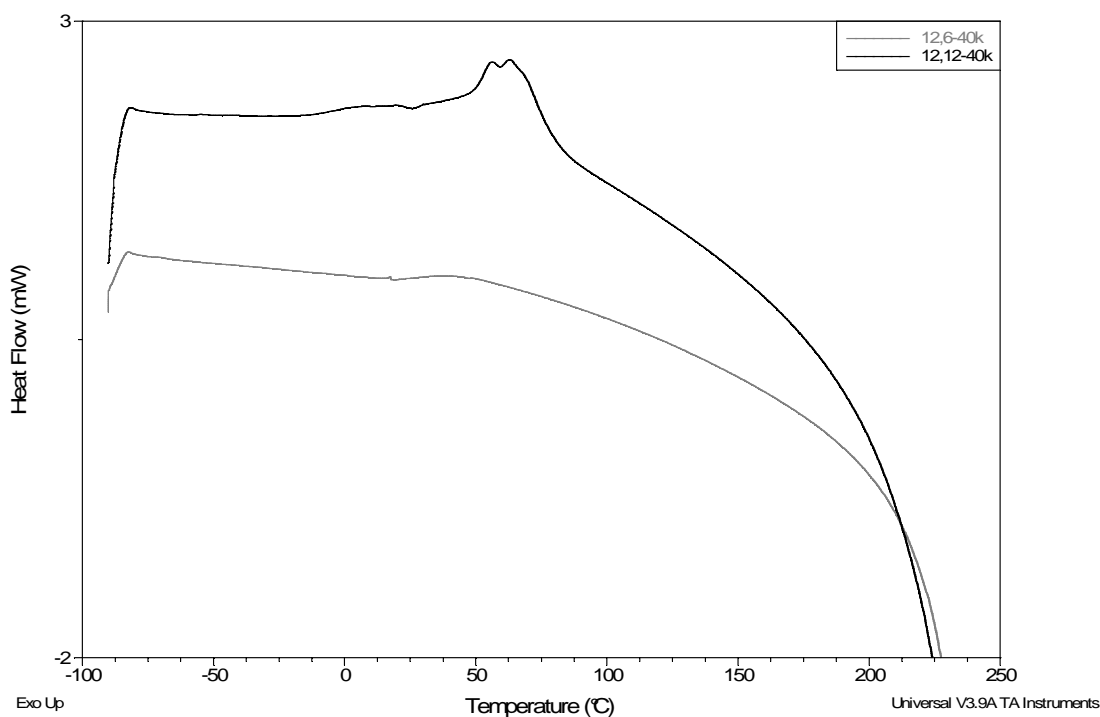


Figure 3.8: Samples were heated to 250 °C to erase thermal history, cooled at 3 °C/min to -90 °C, held isothermally for 30 min, and then, heated to 250 °C at 10 °C/min. The cooling cycle is shown. A cooling rate of 3 °C/min allows crystallization to occur in 12,12-40k, but not in 12,6-40k.

Thermal gravimetric analysis (TGA) was used to determine the degradation temperatures of each ionene (Figure 3.9). The primary method of degradation for ionenes is dequaternization of the amine groups in the backbone via a Hofmann elimination reaction.²² The 5% weight loss temperature for 12,6-20k and 12,6-40k was 234 °C and 247 °C, respectively. 12,12-20k and 12,12-40k had 5% weight loss temperatures of 237 °C and 241 °C. Throughout the remainder of the degradation process from 5% weight loss until complete degradation at 350 °C, the higher molecular weight ionenes degraded slower due to a higher content of quaternized nitrogen groups. Furthermore, 6,6-20k had a 5% weight loss temperature of 265 °C; the higher degradation

temperature was attributed to the highly ordered crystalline structure of ammonium 6,6-ionene, which restricted the mobility of the quaternized nitrogen groups.

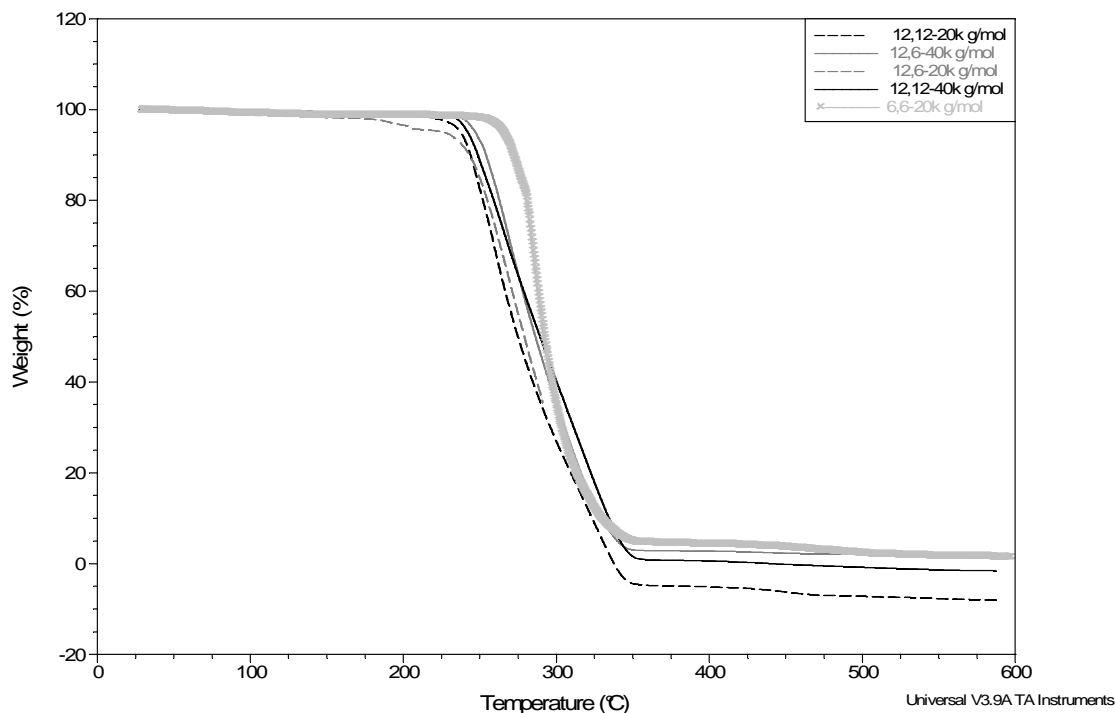


Figure 3.9: TGA results for ammonium 6,6-, 12,6- and 12,12-ionenes.

3.5 CONCLUSIONS

Ammonium 6,6-, 12,6- and 12,12-ionenes were investigated to determine the relationship between charge density, structural symmetry and thermal and mechanical properties. Number average molecular weights between 14,600 and 19,200 g/mol with weight averages between 20,300 and 23,000 g/mol were investigated and compared to ionenes with number average molecular weights between 25,300 and 30,700 g/mol and weight average molecular weights between 39,300 and 43,300 g/mol. Structural symmetry and charge density both positively influenced the ability of ionenes to crystallize, which was observed from the endothermic peaks in the DSC traces.

Crystallization of ammonium 6,6-ionene restricted mobility of polymer chains, which increased the onset of degradation temperature compared to ammonium 12,6- and 12,12-ionenes. Furthermore, tensile properties were stronger for the ionenes with structural regularity, but dynamic mechanical relaxations were similar for both ammonium 12,6- and 12,12-ionenes.

3.6 ACKNOWLEDGMENTS

We would like to acknowledge the generous support of Kimberly-Clark Corporation for financial support of this research. We would also like to thank the U.S. Army Research Laboratory and the U.S. Army Research Office under grant number DAAD19-02-1-0275 Macromolecular Architecture for Performance (MAP) MURI for additional support.

3.7 REFERENCES

¹ C. F. Gibbs, E. R. Littman, C. S. Marvel, Quaternary Ammonium Salts from Halogenated Alkyl Dimethylamines. II. The Polymerization of Gamma-Halogenopropyldimethylamines, *J. Am. Chem. Soc.*, **1933**, 753-757.

² M.R. Lehman, C.D. Thompson and C.S. Marvel, Quaternary Ammonium Salts from Hologenated Alkyl Dimethylamines. III. Omega-Bromo-Heptyl-, -Octyl-, -Nonyl-, and -Decyl-dimethylamines. *J. Am. Chem. Soc.*, **1935**, 57, 1137-1139.

³ C.F. Gibbs and C.S. Marvel, Quaternary Ammonium Salts from Bromopropyldialkylamines. IV. Formation of Four-Membered Rings.

⁴ C.F. Gibbs and C.S. Marvel, Quaternary Ammonium Salts from Bromopropyldialkylamines. V. Conversion of Cyclic Ammonium Salts to Linear Polymers.

⁵ H. Noguchi and A. Rembaum, Reactions of N,N,N',N'-Tetramethyl- α,ω -diaminoalkanes with α,ω -Dihaloalkanes. I. 1-y Reactions. *Macromolecules*, **1972**, 5 (3), 253-260.

⁶ H. Noguchi and A. Rembaum, Reactions of N,N,N',N'-Tetramethyl- α,ω -diaminoalkanes with α,ω -Dihaloalkanes. II. 1-y Reactions. *Macromolecules*, **1972**, 5 (3), 261-269.

-
- ⁷ T. Narita, R. Ohtakeyama, M. Nishino, J.P. Gong, Y. Osada, Effects of charge density and hydrophobicity of ionene polymer on cell binding and viability. *Colloid Polym. Sci.*, **2000**, 278, 884-887.
- ⁸ Zelinkin, A. N., Putnam, D., Shastri, P., Langer, R., Izumrudov, V. A., Aliphatic Ionenes as Gene Delivery Agents: Elucidation of Structure-Function Relationship through Modification of Charge Density and Polymer Length. *Bioconjugate Chem.*, **2002**, 13, 548-553.
- ⁹ Wittgren, B.; Welinder, A.; Porsch B. Molar mass characterization of cationic methacrylate ethyl acrylate copolymers using size-exclusion chromatography with online multi-angle light scattering and refractometric detection. *J. Chromatogr. A* **2003**, 1002:101Y109.
- ¹⁰ Jiang, X.; van der Horst, A.; van Steenbergen, M.J.; Akeroyd, N.; van Nostrum, C.F.; Schoenmakers, P.J.; Hennink, W.E. Molar-Mass Characterization of Cationic Polymers for Gene Delivery by Aqueous Size-Exclusion Chromatography. *Pharmaceutical Research*, **2006**, 23(3), 595-603.
- ¹¹ Borgerding, E., Layman, J., Heath, W., Williams, S., Long, T. Aqueous Size Exclusion Chromatography of Aliphatic Ammonium Ionenes for Absolute Molecular Weight Determination. **2007** *In Preparation*.
- ¹² Williams, S. R.; Borgerding, E. M.; Long, T. E., Synthesis and Characterization of Novel 12,12-Ammonium Ionenes: Evaluating Mechanical Properties as a Function of Molecular Weight. *In preparation*.
- ¹³ Tsutsui, T.; Tanaka, R.; Tanaka, T. Mechanical Relaxations in Some Ionene Polymers. I. Effect of Ion Concentration. *J. Polym. Sci. Polym. Phys. Ed.* **1976**, 14, 2259-2271.
- ¹⁴ Tsutsui, T.; Tanaka, R.; Tanaka, T. Mechanical Relaxations in Some Ionene Polymers. II. Influence of Counterions and Absorbed Water. *J. Polym. Sci. Polym. Phys. Ed.* **1976**, 14, 2273-2284.
- ¹⁵ Tsutsui, T.; Tanaka, R.; Tanaka, T. Dynamic Mechanical Properties of Some Ionene Polymers. *J. Polym. Sci. Polym. Phys. Ed.* **1975**, 13, 2091-2102.
- ¹⁶ Feng, L.N. Venkateshwaran, G.L. Wilkes, C.M. Leir and J.E. Stark, Structure-Property Behavior of Elastomeric Segmented PTMO-Ionene Polymers. II. *J. Appl. Polym. Sci.*, **1989**, 37, 1549-65.
- ¹⁷ Colthup, N. B., Daly, L. H., Wiberley, S. E. *Introduction to Infrared and Raman Spectroscopy*, 3rd Ed.; Academic Press: New York, **1975** (page 344).
- ¹⁸ Rembaum, A., Rile, H., Somoano, R. V. Kinetics of Formation of High Charge Density Ionene Polymers. *Polymer Letters*, **1970**, 8, 457-466.
- ¹⁹ Eisenberg, A., Matsuura, H., Yokoyama, T. The Glass Transition of Aliphatic Ionenes. *Polymer Journal*, **1971**, 2(2), 117-123.
- ²⁰ Sisson, A. L., Shah, M. R., Bhosale, S., Matile, S. Synthetic ion channels and pores. *Chem. Soc. Rev.*, **2006**, 35, 1269-1286.
- ²¹ Eisenberg, A., Matsuura, H., Yokoyama, T. The Glass Transition of Aliphatic Ionenes. *Polymer Journal*, **1971**, 2(2), 117-123.
- ²² Berwig, E., Severgnini, V.L.S., Soldi, M.S., Bianco, G., Pinheiro, E.A., Pires, A.T.N., Soldi, V. Thermal degradation of ionene polymers in inert atmosphere. *Polymer Degradation and Stability*, **2003**, 79, 93-98.

Chapter 4

SYNTHESIS AND CHARACTERIZATION OF LINEAR AND BRANCHED POLY(TETRAMETHYLENE OXIDE) BASED IONENES

Erika M. Borgerding¹, Ann R. Fornof¹, Fredrick Beyer², Shadpour Mallakpour¹, and
Timothy E. Long^{1*}

¹Department of Chemistry, Macromolecules and Interfaces Institute, Virginia Polytechnic
Institute and State University, Blacksburg, Virginia 24061

²U.S. Army Research Laboratory, Aberdeen Proving Ground, Maryland 21005

4.1 ABSTRACT

Ionenes are polycations that contain quaternized nitrogen groups in the main chain as opposed to pendant sites. Bis(dimethylamino) poly(tetramethylene oxide) (BAPTMO) segments were prepared from the living cationic polymerization of tetrahydrofuran (THF) and functionalized with dimethyl amine end groups. Linear and branched ionenes were synthesized from well-defined 2000 g/mol and 7000 g/mol BAPTMO and a di-functional or tri-functional benzylic halide, respectively. Ionenes were investigated to determine how branching and charge density influenced thermal and mechanical properties. Thermal properties were measured using differential scanning calorimetry (DSC) and thermal gravimetric analysis (TGA), and were found to be similar for all ionenes despite topology. Mechanical properties were measured using an Instron and dynamic mechanical analysis (DMA). Linear ionenes exhibited stronger tensile properties, which included higher stresses at break, higher elongations at break and higher elastic moduli than branched ionenes. Furthermore, DMA indicated linear ionenes flowed at higher temperatures and had rubbery plateaus that extended to 200 °C,

compared to 100 °C for branched ionenes. Small angle x-ray scattering was used to determine if regular spacing between ionic domains was present in the ionenes.

Keywords: ammonium ionene, branching, mechanical properties, ionic aggregation

4.2 INTRODUCTION

Ionenes are macromolecules that contain quaternary nitrogen groups in the backbone of the chain. Early ionene synthesis involved the homopolymerization of an ω -halo-alkyl dialkylamine,^{1,2,3} but a more traditional synthetic methodology involves the condensation polymerization of a di-tertiary amine and an alkyl dihalide via the Menshutkin reaction.⁴ Monomer selection is a critical parameter in the design of novel ionene systems for the purposes of controlling charge density and polymer characteristics. The ability to control charge density through monomer selection provides a metric for investigating cell binding and viability,⁵ solution properties,⁶ and gene transfection efficacy⁷ of ionenes. More conventional synthetic methodologies for ionenes involve tailoring monomers via incorporation of low molecular weight polymer segments, such as poly(ethylene oxide) (PEO)^{8,9} or poly(tetramethylene oxide) (PTMO),¹⁰ to yield desired properties, such as water solubility and biocompatibility, or elasticity, respectively.

The living cationic polymerization of PTMO was first reported by Smith and Hubin and has been utilized in the design of several novel ionenes containing PTMO segments.¹¹ In addition, several studies were performed using linear ionenes synthesized from bis(dimethylamino) poly(tetramethylene oxide) (BAPTMO) and a difunctional halide. These studies include the investigation of photochromic behavior,¹² polyelectrolyte behavior,¹³ and reaction rates and thermal stability as a function of

dihalide structure.⁹ Furthermore, structure-property relationships were analyzed to understand the elastomeric properties incorporated with the PTMO soft-segments.¹⁴ While the synthesis and characterization of linear PTMO based ionenes have been thoroughly studied, the influence of branching on these ionene systems has not, yet, been investigated.

We were interested in how topology influenced the thermal and mechanical properties of BAPTMO based ionenes. Branching has been shown to influence melt viscosity and improve melt processibility, and several reviews have been written on this topic.^{15,16} Our research group has developed the *oligomeric A₂* plus monomeric B₃ methodology for polymerization of highly branched macromolecules,^{17,18} where the distance between branching sites is determined by linear oligomers. This architecture allows for both a high degree of branching and acceptable mechanical properties.¹⁹ We utilized this polymerization technique to synthesize branched BAPTMO based ionenes.

Herein, we report on the synthesis of linear and branched ionenes from well-defined 2000 g/mol and 7000 g/mol BAPTMO. Thermal characterization was performed using differential scanning calorimetry (DSC) and thermal gravimetric analysis (TGA), and mechanical testing was performed using tensile testing and dynamic mechanical analysis (DMA). Furthermore, ionic aggregation was studied using small angle x-ray scattering to determine how ionic domains contributed to morphological characteristics and microphase separation. Ionene samples are referred to using L or HB to represent the topology and 2k or 7k to represent the molecular weight of the BAPTMO segments used in the synthesis. For example, L-2k refers to the linear ionene made from 2000 g/mol BAPTMO.

4.3 EXPERIMENTAL

4.3.1 Materials and Methods

High performance liquid chromatography grade tetrahydrofuran (THF) was purchased from EMD Chemicals and dried in a Pure Solv system. Irganox 1076 was obtained from Ciba Specialty Chemical Co. Trifluoromethanesulfonic anhydride (TFMSA) and 2,4,6-tris(bromomethyl)mesitylene (TBMM) were purchased from Sigma-Aldrich and used without further purification. Methyl 3-(dimethylamino) propionate was purchased from Sigma-Aldrich and distilled from calcium hydride (reagent grade, 95%), which was obtained from Sigma-Aldrich and used as received. α,α' -dibromo-*p*-xylene was purchased from Sigma-Aldrich and recrystallized with chloroform. Dichloromethane (DCM) was purchased from EMD Chemicals and distilled from calcium hydride. Hexanes and toluene were purchased from EMD Chemicals and used without further purification.

4.3.2 Synthesis of bis(dimethylamino) poly(tetramethylene oxide)

THF (10 g, 0.1389 mol) was added via a cannula to DCM (10 g, 0.1177 mol) in a three-necked 250-mL round-bottomed flask in an ice bath (Figure 4.1). Mechanical stirring was begun, and TFMSA (3.38 mL, 0.02 mol) was syringed into the solution to initiate the polymerization. After 15 min, THF (30.00 g, 0.4167 mol) was added dropwise to the solution, and the reaction was mechanically stirred for an additional 90 min at 0 °C. Methyl 3-(dimethylamino) propionate (11.4 mL, 0.08 mol, 2.1 molar excess) was syringed into the viscous white solution, and the reaction was removed from the ice bath and allowed to warm to 23 °C with mechanical stirring. The reaction continued for 30 min, and then, was precipitated into hexanes twice to remove excess

end-capping agent. The hexanes were decanted and the polymer was dissolved in toluene (50 mL). The solution was added to 40 g 25 wt% aqueous NaOH in a 250-mL, round bottom flask and refluxed at 70 °C for 30 min. to remove methyl acrylate from the end groups via a reverse Michael addition reaction to yield dimethylamino end groups. The layers were separated and the toluene layer was dried over MgSO₄ and filtered, and subsequently, precipitated into hexanes to remove methyl acrylate. The BAPTMO product was dried in vacuo at 60 °C for 24 h to ensure removal of residual solvent. The number average molecular weight was determined via end group analysis using ¹H NMR spectroscopic characterization and with acid titration using 0.10 N HCl in isopropanol in a solution of THF:isopropanol (2:1 v:v mixture).

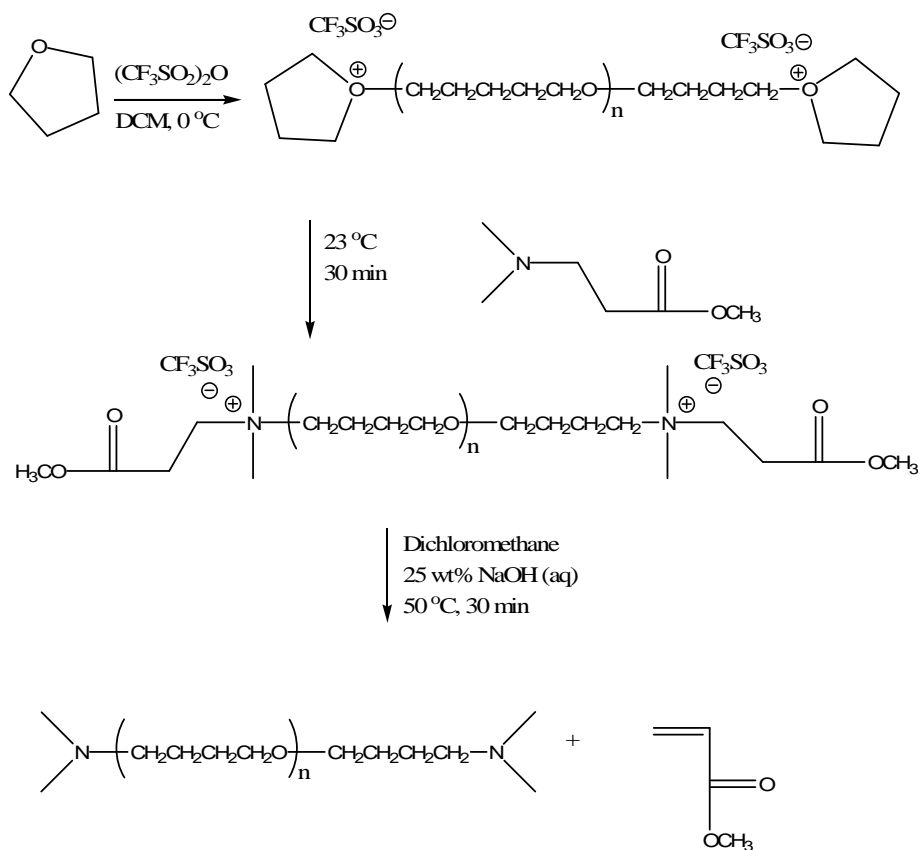


Figure 4.1: Synthetic Scheme for BAPTMO.

4.3.3 Synthesis of linear ionenes

2000 g/mol BAPTMO (4.7680 g, 2.384 mmol) and 1,4-dibromo-*p*-xylene (0.6293 g, 2.384 mmol) was dissolved in THF (50 mL) in a 500-mL round-bottomed flask (Figure 4.2). The reaction was magnetically stirred under reflux for ~1 h until the viscosity became too high for stirring to continue. Irganox 1076 (0.02 g) was dissolved in the reaction mixture, and the solution was cast onto a glass plate and allowed to dry in the hood overnight. Residual solvent was removed in vacuo at 60 °C for 24 h.

4.3.4 Synthesis of branched ionenes

2000 g/mol BAPTMO (4.7680 g, 2.384 mmol) was dissolved in THF at 15 wt% and slowly added dropwise to a 3 wt% solution of TBMM (0.9516 g, 2.384 mmol) in THF, under reflux, in a two-necked 500-mL round-bottomed flask (Figure 4.3). The reaction was magnetically stirred for 1 h. Irganox 1076 (0.02 g) was dissolved in the reaction mixture, and the solution was cast onto a glass plate and allowed to dry in the hood overnight. Residual solvent was removed in vacuo at 60 °C for 24 h.

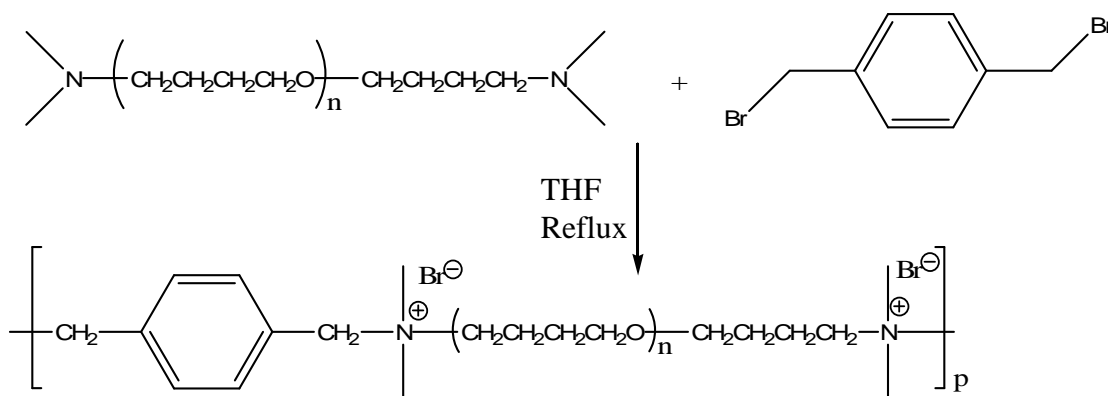


Figure 4.2: Synthetic scheme for linear ionene.

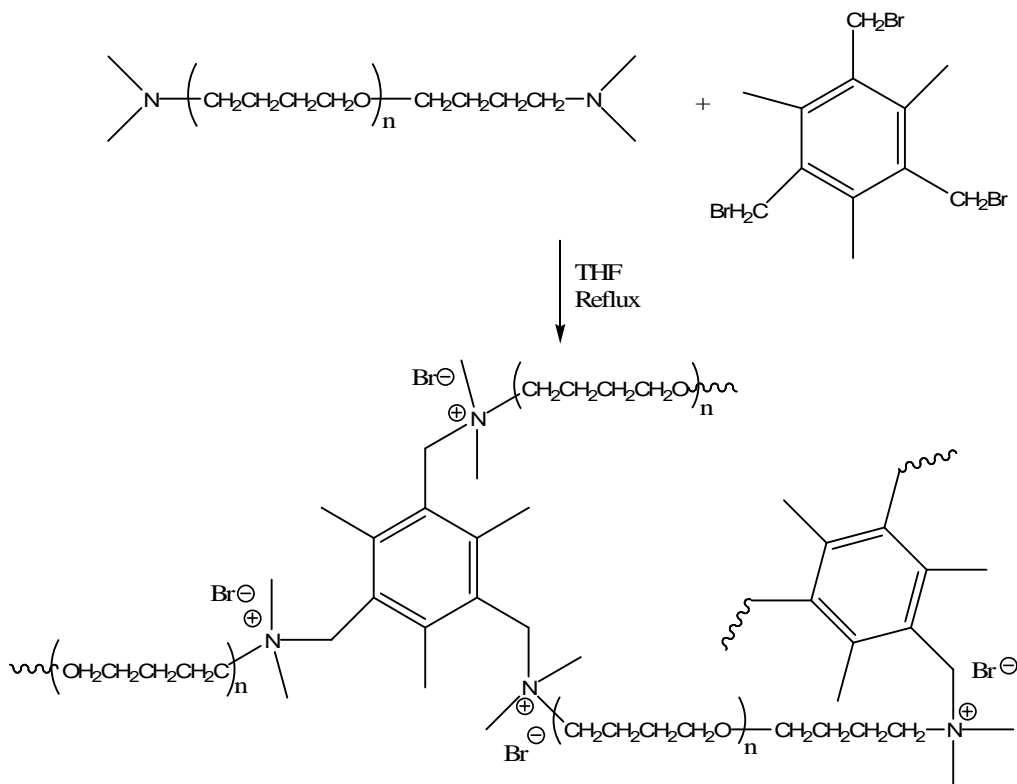


Figure 4.3: Synthetic scheme for highly branched ionene.

4.3.5 Characterization methods

^1H NMR spectra were recorded on a Varian Inova 400 MHz nuclear magnetic resonance instrument used at 25 °C with *d*-chloroform. Dynamic mechanical analysis (DMA) was performed on a DMA Q800 instrument in tension mode at 3°C/min and 1 Hz. Tensile testing was performed on an Instron Model 1123 Universal Testing system using mini dog-bone-shaped samples cut using a bench-top die (2.91 mm x 10 mm) from cast films and a Bluehill software package. Four repetitions per polymer sample were completed, and films were deformed until failure at a cross-head speed of 50 mm/min at 23°C. Prior to testing, samples were heated to 55 °C for 30 min to eliminate crystallinity and cooled to room temperature. Differential scanning calorimetry (DSC) was performed using a TA Instruments Q1000 instrument with a heating rate of 10°C/min under a nitrogen flow of 50 ml/min. Thermal gravimetric analysis (TGA) 2950 was used with a

heating rate of 10°C/min from 25°C to 600°C under nitrogen. Small angle x-ray scattering was performed on a Rigaku Ultrax 18 rotating anode X-ray generator operated at 45 kV and 100 mA. The distance between the beam center and the sample was approximately 1.5 m.

4.4 RESULTS AND DISCUSSION

4.4.1 Synthesis of linear and branched ionenes

BAPTMO segments of 2000 g/mol and 7000 g/mol were synthesized and used as precursors for linear and branched ionenes. BAPTMO was prepared from the living cationic polymerization of THF and end-capped with methyl 3-(dimethylamino) propionate to avoid further alkylation, which occurred when dimethyl amine was used for end-capping. Sodium hydroxide was used to remove methyl acrylate from the end-groups in a reverse Michael addition and to convert the quaternary amine to a tertiary amine. BAPTMO molecular weights were confirmed using acid titration and ¹H NMR spectroscopic characterization (Figure 4.4), which were determined to be above and below the critical molecular weight of entanglement, M_e , for PTMO, 2500 g/mol (Table 4.1). Molecular weight was controlled through adjustment of monomer to initiator ratio using trifluoromethanesulfonic anhydride as the initiator. Branched ionene films were prepared from a 1:1 molar ratio of BAPTMO and tris(bromomethyl)mesitylene; slow addition of the BAPTMO was necessary to reduce the chance of crosslinking. Furthermore, a low concentration of reactants (below 6 wt% solids final concentration) was necessary to avoid crosslinking. Linear ionene films were prepared from a 1:1.025 molar ratio of BAPTMO and 1,4-dibromo-*p*-xylene, as outlined in the previous

literature.¹⁰ The resulting films were either white and opaque, or clear and transparent and ductile. Molecular weight characterization of the ionenes was not performed since they were insoluble in all known mobile phase compositions used for size exclusion chromatography (SEC). Because molecular weight positively influences thermal and mechanical properties, it is important to note that we were not comparing the extent of these properties, but rather, we were investigating the influence of topology on these properties.

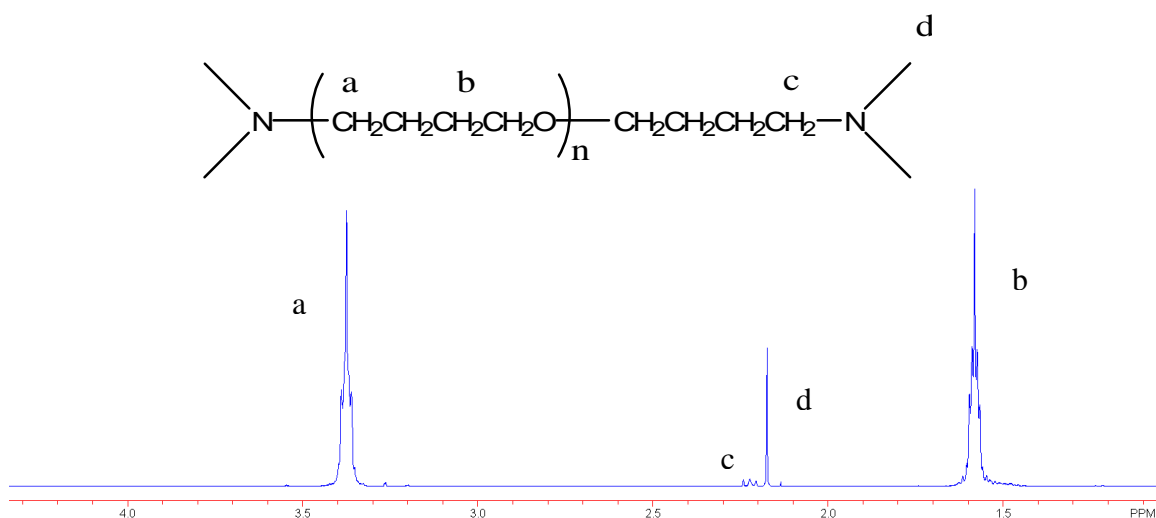


Figure 4.4: ¹H NMR of BAPTMO. A comparison of the integration of peak a and peak c was used to determine the degree of polymerization and calculate the number average molecular weight.

Table 4.1: Molecular weight characterization of BAPTMO.

	^a BAPTMO M _n (g/mol)	^b BAPTMO M _n (g/mol)
L-2k	1900	1600
HB-2k	1600	1900
L-7k	5500	6400
HB-7k	5500	6400

^a ¹H NMR end group analysis

^b HCl acid titration

4.4.2 Mechanical Properties

The stress-strain behaviors of linear and branched PTMO-based ionenes are shown in Figure 4.5. Linear ionenes had stronger tensile properties than branched ionenes (Table 4.2). Linear ionenes exhibited elongations at break greater than 1000%; L-2k had an elongation at break of 1160% and L-7k at 1061%. The tensile strain at break for branched ionenes was less than linear ionenes; HB-2k had a tensile strain at break of 505% and HB-7k at 835%. The greater elongation at break for HB-7k could be due to a higher molecular weight or a lower degree of branching than HB-2k. Elongations greater than 1000% are consistent with other linear PTMO based ammonium ionenes.¹⁴ Furthermore, Loveday showed that good mechanical properties were dependent upon regular spacing of ionic groups in the backbone.²⁰ The upturn in the stress-strain curves at higher elongations was attributed to strain-induced crystallization of the PTMO segments. The ultimate tensile stress for linear ionenes was greater than that of branched ionenes. L-2k and L-7k had stresses at break of 15 and 16 MPa, where as, HB-2k and HB-7k had stresses at break of 0.1 and 6 MPa, respectively. The average elastic modulus for L-2k was 4 MPa, where as, HB-2k had an elastic modulus of 0.4 MPa. The same trend was seen for the 7k system where branched ionenes had a lower elastic modulus than linear ionenes.

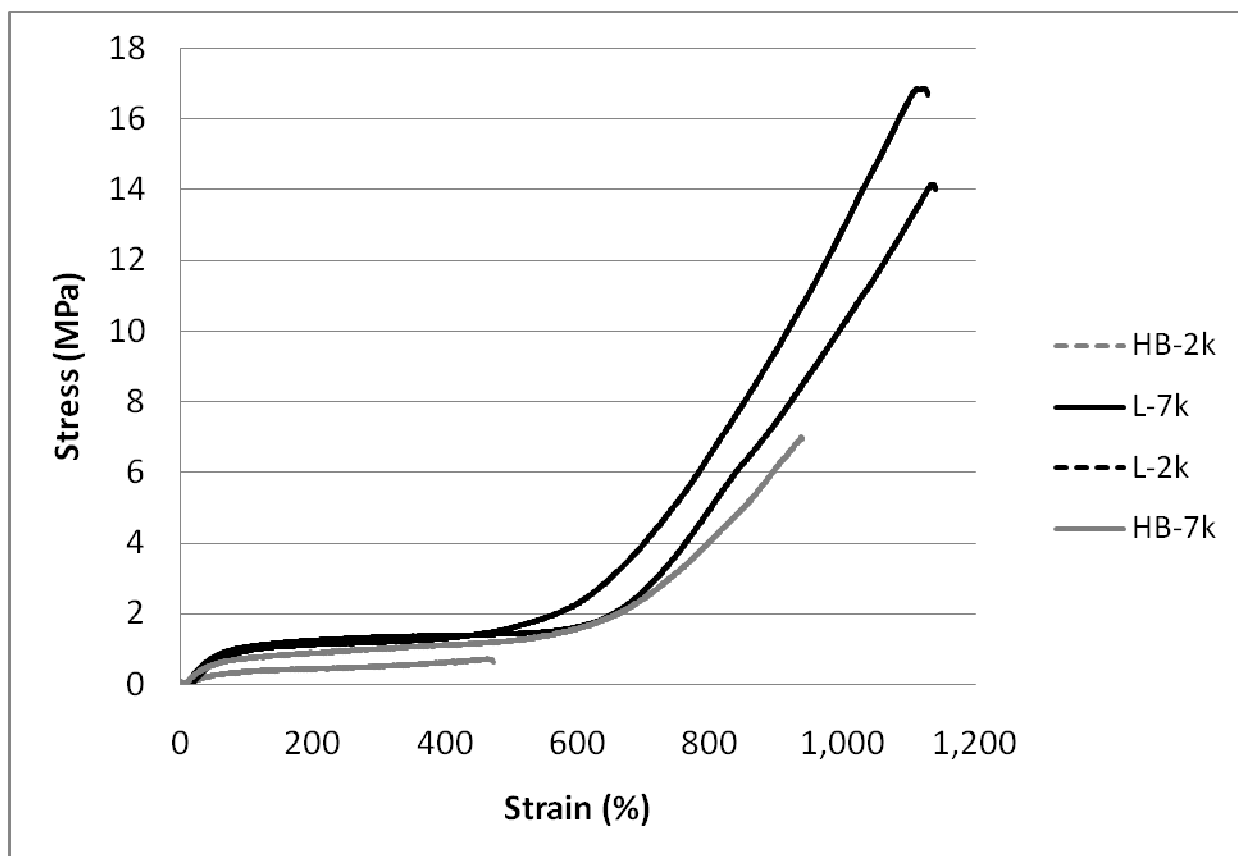


Figure 4.5: Tensile properties of linear (black) and branched (gray) ionenes.

Table 4.2: Tensile properties of linear and branched ionenes.

	Stress at Yield (MPa)	Strain at Break (%)	Stress at Break (MPa)	Young's Modulus (MPa)
L-2k	16 ± 2	1160 ± 57	15 ± 3	4 ± 0.4
HB-2k	0.5 ± 0.2	505 ± 4	0.1 ± 0.2	0.4 ± 0.2
L-7k	3 ± 4	1061 ± 68	16 ± 2	3 ± 0.2
HB-7k	6 ± 1	835 ± 93	6 ± 1	2 ± 0.2

Crystallization in PTMO-based ionene films was previously reported to develop slowly over the period of a week.²¹ Because ionenes were stored at room temperature and PTMO crystallization occurs at room temperature, ionene films were heated to 55 °C prior to tensile testing to erase any crystallinity. Erasing thermal history was critical since we were not interested in the effects crystallization had on mechanical properties, but rather, we were interested in the effects topology had on ionic aggregation and mechanical properties. Figure 4.6 shows how tensile properties changed when crystallization was present in ionenes. The crystalline sample was allowed to sit at room temperature for a week prior to testing, and the amorphous sample was heated to 55 °C and subsequently, cooled to room temperature prior to testing. The crystalline sample had higher stresses at yield (4 MPa) and break (8 MPa) than the amorphous sample, and the ultimate tensile strain was reduced to 500 %.

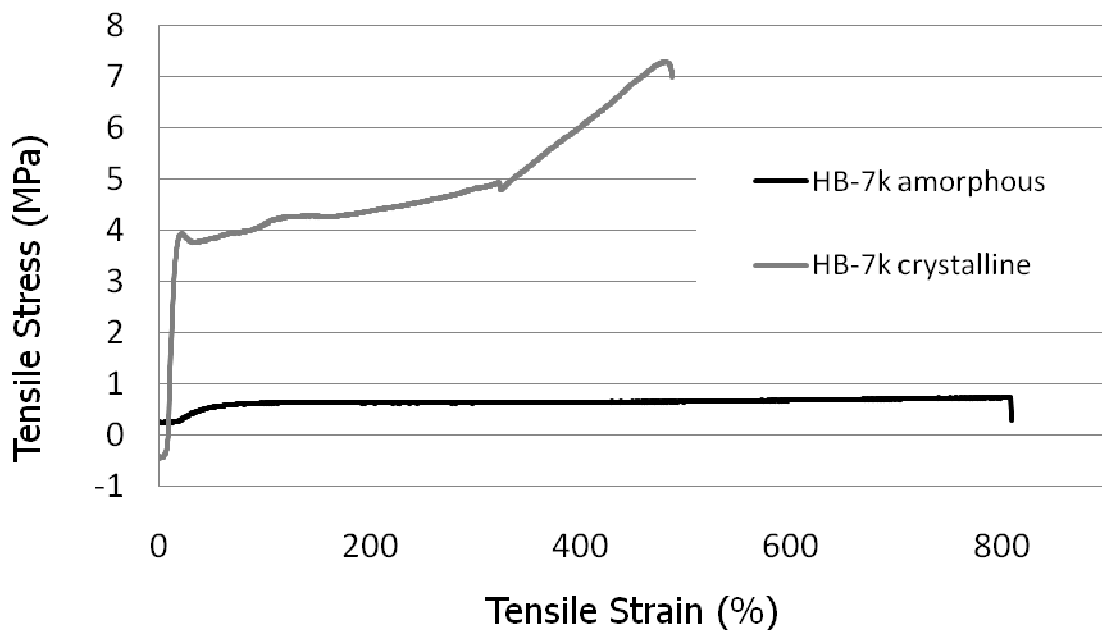


Figure 4.6: Influence of crystallization on tensile properties of PTMO-based ammonium ionenes.

Dynamic mechanical analysis was performed on linear and branched ionenes to probe the influence of temperature on storage modulus (Figure 4.7). Two distinct relaxations were observed for linear and branched ionenes at -60 °C and 23 °C. The first relaxation was attributed to the glass transition temperature of PTMO, and a peak in the $\tan \delta$ curve also denoted this transition (Figure 4.8). A plateau from -50 to 50 °C was observed for both linear and branched ionenes during which melting and crystallization of PTMO occurred. The second mechanical relaxation was attributed to melting of the crystalline phase in the PTMO segments. These transitions were similar for all ionenes regardless of topology or PTMO soft segment length.

The third relaxation was attributed to polymer flow, which was preceded by a rubbery plateau corresponding to the dissociation of ionic groups. Both L-2k and L-7k flowed at 187 °C, and HB-2k flowed at 80 °C while HB-7k flowed at 94 °C. Ionic aggregation was more favorable in linear ionenes because linear ionenes were less sterically hindered than branched ionenes and could pack together more tightly, thus, requiring more thermal energy to reach flow. This was exemplified as linear ionenes had both a higher modulus after PTMO crystals had melted and a rubbery plateau that extended to higher temperatures (50 – 200 °C), as compared to branched ionenes whose rubbery plateau only extended from 50 to 95 °C. Despite the fact that branched ionenes contain three chemically bonded ionic sites versus only two chemically bonded ionic sites in the linear ionenes, a quaternary nitrogen atom was not present at every branching site because a 1:1 molar ratio of BAPTMO to tri-functional branching agent was used in the synthesis. Thus, while one might think that ionic associations were favored in branched

ionenes due to the covalently bound ionic groups, this was not the case based on our DMA results. Furthermore, the chemically bonded ionic groups in branched ionenes did not aggregate as well as in linear ionenes because of steric hindrance.

Charge density also contributed to ionic associations, but to a lesser degree than topology. Higher charge densities allowed for an increased number of ionic associations and a higher modulus after the PTMO crystalline phase melted, thus, L-2k, which had the highest charge density and a linear topology, had the highest modulus and most expansive rubbery plateau preceding flow. L-7k had the second highest storage modulus above the crystalline melting temperature of PTMO because the topology allowed for more ionic associations than in branched ionenes, and HB-2k had a higher modulus than HB-7k because of a higher charge density.

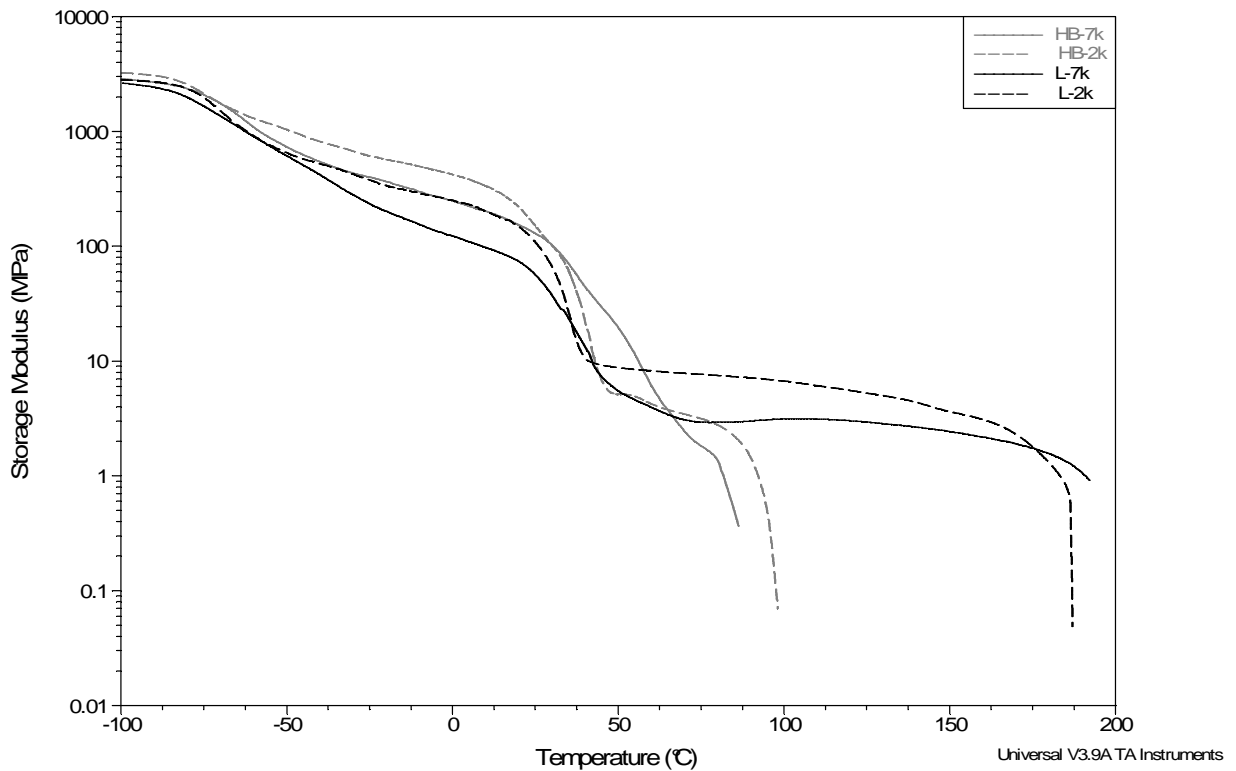


Figure 4.7: DMA results for linear (black) and branched (gray) ionenes.

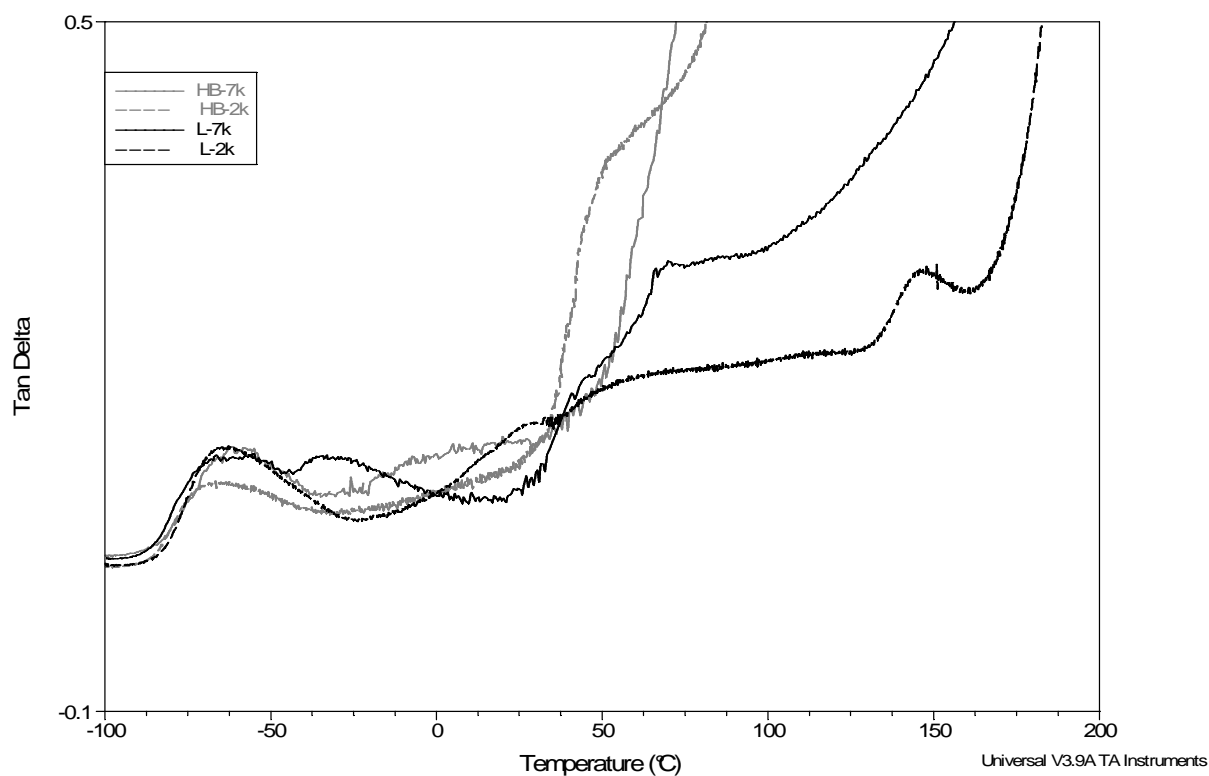


Figure 4.8: Tan δ curves for linear and branched PTMO-based ionenes.

4.4.3 Thermal Properties

Thermal properties were less affected by topology than mechanical properties. DSC results for all linear and branched ionenes showed a T_g of -70 °C, which corresponds closely to the T_g of PTMO. Crystalline melting temperatures (T_m) and temperatures of crystallization (T_c) were also similar for both linear and branched ionenes regardless of charge density or topology and occurred around 23 °C and -10 °C, respectively (Table 4.3). Enthalpy measurements were used to compare the degree of crystallinity of both ionene topologies, and it was determined that branching did not disrupt the crystallinity in the PTMO segments.

Table 4.3: Thermal transitions of linear and branched ionenes as measured from DSC analysis.

	T _g (°C)	T _m (°C)	T _c (°C)
L-2k	-78	21	-9
HB-2k	-79	25	-7
L-7k	-81	23	-11
HB-7k	-75	24	-12

Thermal gravimetric analysis (TGA) results corresponded with degradation temperatures of other ionene systems.²² L-2k had a 5% weight loss at 204 °C and HB-2k had a 5% weight loss at 184 °C, where as, L-7k and HB-7k had a 5% weight loss at 244 °C and 258 °C, respectively (Figure 4.9). The primary degradation process was dequaternization of the amine groups in the backbone via a Hofmann elimination reaction; therefore, similar degradation temperatures for all ionenes was expected and observed.¹⁰ Beyond the 5% weight loss temperature, from 250 – 400 °C, ionenes synthesized from 7000 g/mol BAPTMO degraded slower than the ionenes made from 2000 g/mol BAPTMO because the number of quaternized nitrogen groups in the chain was less for ionenes with lower charge densities. Degradation occurred faster in ionenes with higher charge density because there were more sites for degradation to occur.

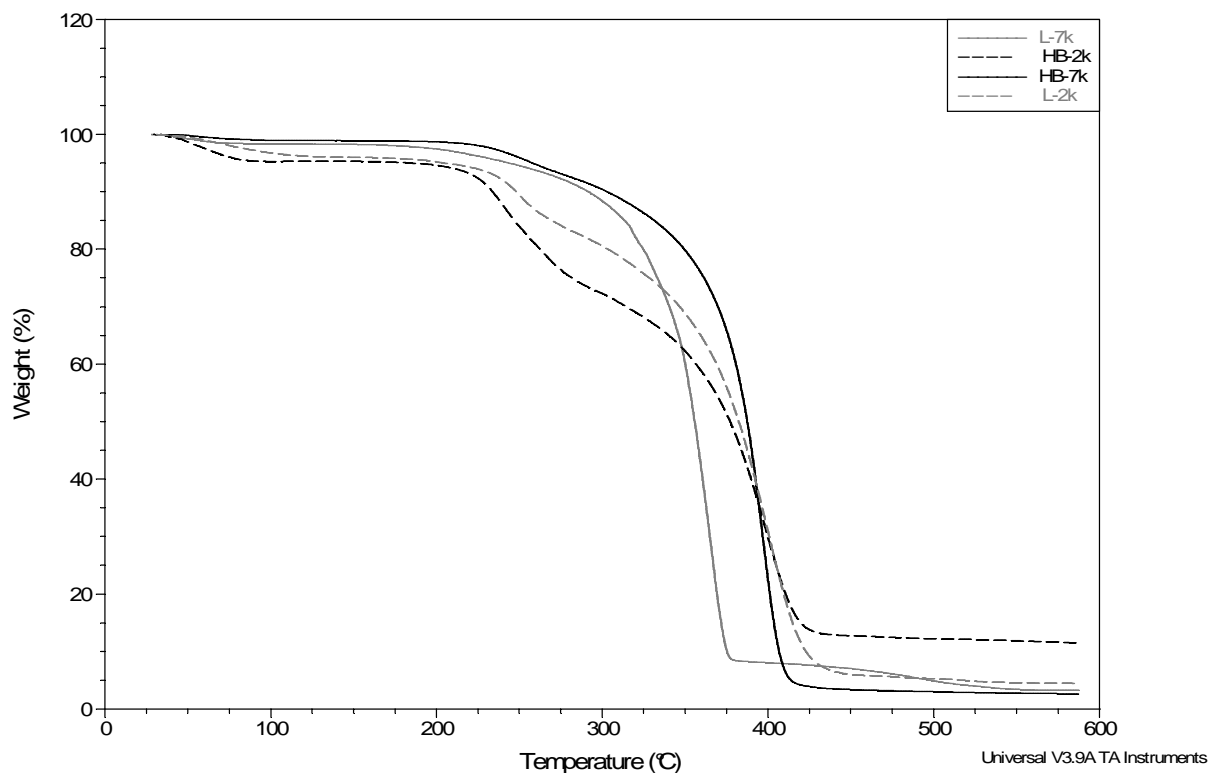


Figure 4.9: TGA data for linear and branched ionenes.

4.4.4 Small angle x-ray scattering (SAXS)

Small angle x-ray scattering (SAXS) data was obtained for L-2k and HB-2k to determine if regular spacing between ionic domains was present. Feng previously determined that linear BAPTMO based ionenes had lamellae arranged normal to the plane of the film, which were postulated to be due to hexagonal associations between four quaternized nitrogen groups and two bromide counterions that stacked on top of each other.²¹ However, our SAXS data showed ill-defined, broad peaks, which did not suggest a well-ordered morphology (Figure 4.10). This lack of order was presumed to be due to the quick drying process we adopted during film formation. It is thought that if the drying process was prolonged for at least three days, the polymer chains would have

enough time and mobility to become ordered, and thus, the SAXS peaks would be more defined.

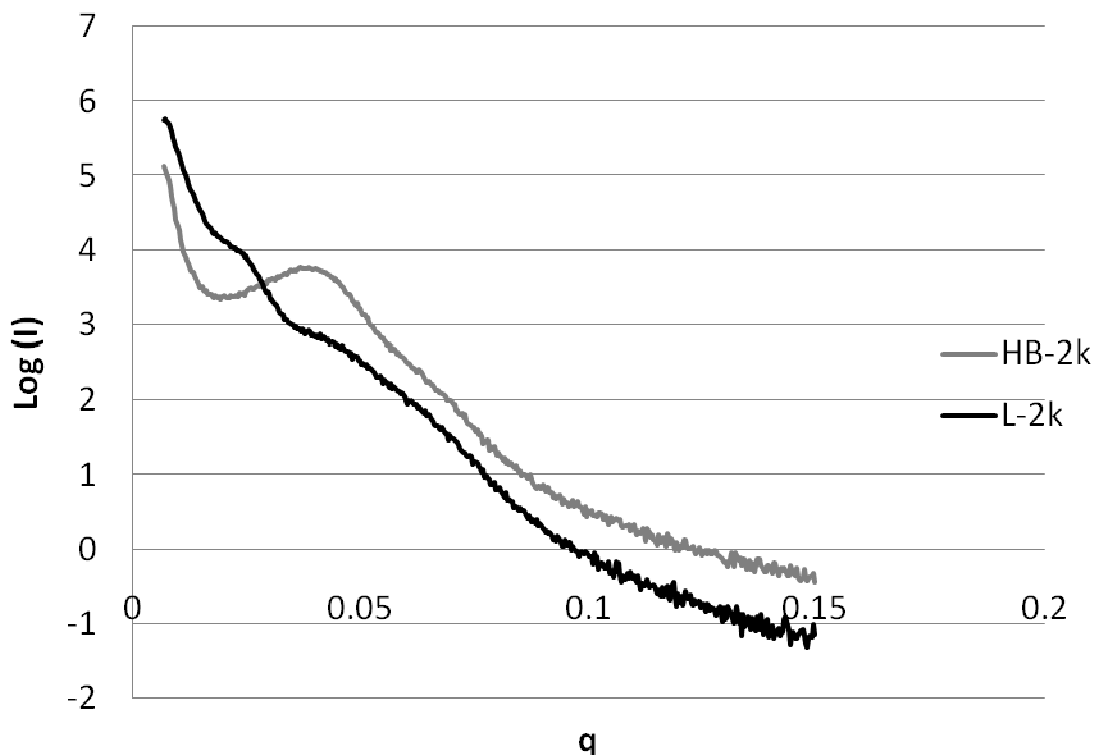


Figure 4.10: SAXS data for linear and branched ionenes.

4.5 CONCLUSIONS

The synthesis of 2000 and 7000 g/mol bis(dimethylamino) poly(tetramethylene oxide) was achieved through the living cationic polymerization of THF followed by end-capping with methyl-3(dimethylamino)propionate and removal of methyl acrylate via a reverse Michael addition reaction. These oligomers were utilized in the synthesis of both linear ionenes and branched ionenes via an oligomeric A_2 plus monomeric B_3 polymerization to probe the influence of branching on thermal and mechanical properties.

Three mechanical relaxations were observed for linear and branched ionenes. The first relaxation was attributed to T_g of PTMO, which occurred at $-60\text{ }^\circ\text{C}$, and the second relaxation was attributed to T_m of PTMO, which occurred at $23\text{ }^\circ\text{C}$. While topology did not affect the first two transitions, the third transition, which corresponded to polymer flow, was affected. Branched ionenes flowed at $100\text{ }^\circ\text{C}$ less than linear ionenes, which supports the previous literature suggesting that branching positively influences melt processibility. Linear ionenes had more ionic aggregation, as observed from the expansive rubbery plateau preceding polymer flow, and steric hindrance prevented the branched ionenes from forming ionic aggregations as easily.

Branching was also determined to influence tensile properties. Branched ionenes had lower moduli and stresses at break than linear ionenes. Linear ionenes also had higher elongations and more strain-induced crystallization at the higher tensile strains.

Thermal properties were similar in all ionenes regardless of topology because PTMO segments dictated these transitions. T_g and T_m of linear and branched ionenes, as observed from DSC, corresponded to the T_g and T_m of PTMO. Furthermore, degradation temperatures were influenced by charge density rather than topology since the primary method of degradation was dequaternization of the amine groups in the backbone. Onset of degradation was above $200\text{ }^\circ\text{C}$, and ionenes with higher charge densities degraded faster than those with lower charge densities because ionenes with higher charge densities had more sites for degradation to occur.

Preliminary SAXS data suggests our ionenes do not have an ordered morphology associated with regular spacing between ionic domains. Future work will include a slower drying process during film formation to encourage a more ordered structure.

4.6 ACKNOWLEDGMENTS

We would like to thank the U.S. Army Research Laboratory for financial support under the Army Materials Center of Excellence Program, contract W911NF-06-2-0014. We would also like to acknowledge the U.S. Army Research Laboratory and the U.S. Army Research Office under grant number DAAD19-02-1-0275 Macromolecular Architecture for Performance (MAP) MURI for support of this work.

4.7 REFERENCES

¹ M.R. Lehman, C.D. Thompson and C.S. Marvel, Quaternary Ammonium Salts from Hologenated Alkyl Dimethylamines. III. Omega-Bromo-Heptyl-, -Octyl-, -Nonyl-, and -Decyl-dimethylamines. *J. Am. Chem. Soc.*, **1935**, *57*, 1137-1139.

² C.F. Gibbs and C.S. Marvel, Quaternary Ammonium Salts from Bromopropylalkylamines. V. Conversion of Cyclic Ammonium Salts to Linear Polymers.

³ C.F. Gibbs and C.S. Marvel, Quaternary Ammonium Salts from Bromopropylalkylamines. IV. Formation of Four-Membered Rings.

⁴ H. Noguchi and A. Rembaum, Reactions of N,N,N',N'-Tetramethyl- α,ω -diaminoalkanes with α,ω -Dihaloalkanes. I. 1-y Reactions. *Macromolecules*, **1972**, *5* (3), 253-260.

⁵ T. Narita, R. Ohtakeyama, M. Nishino, J.P. Gong, Y. Osada, Effects of charge density and hydrophobicity of ionene polymer on cell binding and viability. *Colloid Polym. Sci.*, **2000**, *278*, 884-887.

⁶ D. Casson and A. Rembaum, Solution Properties of Novel Polyelectrolytes. *Macromolecules*, **1972**, *5* (1), 75-81.

⁷ Zelinkin, A. N., Putnam, D., Shastri, P., Langer, R., Izumrudov, V. A., Aliphatic Ionenes as Gene Delivery Agents: Elucidation of Structure-Function Relationship through Modification of Charge Density and Polymer Length. *Bioconjugate Chem.*, **2002**, *13*, 548-553.

⁸ I.V. Dimitrov, I.V. Berlinova, Synthesis of Poly(ethylene oxide)s Bearing Functional Groups along the Chain. *Macrom. Rapid Com.*, **2003**, *24*, 551-555.

-
- ⁹ H. Han, P.R. Vantine, A.K. Nedeltchev, P.K. Bhowmik, Main-Chain Ionene Polymers Based on trans-1,2-(4-pyridyl)ethylene Exhibiting Both Thermotropic Liquid-Crystalline and Light-Emitting Properties. *J. Polym. Sci.: Part A: Polym. Chem.*, **2006**, *44*, 1541-1554.
- ¹⁰ C.M. Leir and J.E. Stark, Ionene Elastomers from Polytetramethylene Oxide Diamines and Reactive Dihalides. I. Effect of Dihalide Structure on Polymerization and Thermal Reversibility. *J. Appl. Polym. Sci.*, **1989**, *38*, 1535-47.
- ¹¹ S. Smith and A.J. Hubin, Preparation and chemistry of dicationically active polymers of tetrahydrofuran. *J. Macromol. Sci. -Chem.*, **1973**, *7* (7), 1399-413.
- ¹² S. Kohjiya, T. Hashimoto, S. Yamashita and M. Irie, Synthesis and Photochromic Behavior of Elastomeric Ionene Containing Viologen Units. *Chem. Lett.*, **1985**, *10*, 1497-500.
- ¹³ S. Kohjiya, T. Ohtsiki, S. Yamashita, Polyelectrolyte Behavior of an Ionene Containing Poly(oxytetramethylene) Units. *Makromol. Chem., Rapid Commun.*, **1981**, *2*, 417-20.
- ¹⁴ D. Feng, L.N. Venkateshwaran, G.L. Wilkes, C.M. Leir and J.E. Stark, Structure-Property Behavior of Elastomeric Segmented PTMO-Ionene Polymers. II. *J. Appl. Polym. Sci.*, **1989**, *37*, 1549-65.
- ¹⁵ Kulkarni, A. S., Beaucage, G., Quantification of Branching in Disordered Materials. *J. Polym. Sci. Part B*, 2006, *44*(10), 1395-1405.
- ¹⁶ Lohse, D. J., Milner, S. T., Fetters, L. J., Xenidou, M., Hadjichristidis, N., Mendelson, R. A., Garcia-Franco, C. A., Lyon, M. K. Well-Defined, Model Long Chain Branched Polyethylene. 2. Melt Rheological Behavior. *Macromolecules*, **2002**, *35*(8), 3066-3075.
- ¹⁷ Unal, S., Oguz, C., Yilgor, E., Gallivan, M., Long, T. E., Yilgor, I. *Polymer*, 2005, *46* (13), 4533-4543.
- ¹⁸ Unal, S., Lin, Q., Mourey, T. H., Long, T. E., *Macromolecules*, **2005**, *38*, 3246-3254.
- ¹⁹ S. Unal, I. Yilgor, E. Yilgor, J.P. Sheth, G.L. Wilkes, and T.E. Long, A New Generation of Highly Branched Polymers: Hyperbranched, Segmented Poly (urethane urea) Elastomers. *Macromolecules*, **2004**, *37*, 7081-4.
- ²⁰ Loveday, D., Wilkes, G. L., Bheda, M. C., Shen, Y. X., Gibson, H. W. *Pure Appl. Chem.* **1995**, *32*(1), 1-27.
- ²¹ Feng, D., Wilkes, G. L. *J. Macromol. Sci.-Chem.*, **1989**, *A26*(8), 1151-1181.
- ²² Berwig, E., Severgnini, V.L.S., Soldi, M.S., Bianco, G., Pinheiro, E.A., Pires, A.T.N., Soldi, V. Thermal degradation of ionene polymers in inert atmosphere. *Polymer Degradation and Stability*, **2003**, *79*, 93-98.

Chapter 5

FUTURE DIRECTIONS

5.1 Molecular Weight Distributions of Aliphatic Ammonium Ionenes Using Aqueous Size Exclusion Chromatography

Currently, we have developed a mobile phase composition for absolute molecular weight determination of aliphatic ammonium ionenes using aqueous size exclusion chromatography. A molecular weight distribution of 2 is expected for macromolecules polymerized in a step-growth fashion; however, the molecular weight distributions we have determined for ammonium 6,6-, 12,6- and 12,12-ionenes are 1.3. The reason for the narrow distributions is unknown despite several attempts to address the issue, including eliminating the possibilities of fractionation and pore volume exclusion. The next step is to investigate reaction kinetics of the ionene polymerization. Extensive studies of reaction kinetics have been performed for ammonium ionenes and it was determined that solvent polarity and salt concentration affect the polymerization.¹ It would be useful to polymerize ammonium ionenes in the presence of salt, such as sodium iodide, and measure how molecular weight and distributions are affected. Furthermore, while we feel the mobile phase composition we developed provides reliable molecular weights for ammonium ionenes, as confirmed with NMR spectroscopy, the mobile phase may still not be perfect for determining distributions. If this is the case, it may be useful to continue searching for a mobile phase that would provide both reliable separations and accurate molecular weight distributions. This study would include changing the salt concentration or type of salt used in the mobile phase and performing aqueous SEC.

Performing aqueous SEC of polyelectrolytes is difficult, and if we can determine why the distributions for our ionenes are less than 2, it will give us a better understanding of aqueous SEC analysis of polyelectrolytes.

5.2 Synthesis of Ammonium Ionenes with Higher Equivalent Molecular Weights

Equivalent molecular weight is determined from dividing the molecular weight of the repeating unit by the number of quaternized ammonium groups in the repeating unit (generally 2).² It has been demonstrated that ionenes with equivalent molecular weights between 750-1400 g/mol are insoluble in aqueous salt solutions above 3 wt%, which is ideal for materials in contact with body fluid since human body fluid contains 2-4 wt% salt. Ammonium 12,6- and 12,12-ionenes have equivalent molecular weights close to 200 g/mol, and are soluble in aqueous salt solutions above 20 wt%. It would be beneficial to synthesize ammonium ionenes with higher equivalent molecular weights. This can be achieved from incorporating PTMO into the ionene backbone, which could be accomplished from reacting bis(dimethylamino) PTMO with a number of dihaloalkanes, such as 1,6-dibromohexane (Figure 5.1).

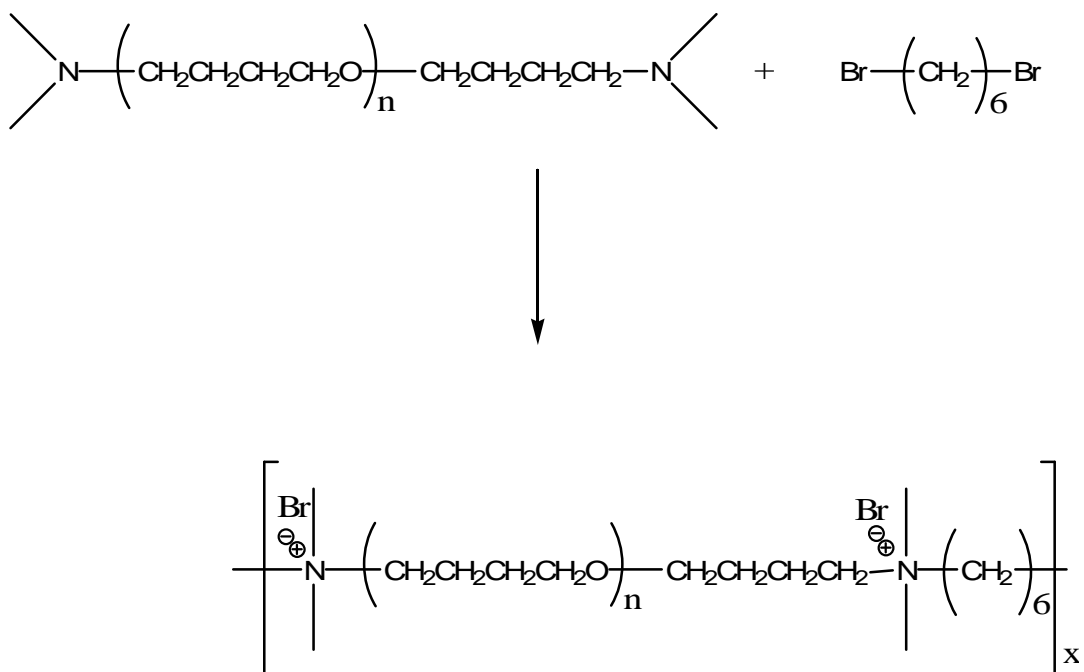


Figure 5.1: Synthesis of ammonium ionene with PTMO segments.

Another synthetic methodology that would lead to higher equivalent molecular weight would be the reaction of bromine end-capped 12,12-ionene with BAPTMO. This would produce a polymer composition similar to a block copolymer, which would have both hydrophobic and hydrophilic blocks (Figure 5.2).

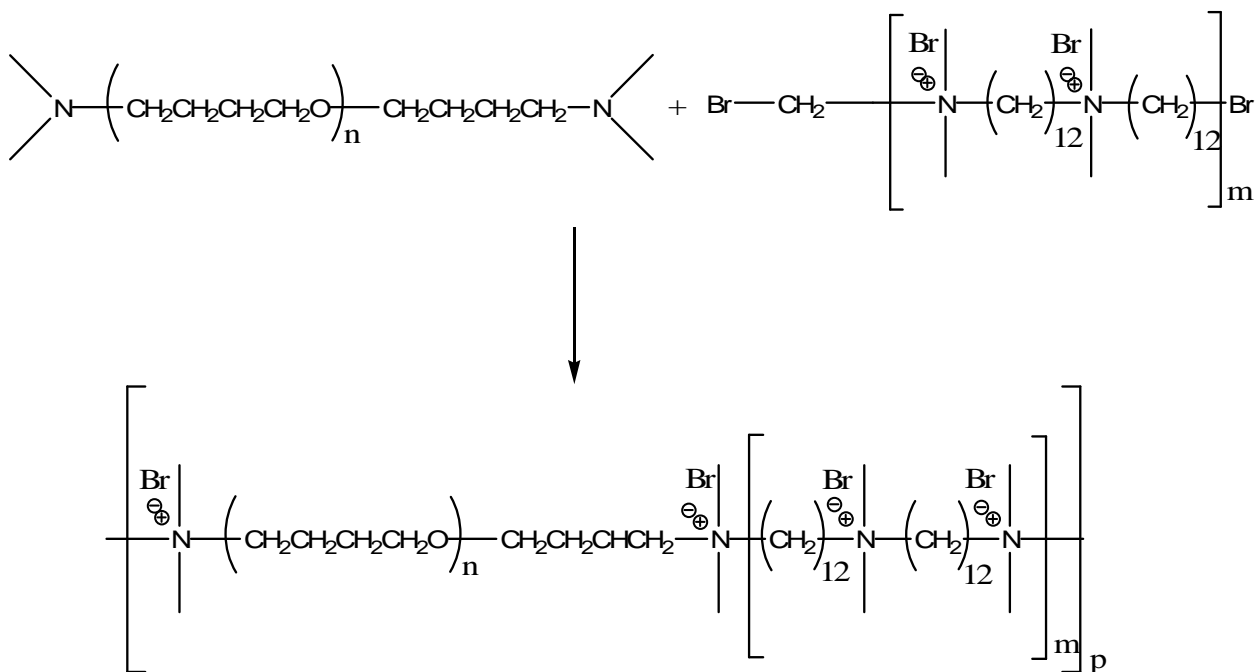


Figure 5.2: Synthesis of ionene with a “block” copolymer type architecture.

Incorporating other hydrophobic segments into the ionene backbone, such as poly(propylene oxide) or poly(caprolactone), would also help to decrease charge density and prevent ionenes from dissolving in aqueous salt solutions above 4 wt%. Increasing equivalent molecular weight affects solubility properties in aqueous salt solutions, which will be useful when developing new materials used in toilet tissue or other personal hygiene items.

5.3 Determination of PTMO based ionene morphologies via SAXS and TEM

We have studied the influence of topology on thermal and mechanical properties of PTMO based ionenes, but the morphology of these materials is unknown. Feng and Wilkes have demonstrated that linear ionenes have unique morphological characteristics where ionic groups and counterions form hexagonal shaped aggregates that stack and

form lamellae normal to the plane of the film.³ It would be useful to determine the influence topology has on morphological characteristics of PTMO based ionenes. Our initial efforts to determine morphology included SAXS analysis of 2k PTMO based ionenes, but wide, broad intensity peaks did not suggest a highly ordered morphology. Furthermore, cryo-microtoming our ionenes was problematic since samples were too rubbery for consistent cutting of thin sections. Sections of ~50 nm are necessary for electron transmission, and we were unable to cut sections thinner than 70 nm. Attempts to overcome this problem included cooling the sample to more than 30 °C below the glass transition temperature, embedding samples in epoxy, cross-linking samples with a ruthenium oxide stain, and cutting with a vibrating diamond knife, but consistent cutting was not achieved. Moreover, when we looked at 70 nm samples beneath the microscope, we did not see any order within the material, and bubbles formed in some sections of the sample because of the heat produced by the electron beam. We are currently attributing the difficulties of cryo-microtoming to a lack of order in the material due to the fast casting procedure we used during film preparation. It would be useful to recast the films from a slow drying process over the period of at least 3 days and then perform SAXS and TEM. We think a slower casting procedure will allow time and mobility for an ordered morphology to develop, which will be detectable with SAXS. Once well-defined peaks are demonstrated with SAXS, cryo-microtoming should be attempted for TEM. It is thought that ionenes with highly ordered morphologies will be easier to microtome. It is expected that the morphology of linear PTMO ionenes will be similar to the results seen in Feng and Wilkes's work, but the morphology of branched ionenes will be less ordered.

5.4 REFERENCES

¹ Wang, J., Meyer, W., Wegner, G. On the polymerization of N,N,N',N'-tetramethyl- α,ω -alkanediamines with dibromoalkanes – an in-situ NMR study. *Macromol. Chem. Phys.* **1994** 195, 1777-1795.

² Branham, K. D., Chang, Y., Lang, F. J., McBride, E., Bunyard, C. Water-dispersible, cationic polymers, A method of making same and items using same. **2002**, USPatent WO02077048.

³ Feng, D., Wilkes, G. L. *J. Macromol. Sci.-Chem.*, **1989**, A26(8), 1151-1181.

Vita

Erika M. Borgerding was born in Winston-Salem, North Carolina on April 19, 1983 to Michael and Teresa Borgerding. She graduated from Mount Tabor High School in 2001. She entered the University of North Carolina at Chapel Hill in 2001 and graduated with a Bachelor of Science in Biology and a double major in Chemistry in 2005. She joined the Chemistry graduate program at Virginia Tech in 2005.